The rabies virus phosphoprotein P: a key regulator of innate immune responses

Dissertation der Fakultät für Biologie
der Ludwig-Maximilians-Universität München
zur Erlangung des Dr. rer. nat.

vorgelegt von
Krzysztof Brzózka
München, April 2006

Erstgutachter:	**PD Dr. Bettina Kempkes**
Zweitgutachter:	**Prof. Dr. Michael Boshart**
Sondergutachter:	**Prof. Dr. Karl-Klaus Conzelmann**

Tag der mündlichen Prüfung: **22 November 2006**

1 TABLE OF CONTENTS

2 ABBREVIATIONS

AP1	**activator protein 1**
Akt	**alpha serine/threonine-protein kinase**
BDV	**Borna disease virus**
CARD	**caspase activation and recruitment domain**
Cardif	**CARD adapter inducing interferon-beta**
CBP	**cAMP-responsive-element-binding protein (CREB)-binding protein**
CNS	**central nervous system**
CpG	**cytidine-phosphate-guanosine**
CRM1	**chromosome region maintenance 1**
dsRNA	**double stranded RNA**
dsDNA	**double stranded DNA**
GAF	**gamma-activated factor**
GAS	**gamma-activated sequence**
IFN	**interferon**
IFNAR	**interferon alpha receptor**
IFNGR	**interferon gamma receptor**
IKK	**IκB kinase**
IL	**interleukin**
IPS-1	**interferon-beta promoter stimulator 1**
IRAK	**IL-1 receptor associated kinase**
ISG	**interferon stimulated gene**
ISGF3	**IFN-stimulated gene factor 3**
ISRE	**interferon stimulated response element**
IRF	**interferon regulatory factor**
JAK	**Janus kinase**
Lgp2	**probable ATP-dependent helicase**
MAVS	**mitochondrial antiviral signaling protein**
MDA5	**melanoma differentiation-associated gene 5**
MHC	**major histocompatibility complex**
MyD88	**myeloid differentiation primary response protein 88**
NFκB	**nuclear factor kappa-B**
NNSV	**non-segmented negative strand RNA viruses**
2'-5'OAS	**2'-5'oligoadenylate synthetase**
pDC	**plasmacytoid dendritic cell**
PAMP	**pathogen-associated molecular patterns**
PI3K	**phosphoinositide-3 kinase**
PKR	**protein kinase R**
PML	**promyelocytic leukemia protein**
RIG-I	**retinoic acid inducible gene-I**
RNP	**ribonucleoprotein**
RSV	**respiratory syncytial virus**
RV	**rabies virus**
ssRNA	**single strand RNA**
SOCS	**suppressor of cytokine signaling**
STAT	**signal transducer and activator of transcription**
TANK	**TRAF-associated NFκB kinase**
TBK-1	**TANK-binding kinase 1**
TIR	**Toll/IL-1 receptor**
TNF	**tumour necrosis factor**
TRAF	**TNF Receptor-Associated Factor**
TRIF	**Toll/IL-1R domain-containing adaptor inducing IFN-β**

TRAM	**TRIF-related adaptor molecule**
TLR	**Toll-like receptor**
VISA	**virus-induced signaling adaptor**
VSV	**vesicular stomatitis virus**
VV	**vaccinia virus**

3 INTRODUCTION

3.1 Rabies virus (RV)

3.1.1 Pathogenicity

Rabies belongs to one of the oldest known infectious diseases. Already first known reports that are found in Egyptian writings, associate the consequences of a contact with a “mad” dog with an acute, progressive and incurable encephalitis (Hemachudha et al., 2002; Rupprecht et al., 2002). Rabies is caused by a neurotropic RNA virus of the *Rhabdoviridae* family, genus *Lyssavirus*. Bites and scratches represent the typical transmission route of this virus. After initial replication in the peripheral wound RV is transported in a retrograde way to the central nervous system (CNS). The incubation period ranges from one week to several months. The neurotropism of RV is at least in part caused by the use of several receptors in the CNS to facilitate virus entry into neurons: the neural cell adhesion molecule (Thoulouze et al., 1998), the p75 neurotrophin receptor (p75NTR) (Tuffereau et al., 2001; Tuffereau et al., 1998) and the acetylcholine receptor (Lentz et al., 1982). Rabies is characterized by very little neuronal pathology and mild CNS inflammation. Clinical presentation of rabies disease comes in two major forms, encephalitic (furious) and paralytic (dumb), but there is no clear explanation for this dysfunction of the limbic system. Direct post exposure treatment encompasses wound treatment, vaccine administration and inoculation of rabies virus neutralizing immunoglobulins. This treatment is mostly effective when applied in time, but once first symptoms of rabies encephalitis occur, the outcome of the disease is almost always fatal and the management of the disease is palliative (Jackson et al., 2003; Warrell and Warrell, 2004).

Recent studies addressed the question of rabies virus pathogenicity and activation of the immune response system. Inflammation and production of neutralizing antibodies, which depend on B lymphocytes and CD4+ T cells, are crucial for clearance of RV from the CNS (Dietzschold, 1993; Dietzschold et al., 1992; Perry and Lodmell,

1991; Hooper et al., 1998). As mature neurons are relatively resistant to either cell or cytokine induced cytolysis, the role of cytotoxic CD8+ T cells in RV clearance is considered minor. A major role can be attributed to cytokine production, mainly IFN-γ. Infection with pathogenic rabies virus results in chemokine production and infiltration of the CNS by mononuclear inflammatory cells (NK cells, T and B lymphocytes). In contrast to attenuated RV, no or only slight activation of innate immune response was observed (Wang et al., 2005; Nakamichi et al., 2004; Nakamichi et al., 2005; Lafon, 2005). Additionally, rabies virus infected neurons retain their integrity but upregulate FasL levels, and thereby induce apoptosis of T-cells, shortly after the T-cells cross the blood-brain barrier (Baloul et al., 2004).

3.1.2 Virus structure and replication

RV is a prototypic virus of the *Mononegavirales* order, the nonsegmented negative strand RNA viruses (NNSV). The RV single strand RNA genome of approximately 12 kb is packed into a bullet-shaped, enveloped virion of approximately 250 nm length and 70 nm width (Figure 1). It comprises five genes encoding nucleoprotein (N), phosphoprotein (P), matrixprotein (M), glycoprotein (G) and polymerase (L) in the order 3'-N-P-M-G-L-5'. All the five proteins are structural proteins of the virion and are essential for virus replication and spread.

The viral RNA is tightly enwrapped by the highly conserved nucleoprotein N and forms a ribonucleoprotein complex (RNP). The RNP serves as a template for the viral polymerase which is composed of a large catalytic subunit L and the polymerase cofactor P. The RNA synthesis, as well as the whole replication cycle, takes place in the cytoplasm. In the transcription mode, a gradient of monocistronic, capped- and polyadenylated mRNAs is synthesized using genomic RNA ("-"strand) as a template. In this model, the mRNAs of the genes most proximal to the 3' leader promoter are the most abundant ones and the amounts of transcribed mRNAs decrease with the distance from the leader sequence due to dissociation of the polymerase at the gene borders. In the replication mode, full-length RNA is synthesized on both genomic and anti-genomic RNPs (Finke and Conzelmann, 2005). Recombinant rabies viruses can be created from cDNA using a "reverse genetics" approach. Co-transfection of cDNA expressing the viral

anti-genome RNA together with support plasmids expressing rabies virus N, P and L proteins into stable cell line constitutively expressing T7 polymerase (BSR T7/5 cells) results in production of virus particles (Schnell et al., 1994; Buchholz et al., 1999). Recovery of genetically engineered rabies viruses with defined changes in the genome greatly facilitated studies on the different steps of virus life cycle, the determination of viral pathogenicity factors, and on host-virus interactions. The balance between RNP replication and mRNA transcription is regulated by the structural matrix (M) protein (Finke and Conzelmann, 2003; Finke et al., 2003). The M protein, together with the spike glycoprotein (G), is also essential for budding of virus particles. The glycoprotein is the major viral antigen and pathogenicity factor of rabies virus, as shown by *in vivo* experiments, involving the exchange of glycoproteins of pathogenic and attenuated rabies virus. Infection with a chimeric virus expressing G protein of an apathogenic strain resulted in abortive infection and increased the survival rate of infected mice (Morimoto et al., 2000; Finke and Conzelmann, 2005). High levels of glycoprotein expression were found to be responsible for induction of apoptosis in infected cells. Downregulation of G expression prevents induction of apoptosis and correlated with virus pathogenicity (Faber et al., 2002; Morimoto et al., 1999; Prehaud et al., 2003; Sarmento et al., 2005).

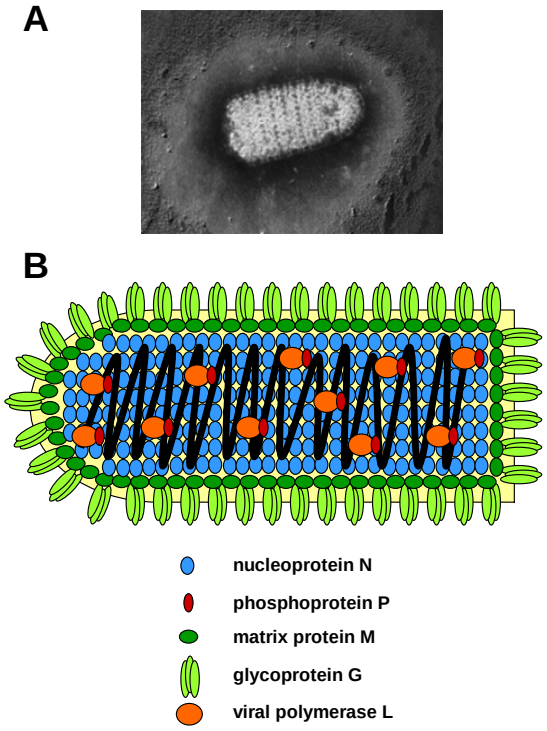

Figure 1. (A) Rabies virus belongs to the family of ssRNA enveloped viruses. The mature rabies virion has a characteristic bullet-shaped appearance of approximately 80 nm diameter and length varying between 130 and 300 nm. (B) Negative stranded RNA genome codes for 5 proteins; nucleoprotein (N), phosphoprotein (P), matrix protein (M), glycoprotein (G) and polymerase (L). All proteins are structural and can be divided in two groups: a helical ribonucleoprotein core (RNP) and a surrounding envelope. In the RNP, the viral RNA-dependent RNA polymerase consisting of P and L proteins is associated with genomic RNA tightly encased by the N protein. The M protein is associated with both RNP and the envelope and plays an essential role in rabies virus assembly. The rabies glycoprotein forms approximately 400 trimeric spikes which are tightly arranged on the surface of the virus.

3.1.3 Multifunctional phosphoprotein P

The multifunctional phosphoprotein P (Figure 2) of rabies virus is an essential and structural protein of 297 aa length. P-deficient rabies viruses are unable to replicate (Shoji et al., 2004; Finke et al., 2004), as RV P serves as a scaffold protein that associates with nucleoprotein (N) and the large subunit of vital polymerase (L). The very N-terminus of RV P is responsible for binding to L protein, with the 19 first aa residues being crucial for interaction with the C-terminal domain of L protein (Chenik et al., 1998). There are two independent N-binding domains, one is localized between aa 69-177 and most likely serves as a chaperone for non-RNA bound N protein, and the other in the C-terminus (aa 268-297) is essential for transcriptional activity of P (Chenik et al., 1994; Jacob et al., 2001; Mavrakis et al., 2004; Mavrakis et al., 2003). Phosphoprotein P contains an internal homooligomerization domain (Gigant et al., 2000; Jacob et al., 2001), and is phosphorylated by two cellular kinases, a yet uncharacterized rabies virus protein kinase (RVPK) and four isomers of protein kinase C (PKC) (Gupta et al., 2000). An interaction between RV P and a component of the microtubular transport complex, the dynein light chain (LC8), was suggested to play a role in axonal retrograde transport of rabies virus (Raux et al., 2000; Jacob et al., 2000). The importance of this interaction in rabies pathogenicity has been questioned by *in vivo* experiments, where mutant viruses that lack the LC8 binding domain were only slightly attenuated in comparison to wt virus (Mebatsion, 2001; Rasalingam et al., 2005).

Several N-terminally truncated forms of RV P are generated due to a ribosomal leaky scanning mechanism (Chenik et al., 1995; Eriguchi et al., 2002). Three such forms are detectable in RV SAD L16 infected cells, starting form internal AUG methionine codons in position 20, 53 and 83, called P2, P3 and P4, respectively. As shown by our own work, mutant SAD L16 with these internal methionine residues substituted by isoleucine (SAD P1xxx) could be “rescued” and showed only minor growth attenuation. This indicated that mutated P protein is able to support viral transcription and replication and the presence of truncated P forms is not required for RV replication *in vitro* (Brzózka et al., 2005).

In the present work, a new important role of RV P, namely in antagonizing specific functions of the innate immune system has been discovered. As RV is a rather slowly

replicating virus, it is of immense importance that initial steps of RV infection remain undetected by the host. This work shows that RV P is able to inhibit the activation of a crucial transcription factor IRF3 (interferon regulatory factor 3), thereby preventing production of interferon beta (IFN-β), a cytokine that regulates antiviral response (Brzózka et al., 2005). In addition, I was able to show that RV P is also responsible for preventing IFN-α/β as well as IFN-γ signaling. This occurrs by binding of RV P to activated STATs (signal transducer and activator of transcription) and their retention in the cytoplasm (Brzózka et al., 2006). Whereas 10 aa residues of the C-terminal domain of P were crucial for counteracting Janus kinase - signal transducer and activator of transcription (JAK-STAT) signaling, another stretch of 10 aa (residues 176-186) was required for inhibition of IFN-β production (unpublished data). This demonstrates that P possesses two independent functions in antagonizing the IFN system.

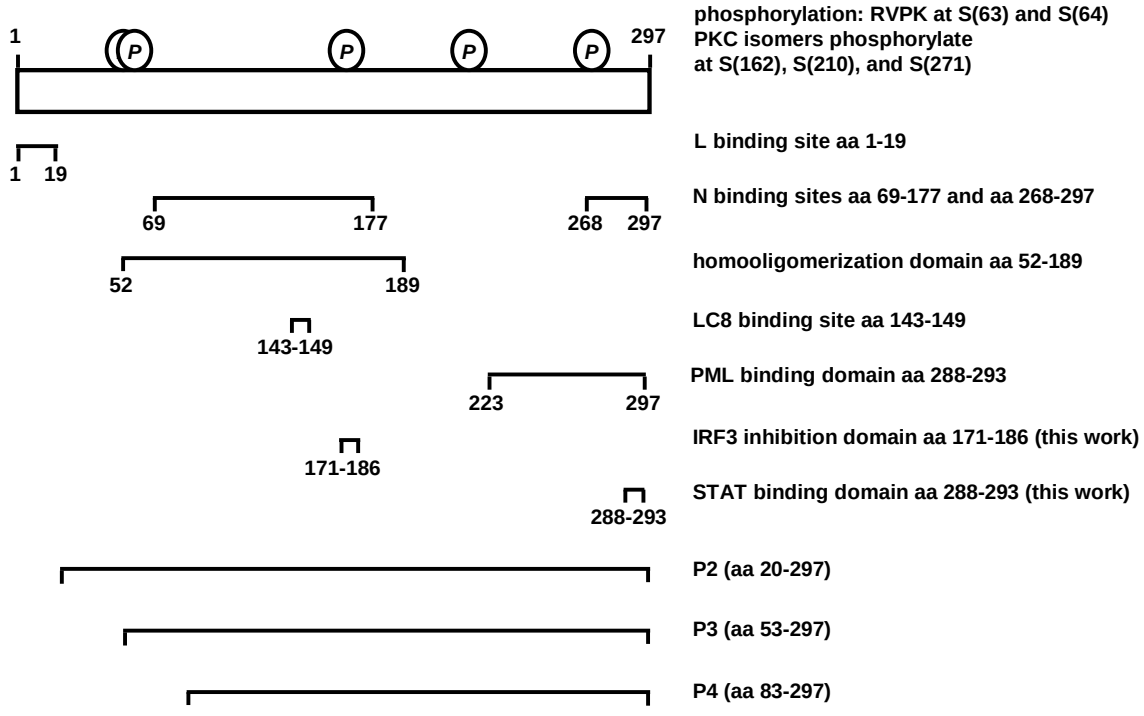

Figure 2. Schematic representation of rabies virus phosphoprotein domains. For abbreviations and detailed description see text. P2, P3 and P4 stand for short forms of RV P created by ribosomal leaky scanning mechanism from internal AUG codons.

3.2 Innate immunity: Interferon

Innate immunity is the first line of defense against viral and bacterial pathogens. Already minutes and hours after invasion of the pathogen can decide on the infection outcome – death or survival. For many years this response was underestimated and presented as basic and crude, in contrast to the sophisticated adaptive immunity. The situation changed during the last decade, with the discovery of a range of specialized receptors recognizing foreign molecular patterns and links to the adaptive immunity. Activation of the innate immune response plays a crucial role in the survival of the infected host as it occurs long before adaptive immune responses like activation of cytotoxic T lymphocytes or production of neutralizing antibodies.

3.2.1 Interferon induction

Among cytokines involved in innate immune response, interferons play a key role in turning on mechanisms of antiviral defense and shaping adaptive immunity. Initially discovered by Isaacs and Lindenmann in 1957, the family of interferons consists of two main types. The mammalian type I interferons comprise a single IFN-β protein and a dozen of IFN-α subtypes, whereas type II interferon consists of the single IFN-γ. Time course and interferon types produced vary between cell types. Whereas IFN-γ is produced only by certain cells like natural killer (NK) cells, CD4+ and CD8+ T lymphocytes, macrophages and also by neurons, the type I interferons can be produced by most cell types. A specialized cell type, the plasmacytoid dendritic cell (pDC) is the main source of IFN-α in humans.

Invading pathogens can be recognized by extracellular or intracellular receptors. Membrane associated Toll-like receptors (TLRs) recognize a broad spectrum of pathogen-associated molecular patterns (PAMPs), presented by viruses and bacteria. TLRs are present on many cell types, in particular on hematopoetic cells. There are twelve different TLRs, all of them capable to trigger nuclear factor κB-dependent (NFκB-dependent) cytokine production. Among them, five TLRs are known to stimulate type I

IFN synthesis (TLR3/4 and TLR7/8/9). Recognition of PAMPs leading to IFN production also occurs by poorly characterized cytoplasmic receptors, expressed in virtually all cell types. The transcription of interferon genes is tightly controlled by latent transcription factors, which are activated upon PAMPs recognition by TLRs or the cytoplasmic receptors (Figure 3).

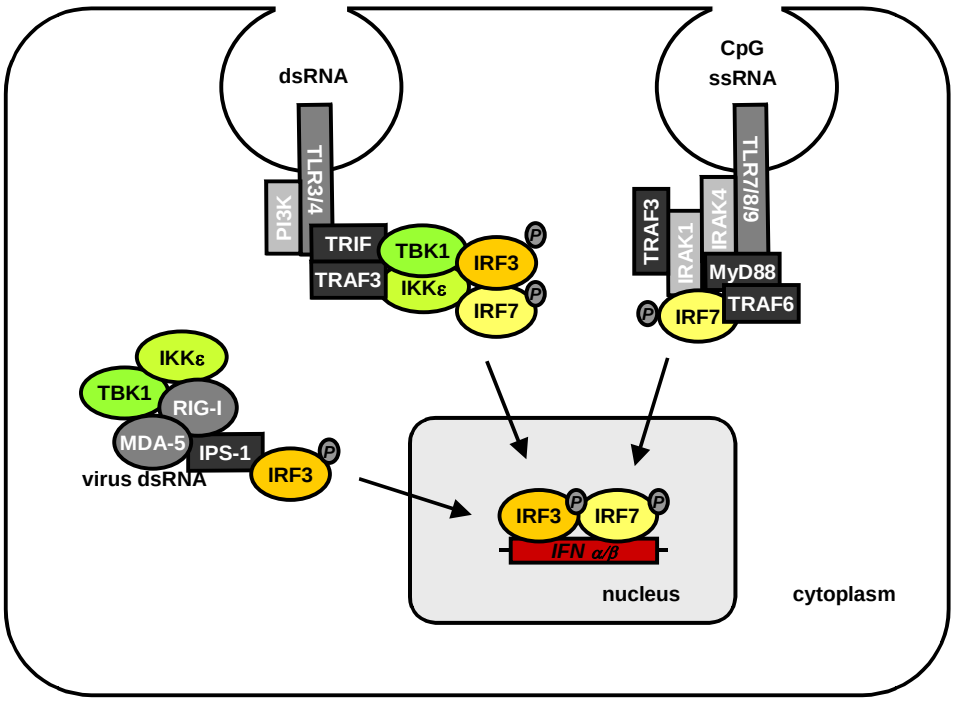

Figure 3. Cellular pathways, leading to interferon production. TLR7/9 signaling is a MyD88- and IRAK1-dependent pathway in which IRF7 is phosphorylated by IRAK1 in a complex with TRAF6 and IRAK4. TLR3/4 utilize a MyD88-independent pathway for downstream signaling. The adaptor protein TRIF binds to TLR3 upon ligand recognition. Recruitment of TBK1 or IKKε leads to phosphorylation of IRF3 or IRF7, their nuclear translocation and activation of type I IFN production. Binding of double stranded RNA (dsRNA) to the cytoplasmic receptors RIG-I and MDA5 triggers downstream signals via a CARD-domain containing protein IPS-1 (MAVS, VISA, Cardif). This complex recruits TBK1 or IKKε and leads to phosphorylation of IRF3 (for details and abbreviations see text).

3.2.1.1 Interferon regulatory factors

Two transcription factors are essential for IFN-α/β gene expression, the ubiquitously expressed interferon regulatory factor 3 (IRF3) that regulates expression of IFN-β (Yoneyama et al., 2002; Yoneyama et al., 1998; Lin et al., 1998; Lin et al., 1999), and interferon regulatory factor 7 (IRF7) that controls production of IFN-α subtypes. IRF7 is constitutively expressed only in pDCs (plasmacytoid dendritic cells), in other cells its expression is induced by IFN (Lin et al., 2000; Honda et al., 2005b; Caillaud et al., 2005; Civas et al., 2005; Sato et al., 2000). A hallmark of the IRF family is a highly conserved N-terminal DNA binding domain with five characteristic tryptophan repeats and a C-terminal serine-rich domain. IRF3 and IRF7 form hetero- or homodimers after activation by phosphorylation. Following nuclear translocation, IRFs bind to the IFN promoter sequence and transcription of IFN is switched on. Other transcription factors and co-factors like AP1, NFκB, or p300/CBP (directly interacting with IRFs) further support activation of IFN-β mRNA transcription. As shown recently, the critical IRF3 phosphorylation step is executed by kinases of the IKK family (see below). Activation by phosphorylation of IRF3 and IRF7 seems to be a bottle neck where all the pathways leading to IFN production converge.

IKKε (called also IKK-i) and TBK1 (known also as NAK) are members of the IKK kinase family and show structural and functional homology to IKKα and IKKβ which are involved in activation of NFκB. The overall topology of the kinase domain, a leucine zipper-like domain and helix-loop-helix region is similar within the family. Although both IKKε and TBK1 are able to activate NFκB via Ser36 phosphorylation of IκBα, their main and essential role is activation of IRF3 and IRF7 factors (Kishore et al., 2002; Huynh et al., 2002; Tojima et al., 2000; Sharma et al., 2003; Fitzgerald et al., 2003a). In contrast to the constitutively and ubiquitously expressed TBK1, IKKε is mostly expressed in immune cells, but can be also induced in other cells. Both kinases phosphorylate specific C-terminal serine residues of IRF3 and IRF7, leading to IRF dimerization, nuclear translocation and transcriptional activation of IFN-α/β promoters. Whereas the critical phosphorylation residues of IRF7 are still unclear (tenOever et al., 2004; Caillaud et al., 2005), IRF3 phosphorylation was extensively studied in the past years. A

sequential activation model has been proposed, in which a serine cluster containing Ser396 and Ser402 is phosphorylated by TBK1 or IKKε (Servant et al., 2001; tenOever et al., 2004; Qin et al., 2003). This leads to partial IRF3 activation and structural rearrangement that allows phosphorylation of Ser385/386 residues in another serine cluster, by TBK1 or an additional kinase, that has not yet been characterized. This step is essential for dimerization and transcriptional activity of IRF3 (Mori et al., 2004).

3.2.1.2 RNA-helicase pathway

Two molecules, retinoic acid inducible gene-I protein (RIG-I) and melanoma differentiation associated gene 5 protein (MDA5, known also as Helicard) serve as intracellular receptors binding dsRNA and activate IFN production (Yoneyama et al., 2004; Andrejeva et al., 2004). RIG-I and MDA5 are cytosolic proteins containing a carboxy-terminal DExD/H-box RNA helicase domain and two amino-terminal caspase activation and recruitment domains (CARDs). After binding of dsRNA an adaptor protein IPS-1 (interferon-beta promoter stimulator 1, called also MAVS (mitochondrial antiviral signaling protein), VISA (virus-induced signaling adaptor) or Cardif (CARD adapter inducing interferon beta)) associates with both RIG-I and MDA5 via CARD domain interactions (Kawai et al., 2005; Meylan et al., 2005; Seth et al., 2005; Xu et al., 2005). The mitochondrial localization of IPS-1 is essential for its function in IFN induction providing an interesting link between innate immunity and mitochondria (Seth et al., 2005). Most probably, the adaptor protein binds to the activated form of the RNA-helicases, as suggested by co-precipitation of RIG-I ΔC and MDA5 ΔC lacking the auto-inhibitory carboxy-terminal domains. Thus, virus infection stimulates formation of macromolecular signaling complexes consisting of RIG-I or MDA5 with IPS-1 and signaling effectors. However, the recruitment of IRF3 and TBK-1 or IKKε to this complex remains still to be clarified.

A negative feedback regulator of this pathway has been described recently (Yoneyama et al., 2005; Rothenfusser et al., 2005). Like RIG-I and MDA5, the Lgp2 (probable ATP-dependent helicase) protein binds dsRNA with a very high affinity competing with RIG-I/MDA5 for dsRNA. However, Lgp2 lacks the caspase recruitment and activation domain. It is therefore not able to signal downstream via CARD-adaptor

protein and functions as a negative regulator of IFN induction by preventing recognition of viral RNA.

3.2.1.3 Toll-like receptor 3 pathway

Toll like receptor 3 is involved in recognition of exogenous dsRNA. In contrast to other members of the TLR family, downstream signal transduction of this receptor is independent of the common Toll/IL-1 receptor (TIR) - adaptor protein MyD88 (myeloid differentiation primary response protein 88). Stimulation of macrophages and DCs with dsRNA leads to recruitment of an adaptor protein called TRIF (Toll/IL-1R domain-containing adaptor inducing IFN-β) to the receptor via TIR domain interactions (Sato et al., 2003; Yamamoto et al., 2003a). TRIF binds to TBK-1 and IKKε, which in turn phosphorylate IRF3 to activate IFN-β production. Similarly to TLR3, signaling of TLR4 after binding to its ligand LPS (lipopolysaccharide), involves TRIF, but requires an additional adaptor protein called TRAM (TRIF-related adaptor molecule) (Yamamoto et al., 2003b; Fitzgerald et al., 2003b). Recent studies revealed a pivotal role of TNF receptor associated factor-3 (TRAF3) in TLR signaling. Two groups showed that TRAF3 binds to both TRIF and the kinases TBK1 and IKKε (Oganesyan et al., 2006; Hacker et al., 2006). The indispensability of TRAF3 in TLR3 signaling suggests that it serves as a critical link between the TLR adaptor proteins and effector kinases, enabling downstream signaling. Moreover, TRAF3-deficient fibroblasts were defective in IFN production in response to vesicular stomatitis virus (VSV) infection, indicating a role of TRAF3 in TLR-independent virus recognition as well. Another member of the TRAF family proteins, TRAF1, is a negative regulator of the TLR3 signaling pathway. Caspase-dependent cleavage of TRAF1, somehow induced by TRIF adapter protein, leads to interaction of TRIF and TRAF1 that results in inhibition of TRIF-dependent signaling (Su et al., 2006).

A two-step mechanism of IRF3 activation in TLR3 downstream signaling was suggested. Full phosphorylation and activation of IRF3 can be achieved if the phosphoinositide-3 kinase-alpha serine/threonine-protein kinase (PI3K-Akt) pathway is also activated (Sarkar et al., 2004; Spiegel et al., 2005). According to the model, IRF3 is

not completely phosphorylated when PI3K is not recruited to TLR3 after dsRNA binding, or the pathway is blocked by a specific inhibitor. IRF3 then translocates to the nucleus but is unable to drive transcription from the target gene promoter. Most probably, a nuclear kinase different from TBK-1 or IKKε can phosphorylate IRF3 at the crucial S386 residue, allowing its dimerization and DNA binding.

3.2.1.4 Toll-like receptor 7/9 pathway

Plasmacytoid dendritic cells are responsible for production of the majority of type I IFN *in vivo* in response to viral infection. This is due to constitutive expression of TLR7 and TLR9 on the cell surface, and of IRF7 in pDCs (Asselin-Paturel and Trinchieri, 2005). Ligand recognition by TLR7 (ssRNA and synthetic imidazoquinoline-like molecules like imiquimod (R-837) and resiquimod (R-848)) or TLR9 (unmethylated 2'deoxyribo (cytidine-phosphate-guanosine) (CpG) DNA motifs) activates signaling dependent on the TIR adaptor MyD88. An important observation regarding TLR3, TLR7 and TLR8 ligand recognition was made by Kariko et al., indicating that innate recognition of RNA is dependent on its modifications, like methylation, which allows selective recognition of foreign RNA. Unlike cytoplasmic receptors, TLRs do not require viral infection of the cells. The association of MyD88 with TLR7/9 recruits members of IL-1 receptor associated kinase (IRAK) family, namely IRAK4 and IRAK1, that bind to TRAF6 and IRF7 (Kawai et al., 2004; Honda et al., 2004). This leads to phosphorylation of IRF7 by IRAK1 and its translocation to the nucleus to induce production of IFN-α (Uematsu et al., 2005). In contrast to other cell types, pDCs are able to produce abundant amounts of interferon upon TLR7/9 activation. As shown by Honda *et al*., in pDCs but not in conventional dendritic cells, ligand bound TLR9 is retained for long periods in the endosomal vesicles, instead of being rapidly transferred to lysosomal vesicles (Honda et al., 2005a). This retention was suggested to be responsible for the robust type I interferon production by stimulated pDCs.

Better understanding of the TLR7/9 signaling mechanisms included also the discovery of a whole range of negative regulators, that target different signaling components (reviewed in (Liew et al., 2005)). For example, IRAKM, an inactive member

of the IRAK kinase family proteins, is induced upon TLR stimulation and prevents IRAK4/IRAK1 dissociation from the MyD88 complex, disrupting downstream signaling (Kobayashi et al., 2002). SIGIRR (single immunoglobulin interleukin-1 receptor-related protein), a constitutively expressed protein is down-regulated when TLR signaling is activated, binds to both TRAF6 and IRAK, thereby preventing their actions (Wald et al., 2003). Interestingly, also SOCS (suppressors of cytokine signaling), described initially as inhibitors of the JAK-STAT pathway (see below), are also upregulated by TLR ligands independent of type I interferon signaling. Although the mechanism of TLR inhibition by different SOCS are still unclear, recent publication linked SOCS1 mediated degradation of the adaptor Mal to inhibition of TLR2/4 signaling (Kinjyo et al., 2002; Mansell et al., 2006).

3.2.2 Interferon signaling

IFN-α/β and IFN-γ act through binding to ubiquitous receptors, the IFNAR (interferon alpha receptor) and the IFNGR (interferon gamma receptor), respectively. IFN-α/β binding to IFNAR results in receptor dimerization and recruitment of two Janus kinases (JAK) that activate themselves by autophosphorylation. Those activated JAKs, directly or indirectly turn on several downstream signaling pathways (for review see (Platanias, 2005; Aaronson and Horvath, 2002)). The classical and best known signaling pathway involves phosphorylation of STAT1 and STAT2 at the specific tyrosine residues, Y701 and Y689, respectively. Activated STATs form a heteromeric complex containing STAT1, STAT2, and IRF9 (p48), also known as IFN-stimulated gene factor 3 (ISGF3), that enters the nucleus, where it binds to a specific DNA sequence called ISRE (IFN-stimulated response element) initiating gene transcription of interferon stimulated genes (Figure 4). STAT dephosphorylation by nuclear phosphatases causes disruption of the complex and allows STAT reshuttling to the cytoplasm via the CRM1 (chromosome region maintenance 1) export system. Inactivated STATs are shuttling between cytoplasm and nucleus with different speed (for review see (Vinkemeier, 2004; Meyer and Vinkemeier, 2004)). In contrast to IFN-α/β inducing predominantly STAT1/2 heterodimers, IFN-γ signaling involves tyrosine phosphorylation of only STAT1 by the

kinases JAK1 and JAK2. This leads to the formation of STAT1 homodimers, also known as gamma-activated factor (GAF). GAF drives the expression of genes that are controlled by another specific promoter sequence, the gamma activated sequences (GAS). Tyrosine phosphorylation of STATs is the crucial step in IFN mediated signaling, required for nuclear import of the STAT complexes. Serine phosphorylation of STAT1 in the S727 position may further augment transcriptional activity via enhancement of STAT interaction with other co-activators, like p300/CBP. S727 phosphorylation is performed for example by protein kinase Cδ (PKCδ) kinase, the activation of which is PI3K dependent (Deb et al., 2003; Uddin et al., 2002).

One group of IFN-induced proteins acts as feedback inhibitors. It is the family of suppressors of cytokine signaling (SOCS) consisting of eight members (SOCS1-SOCS7 and CIS) that share structural homologies like a central SH2 domain and C-terminal SOCS box (for review see (Ilangumaran et al., 2004; Larsen and Ropke, 2002)). There are several mechanisms by which SOCS inhibit JAK-STAT signaling. They can bind through their SH2-domain to the phoshotyrosine residues of the target protein, either preventing JAK kinase activity or STAT recruitment to the IFN receptor. Another possibility is SOCS-box mediated proteosomal degradation of the target protein.

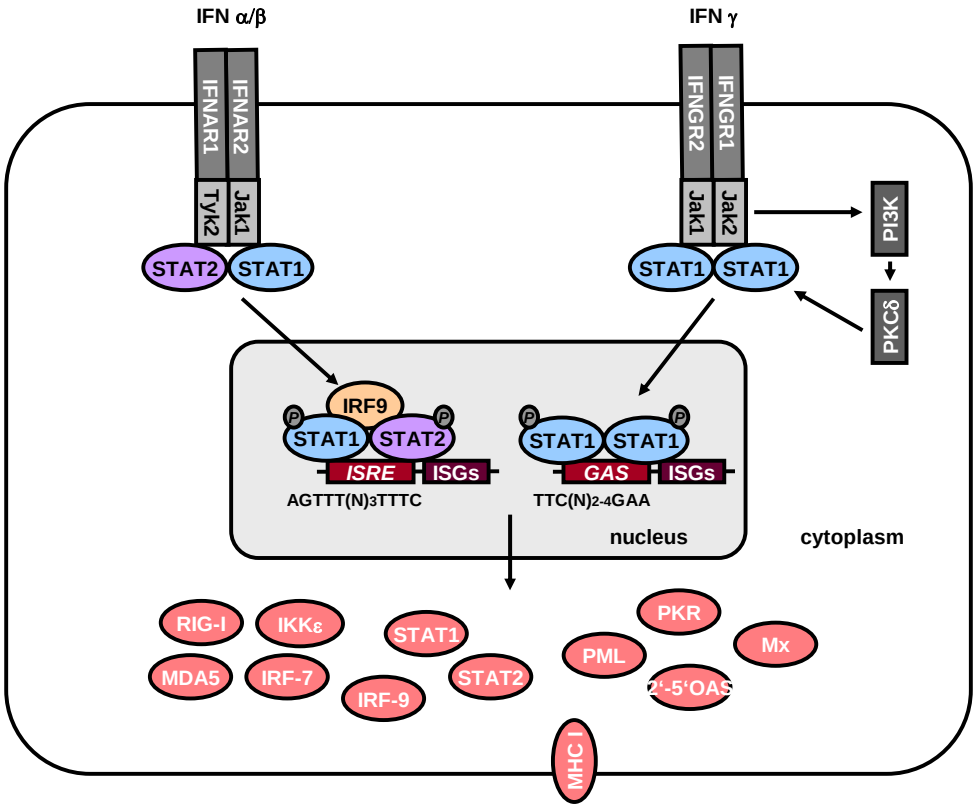

Figure 4. Downstream signaling of interferons. IFN binding to the receptor recruits members of the Janus kinase family, that cross-activate each other STAT proteins, by phosphorylation. Tyrosine phosphorylated STAT homo- and heterodimers translocate to the nucleus and drive transcription of interferon stimulatory genes controlled by the ISRE and GAS sequences (see text for details and abbreviations).

3.2.3 Interferon stimulated genes (ISGs)

Proteins produced upon IFN stimulation include several that exert direct antiviral effects, and others, which cause indirect antiviral effects (for review see (Sarkar and Sen, 2004; Samuel, 2001; Nisole et al., 2005)). For example, 2'-5'oligoadenylase (2'-5' OAS) is an enzyme capable to synthesize short adenosine oligomers that bind latent endoribonuclease and cause its dimerization and activation. Active RNase L degrades cellular and viral RNA. Protein kinase R (PKR) is a kinase capable of binding dsRNA and phosphorylating the α subunit of the translation initiation factor 2 (eIF2), thus causing inhibition of translation. Similarly, a family of P56 proteins blocks different steps

of the translation initiation process by binding to the eIF3 factor. Mechanisms of actions of other antiviral proteins like Mx protein, PML (promyelocytic leukemia protein) or p200 protein family are less clear and may involve direct interaction with viral proteins.

The second group of IFN stimulated genes consists of proteins like IRF7, which control transcription of the "late" IFN-α genes, or other members of the IFN induction and signaling pathways. Increasing their levels sensitizes non-infected cells to invading pathogens. Additionally, a number of cytokines and chemokines are produced as a result of IFN signaling, stimulating mechanisms of the adaptive immune response, including expression of major histocompatibility complex (MHC), activation of NK cells, maturation of dendritic cells, and promoting the T helper cell response toward Th1 type. Taken together, all described mechanisms restrict virus replication and amplification via different means.

3.3 Viral inhibitors of innate immune respose

3.3.1 Viral inhibitors of IFN induction

A broad range of viral IFN inhibitors, employing different strategies in counteracting IFN induction, was described in the past years (extensively reviewed in (Hengel et al., 2005; Conzelmann, 2005; Weber et al., 2004; Katze et al., 2002)). To date however, only two inhibitors of TBK-1 mediated phosphorylation of IRF3 have been reported, borna disease virus phosphoprotein (BDV P) and rabies virus P (RV P) (Unterstab et al., 2005; Brzózka et al., 2005). Another member of the negative strand RNA viruses family, Ebola virus, encodes a protein VP35, that blocks IRF3 activation upstream of TBK1 and IKKε (Basler et al., 2000; Basler et al., 2003; Conzelmann, 2005). Similarly, nonstructural proteins (NS) of respiratory syncytial virus are responsible for IRF3 pathway inhibition, whereas NFκB and AP1 activation remains unchanged (Bossert et al., 2003; Spann et al., 2005; Spann et al., 2004).

Viruses like influenza and vaccinia virus encode for proteins (NS1 and E3L, respectively) that directly bind to dsRNA, therefore preventing its recognition by

intracellular receptors. Andrejeva and colleagues identified MDA5 as a direct target of the V proteins from *Paramyxovirinae* (Andrejeva et al., 2004). V proteins are expressed from the multicistronic P genes *Paramyxovirinae* by a RNA editing mechanism. P and V have therefore identical N-terminal domains, and specific C-terminal domains. The V proteins bind specifically to the RNA helicase MDA5, but not to RIG-I, reducing its IFN-β inducing activity. A serine protease NS3/4A of hepatitis C virus (HCV) causes specific proteolysis of two adaptor proteins, TRIF (Ferreon et al., 2005; Li et al., 2005) and IPS-1 (Meylan et al., 2005), therefore disabling both TLR3 and RIG-I signaling pathways. The vaccinia virus A46R protein is so far the only TIR-domain containing viral protein that targets TLR adaptor molecules, like MyD88, TRAM and TRIF disrupting IRF3 activation (Stack et al., 2005).

With regard to IFN gene expression, also other, unspecific mechanism like general transcription shut down, can be interpreted as developed by viruses to evade host innate immunity. For example, the matrix protein (M) of vesicular stomatitis virus (VSV) is responsible for blocking cellular mRNA transcription by binding to a TFIID RNA polymerase II cofactor (RNAPII) and influencing nuclear transport (Ahmed and Lyles, 1998; Ahmed et al., 2003; Yuan et al., 2001; Yuan et al., 1998). Similarly, the small nonstructural protein (NSs) of Rift Valley Fever virus targets another component of the RNAPII complex, namely the p44 subunit of the TFIIH factor (Le May et al., 2004).

3.3.2 Viral inhibitors of interferon signaling

The mechanism of RV P used to interrupt IFN JAK-STAT signaling is unique among viruses. The related Paramyxoviruses have developed a variety of “weapons of STAT destruction”, which are in particular represented by their V proteins. The V proteins of most Rubulaviruses bind to DDB1 (DNA-damage binding protein 1) which is a component of E3 ubiquitin ligase complexes, and then mediate proteasomal degradation of either STAT1 or STAT2 (Andrejeva et al., 2002; Parisien et al., 2002a; Parisien et al., 2002b; Ulane et al., 2005). Depletion of STAT2 or STAT1 from the infected cells is therefore responsible for the interference with IFNGR and/or IFNAR signaling. Notably, degradation of either STAT requires the presence of the other STAT,

suggesting that hetero(di)meric complexes of STAT1 and STAT2 with V, are required for degradation. The common direct and/or primary binding partner of some V proteins appears to be STAT2. Importantly, however, activation or tyrosine phosphorylation of STAT is not required for binding and degradation. The V proteins of other Paramyxoviruses like measles virus of the Morbillivirus genus or Nipah and Hendra viruses (Henipavirus genus) do not lead to degradation of STATs, but rather interfere with signaling mechanisms. Henipaviruses prevent phosphorylation of STATs and sequester STAT1 and STAT2 in high molecular mass complexes in the cytoplasm (Rodriguez et al., 2002; Rodriguez and Horvath, 2004; Rodriguez et al., 2004; Shaw et al., 2004). The V protein of Measles virus (Morbillivirus genus) V protein, was reported to co-precipitate with STAT1, STAT2, STAT3, and IRF-9, to bind to the IFNAR, and to recruit STATs to viral inclusion bodies, while Tyr-phosphorylation of STATs was possible (Palosaari et al., 2003; Takeuchi et al., 2003; Yokota et al., 2003). The phenotypes caused by measles virus V and RV P seem to be therefore similar. However, measles virus applies a constitutive binding of STATs, and RV P binding occurs on demand when STATs are activated (this thesis).

Also the large poxviruses developed mechanisms of IFN signaling inhibition. They express soluble chemokine receptors (so called viroceptors), like B8R of vaccinia virus, that intercept soluble, secreted IFN and prevent its binding to the cellular receptors (Alcami and Smith, 1996). Other sophisticated mechanisms discovered among large DNA-viruses, are for example STAT2 degradation by m27 protein of CMV (cytomegalovirus) (Zimmermann et al., 2005) or the VH1 phosphatase of vaccinia virus that is able to bind and dephosphorylate STAT1 (Najarro et al., 2001).

4 DISCUSSION

4.1 Inhibition of interferon beta induction by Rabies virus P protein

In this study I present evidence that the phosphoprotein P of RV is an IFN antagonist preventing transcription of IFN β in virus-infected cells (**Brzózka *et al*, 2005**). An initial finding pointing towards a role of RV P in inhibition of host cell defense was the observation that SAD eGFP-P rabies virus was severely attenuated in certain tissue cultures ((Finke et al., 2004) and Finke, unpublished data). This recombinant virus expressed an eGFP-P fusion protein instead of wt RV P. Attenuation of SAD eGFP-P was correlated with the presence of interferon and antiviral response in infected cells, in contrast to the wt SAD L16. Further experiments indicated that reduced levels of the P fusion protein and a possible impediment of P functions by the N-terminal eGFP moiety might be responsible for the inability of GFP-P to prevent IFN production. Indeed, from previous experiments involving complementation of P-deficient RV it appears that the eGFP-P fusion protein has severe defects in mRNA synthesis, while virus formation is well supported.

To further address the role of the essential phosphoprotein P in rabies virus growth, I generated a recombinant virus, SAD ΔPLP, expressing very little of the RV P protein (Brzózka et al., 2005). Since viruses lacking the P gene are not able to replicate, I applied a reverse genetics approach making use of the typical transcription gradient of non-segmented negative strand viruses (NNSV) (Conzelmann, 2004). The P gene was moved from its second position in the genome (that allows abundant transcription of P mRNAs), to the most 3'-end promoter distal position. This resulted in a large decrease in the levels of P mRNA and of P protein in cells infected with SAD ΔPLP, in comparison to wt SAD L16. SAD ΔPLP was only slightly attenuated in the BSR T7/5 cell line with titers approximately one log10 lower than wt, but failed to replicate in HEp-2 cells. This failure was due to efficient transcription of IFN-β upon virus infection. A substantial contribution of the M protein to preventing IFN production, as observed for VSV (Ferran and Lucas-Lenard, 1997), could be excluded since RV replicons encoding N, P, and L did not

induce any IFN response. IFN-induction by SAD ΔPLP was correlated with the activation of the critical transcription factor IRF3, whereas the activity of NFκB and AP1 was unchanged (Figure 5A). This demonstrated that the IRF3 activation pathway is specifically blocked in wt RV-infected cells. In the presence of sufficient P, IRF3 is not activated as demonstrated by the absence of Ser386 phosphorylation and dimerization. In contrast, in SAD ΔPLP-infected cells the crucial phosphorylation at the Ser386 residue of IRF3 dimers was readily detectable, and IRF3-dependent expression of reporter genes was possible (Figure 5B).

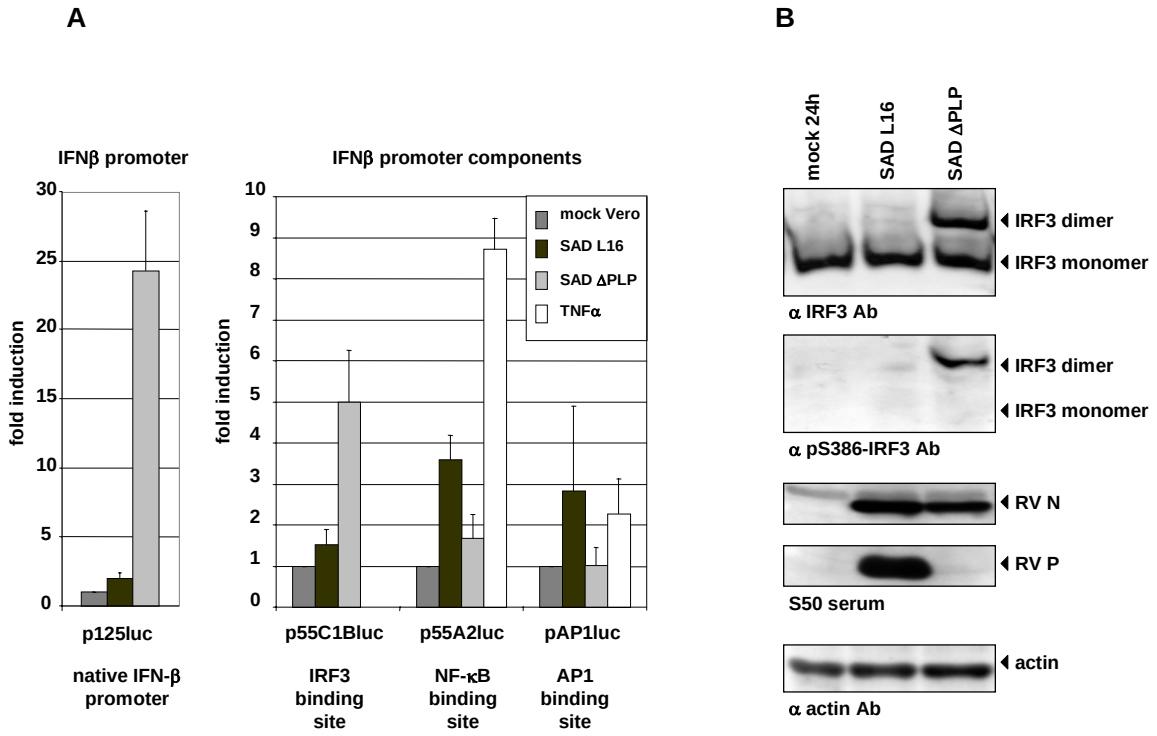

Figure 5. Rabies virus targets the IRF3 activation pathway. (A) Vero cells were transfected with reporter plasmids harbouring the *firefly* luciferase gene under the control of different promoter sequences and were infected at a MOI of 3 with SAD L16 or SAD ΔPLP. Cell lysates were analyzed using the Dual Luciferase reporter system (Promega) for luciferase activity at 48 hrs p.i.. In contrast to SAD ΔPLP, SAD L16 is able to prevent expression of *firefly* luciferase from plasmids containing the IFN-β promoter (p125luc) and the IRF3 binding site (p55C1Bluc). In contrast to IRF3, the activity of NFκB and AP-1 is not further stimulated in SAD ΔPLP-infected cells as compared to SAD L16-infected cells. Incubation of cells with tumor

necrosis factor α (TNF-α) was used as a positive control. (B) Dimerization and Ser 386-phosphorylation of IRF3 in SAD ΔPLP infected cells. HEp-2 cells were infected at a MOI of 1 and cell extracts were analyzed at 24 hrs p.i. by native PAGE and Western blot. In contrast to SAD ΔPLP, wt SAD L16 prevents IRF3 dimerization and phosphorylation on Ser386. The same cell lysates were analyzed by SDS PAGE for expression of viral N and P proteins.

Since overexpression of TBK-1 in cells is sufficient for IRF3 activation, I have utilized this feature to demonstrate that the IFN inhibitory activity of RV involves a downstream target within the IRF3 activation pathway. In cotransfection experiments, RV P alone was sufficient for inhibiting TBK1-mediated IRF3 activation and IFN-β production (Figure 6A). The same effect was observed after expression of RV P with upstream TBK1 activators, TRIF and IPS-1. On the other hand, RV P did not show any effect on constitutively active forms of both IRF3 and IRF7 (unpublished data). Analysis by native PAGE revealed that P precludes not only the critical S386 phosphorylation of IRF3 by TBK-1, but also phosphorylation of IRF7, such that IRF dimerization and transcriptional activity is prevented (Figure 6B and C). A direct interaction between P and IRF3 or IRF7 is unlikely, since in co-immunoprecipitation experiments no association has been observed (data not shown).

Figure 6. Expression of P is sufficient to prevent TBK1 mediated IFN-β induction. (A) HEK 293 cells were transfected with expression plasmids encoding the indicated genes and reporter plasmids harboring the *firefly* luciferase gene under control of the IFN-β promoter (p125luc). Luciferase activities were determined at 48 hrs p.t. using the Dual Luciferase reporter system (Promega). Co-transfection of P, but not of PΔ162-186 with TBK1 almost completely inhibited activation of the IFN-β promoter. (B) Expression of RV P inhibits TBK1-mediated dimerization of endogenous IRF3 and phosphorylation of IRF3 in position Ser386. Cell extracts were harvested 24 hrs p.t. of TBK1 or TBK1 and P-encoding plasmids and were analyzed by native PAGE and Western blot. Expression of Flag-tagged TBK1 (fl-TBK1), RV P and β-actin was confirmed by SDS PAGE and Western blot analysis of the same lysates. (C) Expression of RV P inhibits TBK1-mediated phosphorylation of IRF7. Cell extracts were harvested 24 hrs p.t. of indicated expression plasmids. The typical mobility shift of IRF7, that could be detected upon phosphorylation of IRF7 by TBK1, was not detected in the presence of RV P.

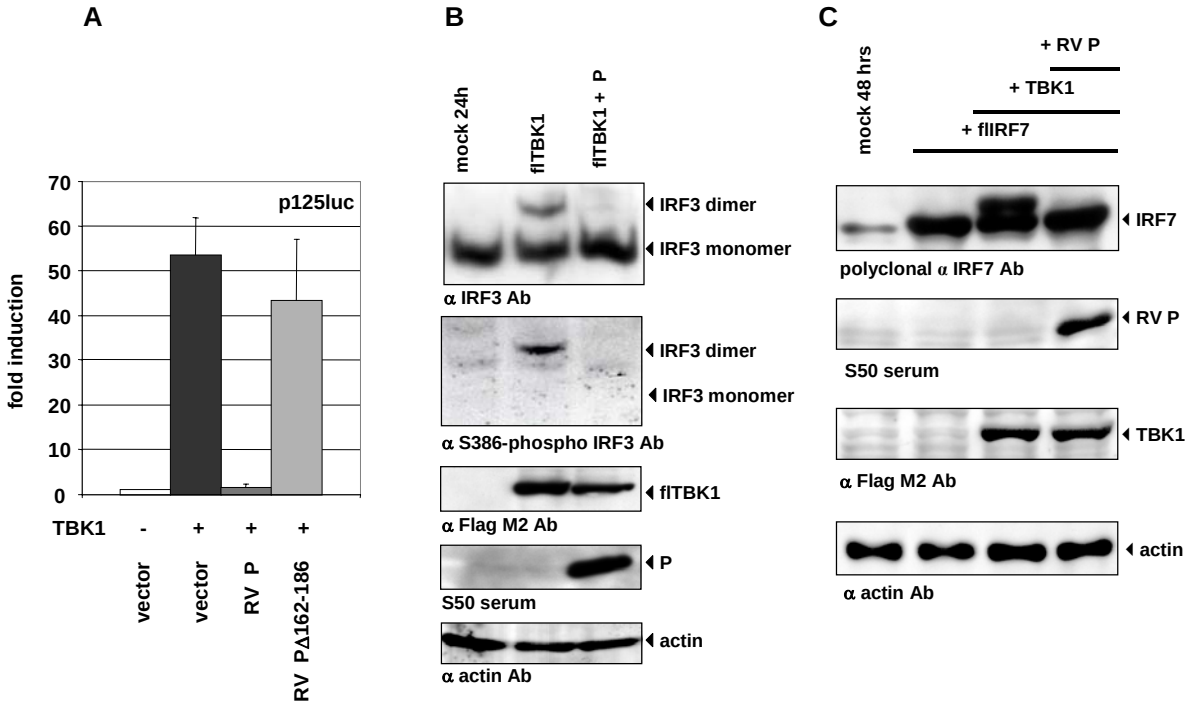

To address which domains of RV P are important for inhibition of IFN induction, I generated a series of P mutants. An internal RV P domain consisting of the aa residues 171-186 was found to be required since a corresponding deletion mutant failed in preventing TBK1-mediated interferon induction (Fig. 6A). Notably, as found later, this domain is not important for another function of P, namely, the binding of STATs and inhibition of JAK-STAT signaling (see below). Therefore, inhibition of IFN induction is a function of RV P that is independent and genetically separable form other functions of P. In future experiments, such P mutants lacking individual functions will be used to identify the cellular interaction partners of P and to dissect the mechanisms of inhibition.

In case of IFN induction, a potential molecular target of P is TRAF3, which was very recently described as part of the protein complex in which IRF-3 is phosphorylated by TBK-1. Binding of P to TRAF3 would provide an elegant explanation for the specific inhibition of the TBK1 pathway and the failure of RV P in inhibiting IRAK-dependent IFN induction. As we could show, RV P is not able to interfere with the TLR7/9 signaling pathway that involves phosphorylation of IRF7 by IRAK1 kinase ((Schlender et al., 2005) and Ch.Pfaller, personal

communication). Therefore infection of pDCs, in which TLR7/9 pathway is active, with rabies virus, in contrast to infection with respiratory syncytial virus (RSV) and Measles virus, results in the efficient production of IFN-α (Fig. 7).

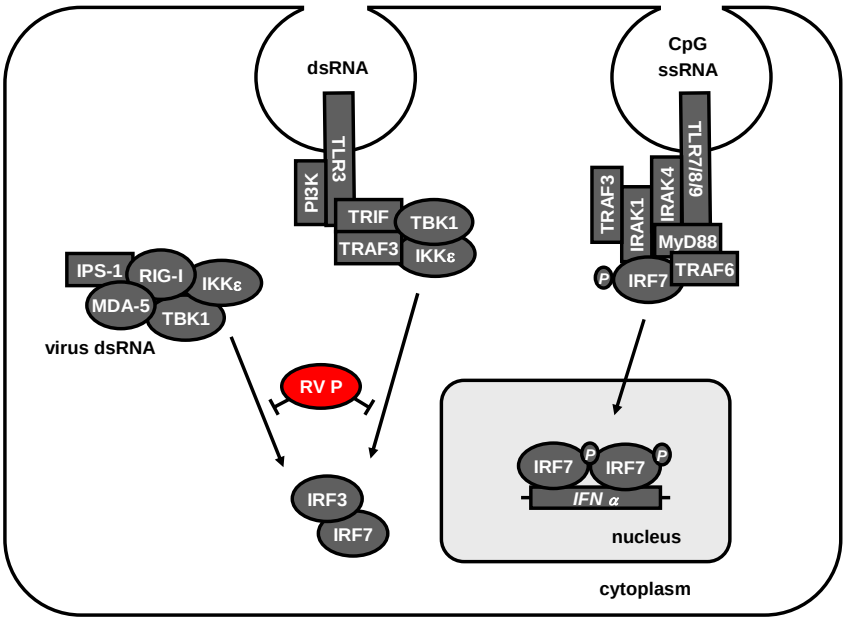

Figure 7. Inhibition of the IFN induction pathway by the rabies virus phosphoprotein P. RV P prevents phosphorylation and activation of the crucial transcription factors IRF3 and IRF7 by the upstream TBK1 and IKKε kinases. Unphosphorylated IRF3 and IRF7 are unable to dimerize and enter the nucleus to switch on transcription of the IFN mRNA. In contrast, the TLR7/8/9 signaling pathway involving phosphorylation of IRF7 by IRAK is not influenced by the RV P.

4.2 Inhibition of interferon signaling by Rabies virus P protein

In the second part of my thesis work I could demonstrate that RV P is responsible for protecting the virus from the effects of IFN, by abolishing IFN-mediated JAK-STAT signaling (**Brzózka *et al*, 2006**). The existence of RV proteins able to counteract IFN signaling was first suggested by the observation that IFN treatment of cells previously infected with RV had no detectable effects on virus gene expression and infectious virus titers, whereas pre-treatment of cells with IFN completely prohibited RV replication. In RV-infected cells an almost complete inhibition of ISRE- and GAS-controlled luciferase

activity was observed after stimulation with IFN-α/β or IFN-γ (Fig. 8). In striking contrast, the recombinant RV expressing low P amounts was not able to prevent the induction of ISRE- and GAS-controlled genes, and was sensitive to the antiviral activities induced by IFN. This suggested the P protein as the inhibitory factor and was verified by expression of P from transfected plasmids (**Brzózka *et al*, 2006)**.

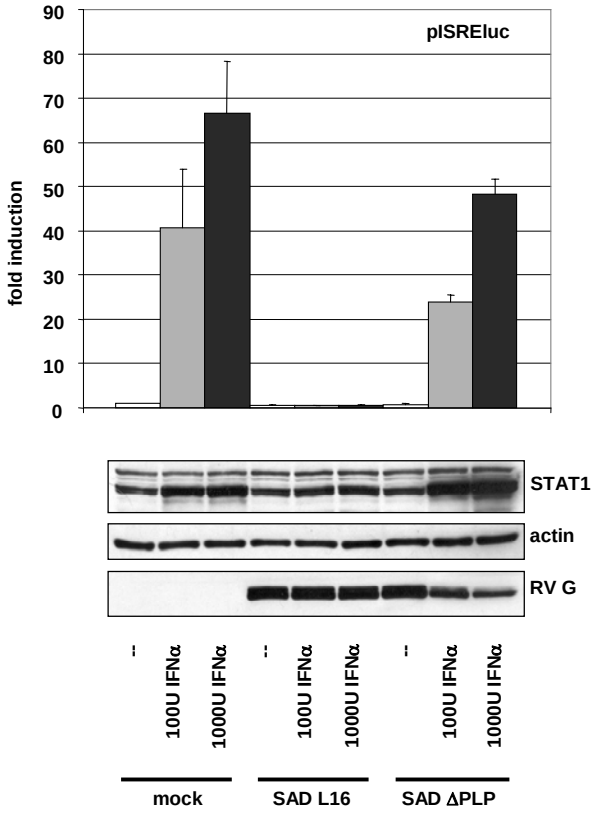

Figure 8. Inhibition of IFN signaling by wt RV SAD L16 but not by a mutant virus expressing low amounts of P protein (SAD ΔPLP). Virus-infected cells expressing *firefly* luciferase under the control of the ISRE sequence were stimulated with IFN-α as indicated. Only wt RV is able to abolish IFN-induced luciferase activities (top) and prevent upregulation of the IFN responsive STAT1 (bottom). SAD ΔPLP is not able to prevent IFN signaling and is therefore sensitive to IFN effects as indicated by decreased accumulation of virus proteins (G).

The following experiments revealed that in the presence of P, STAT1 and STAT2 was correctly phosphorylated by Janus kinases at the critical tyrosine residues after stimulation with IFN-α/β or IFN-γ. Nevertheless, neither activated STAT1 nor STAT2 was able to enter the nucleus as shown by confocal microscopy (Fig. 9).

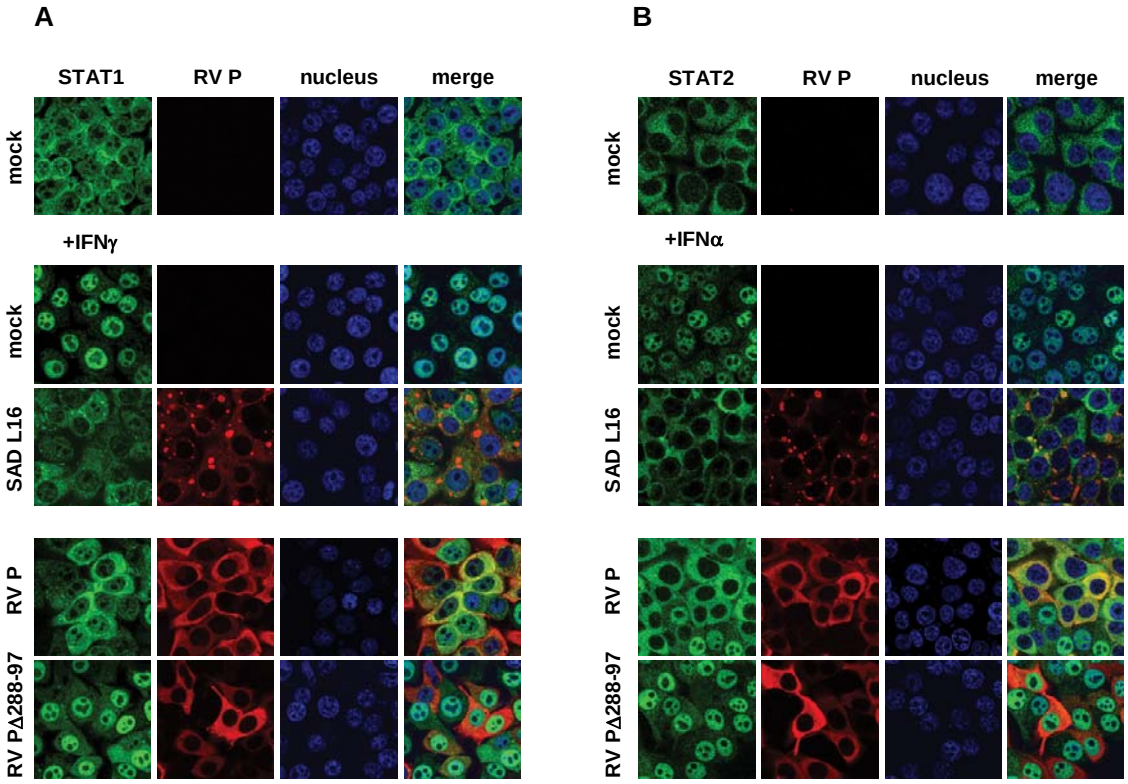

Figure 9. Cytoplasmic retention of IFN-activated STAT1 (A) and STAT2 (B) in RV infected (SAD L16) or P-expressing (RV P) HEp-2 cells. Cells were stimulated with IFN-γ or IFN-α for 45 min at 24 h post infection or transfection, and stained with the indicated antibodies. In contrast to RV, or authentic RV P protein, a deletion mutant lacking the carboxyterminal 10 aa (RV PΔ288-297) is not able to prevent nuclear import of STATs following IFN treatment.

Surprisingly, a direct association of P with STAT1 or STAT2 was not apparent in RV-infected cells or in cells expressing P from transfected plasmids. Since nuclear shuttling of non-activated STATs was not affected, in contrast to IFN-induced nuclear import of STATs, the hypothesis emerged that P might bind selectively to the tyrosine-activated isoforms of STAT1 and STAT2. I could verify this hypothesis by co-precipitation experiments involving cell extracts from IFN-stimulated and non-stimulated cells. Precipitation of STATs was only possible after activation through IFN (Figure 10). The presence of tyrosine-phosphorylated STATs in the precipitates strongly argues in favor of P binding exclusively to tyrosine-phosphorylated STATs. I could further show

that recognition of activated STAT2 is independent of STAT1, as shown by co-precipitation experiments using U3A cells that lack STAT1 (McKendry et al., 1991). Recognition and precipitation of pY689-STAT2 with RV P appears to be very specific, as suggested by the precipitation of these molecules from cell extracts of IFN-γ-stimulated cells, in which they were not detectable by Western blot, or were present in very low amounts among a bulk of non-phosphorylated STAT2. The possibility of a basic low level affinity of P to STATs was recently suggested by a paper (Vidy et al., 2005) in which an interaction of P and STAT1 was indicated in yeast-two-hybrid experiments. Under physiological conditions, however, interaction of RV P with non-phosphorylated STATs was not detectable. This is therefore the first example of a viral IFN antagonist acting in a "conditional" manner and targeting the activated isoform of a transcription factor (**Brzózka *et al*, 2006)** (Figure 11).

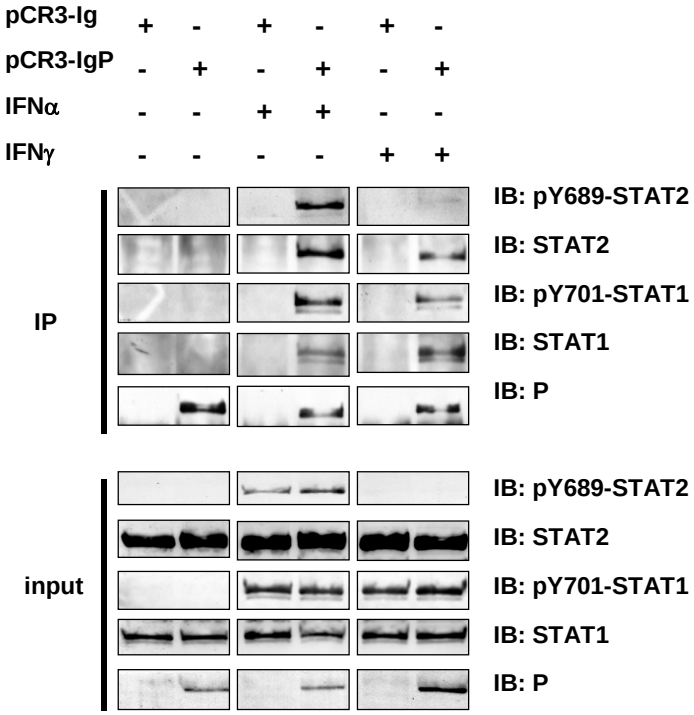

Figure 10. RV P interacts with STATs in an IFN-dependent manner. HEK293 cells were transfected with plasmids encoding immunoglobulin (Ig)-tagged P (pCR3-IgP), or the Ig moiety alone (pCR3-Ig). Prior to extraction and precipitation with Ig-binding Sepharose-A beads, cells were treated with IFN-α or IFN-γ as indicated, or were mock-treated. Precipitates (IP) and 3% of cell extracts (input) were analyzed by Western blot with the indicated antibodies. Only from IFN-treated cells STATs were co-precipitated with Ig-P.

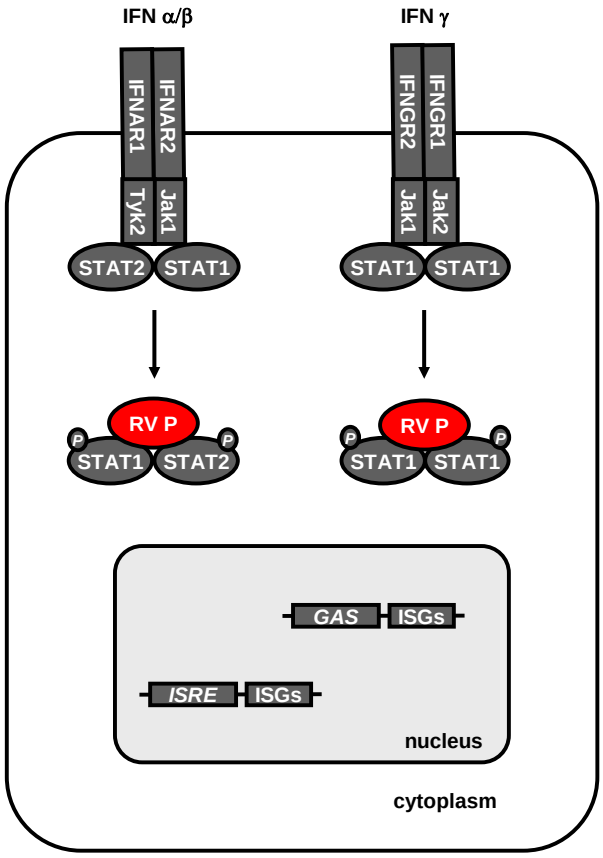

Figure 11. Inhibition of IFN signaling by RV P. Binding of IFNs to IFN receptors results in phosphorylation of tyrosine residues in STAT1 and STAT2 by Janus kinases. RV P specifically binds to the tyrosine-phosphorylated isoforms of STAT1 and STAT2 and precludes their nuclear import.

Additionally, the C-terminal 10 aa residues of RV P are responsible for STAT1 and STAT2 binding, as I could show by analysis of P deletion mutants, whereas the above described internal “TBK1-inhibiting” domain is not important. These findings further confirm that the inhibition of IFN induction and of IFN signaling are two genetically independent functions of RV P. Interestingly, the 10 aa residues responsible for STAT binding lie within a domain that has been described to interact with promyelocytic leukemia protein (PML) (Blondel et al., 2002). Although not suggested by the authors, interaction of PML with RV P could be one of the means to constrict virus growth by the host. A competition between PML and STAT in binding to the C-terminal domain of P could result in lack of IFN signaling inhibition, establishment of the antiviral state and elimination of RV from the cell.

The inability of rabies virus to prevent early IFN synthesis triggered by the IRAK pathway in certain tissues or cell types (Nakamichi et al., 2005; Nakamichi et al., 2004; Prehaud et al., 2005; Wang et al., 2005; Lafon, 2005) has to be compensated by the capability to preclude IFN signaling, in order to support virus growth. The outcome of the

rabies disease seems to depend on both innate and adaptive immune response. The group of Fu proposed that pathogenic rabies viruses evade host innate immune and antiviral response (Wang et al., 2005). *In vivo* experiments using different knock-out mice revealed that the rabies virus specific antibody response is an absolute requirement for recovery upon infection with attenuated strains, as shown by a lethal outcome of infection in mice lacking B cells (Hooper et al., 1998). Also inflammation and infiltrating T cells have been reported to play a role in controlling RV spread in the CNS (Camelo et al., 2000; Baloul and Lafon, 2003). Interestingly, IFNAR-/- or IFNGR-/- mice (lacking either IFN-α/β receptor or IFN-γ receptor), did not succumb to infection with a highly attenuated rabies strain, but the virus could be detected for a longer period in the brain, in comparison to wt mice. *In vivo* experiments in knock-out mice lacking IFNAR, IFNGR or both, are currently being performed with recombinant viruses generated in this work. Especially interesting is the outcome of the SAD ΔPLP infection in single and double IFN receptor knock-out mice. Since IFN-β, and in particular IFN-γ has a major role in the non-cytotoxic clearance of viruses from neurons and the CNS (Griffin, 2003; Burdeinick-Kerr and Griffin, 2005), it is expected that the ability of the wt SAD L16 RV to counteract IFN-α/β and IFN-γ signaling is crucial for RV infection in wt mice. This working hypothesis, can be verified by showing that SAD ΔPLP is able to establish successful infection only in IFN receptor knock-out mice, but not in wt mice.

4.3 Concluding remarks

The work presented here reveals a previously not appreciated role of the RV P protein. RV P was identified as an effective inhibitor of the host interferon system, which is not only the critical first line of defense against viruses but also, as it turned out more recently, a central stimulator and modulator of the adaptive immune response.

RV P is the first specific IFN antagonist of a rhabdovirus described. The closely related and intensely investigated VSV, which is a fast growing virus, causes an early general host cell shut down, thereby killing all host cell responses. This is due to the activity of the VSV matrix (M) protein. The more slowly growing RV depends on the

integrity of cells to reach its final destination, the CNS and therefore must have means to specifically target the antiviral host response.

With respect to the need to specifically counteract IFN, RV is therefore more similar to the more distantly related paramyxoviruses. Paramyxoviruses may afford separate proteins for counteracting IFN, either by encoding proteins from extra genes, or from polycistronic P genes encoding a variety of “accessory” proteins which are active in either counteracting IFN induction or IFN signaling. The combination of polymerase-cofactor, N/RNA chaperone-, IRF inhibition, and STAT inhibitory functions as shown here for the authentic P protein is unique and demonstrates that even viruses with a small coding capacity may encode the full set of functions required for successfully counteracting the host response.

The inhibitory activities of RV P were demonstrated in the context of recombinant viruses, using reverse genetics. The availability of viable recombinant viruses deficient for IFN escape functions will allow to dissect the RV P functions and their importance for RV virulence and pathogenicity *in vivo*.

5 SUMMARY

Interferons are the key cytokines of innate immunity and represent the first line of defense against invading viruses. By activating immediate antiviral mechanisms and stimulating the adaptive immune response, interferon signaling is decisive for the outcome of disease and virus clearance. The work presented in this thesis reveals a central role of the phosphoprotein P of rabies virus (*Rhabdoviridae* family), known as a polymerase cofactor, as an inhibitor of the host interferon system.

Counter-mechanism to escape form recognition by the immune system were previously unknown for the neurotropic rabies virus, which is characterized by the highest case-fatality ratio. In my work I have shown that rabies virus (strain SAD L16) is able to prevent both the production IFN-α/β and the effector functions of IFN-α/β and IFN-γ. The factor responsible is the viral phosphoprotein P. P interferes with transcriptional activation of IFN-α/β by preventing phosphorylation of the essential transcription factors IRF3 and IRF7 by their kinases TBK1 and IKKε. Unphosphorylated IRFs are unable to dimerize and fail to enter the nucleus. In addition, rabies virus P prevents IFN-mediated JAK/STAT signaling and the expression of IFN-stimulated genes which include a broad spectrum of antiviral and immune regulatory genes. The inhibition of JAK/STAT signaling by P involves a unique mechanism, namely, specific binding of the tyrosine-phosphorylated STAT1 and STAT2 isoforms and their retention in the cytoplasm. The inhibitory activities of RV P on IFN induction and signaling are independent functions, as shown by site-directed mutagenesis of P and identification of different short amino acid stretches required for either function.

Importantly, the inhibitory activities of P were demonstrated in the context of recombinant viruses. Using reverse genetics, a rabies virus was constructed, in which P expression was “knocked down” by moving the P gene to a promoter-distal position of the genome (SAD ΔPLP). This virus caused efficient IFNα/β production in infected cells and upregulation of interferon stimulated genes. The IFN sensitivity of SAD ΔPLP was confirmed in cell culture and is now being studied in animal experiments including IFN receptor knock of mice, to verify the relevance of P functions *in vivo*. The described work contributes to the understanding of host responses to virus infections in general and of

rabies virus pathogenicity in particular. In addition, viruses with modified IFN antagonists provide interesting opportunities for development of attenuated vaccines and vectors.

6 ZUSAMMENFASSUNG

Interferone sind Schlüssel-Zytokine des angeborenen Immunsystems und stellen die erste Hürde für eindringende Viren dar. Durch die Aktivierung von direkten antiviralen Mechanismen und die Stimulierung des adaptiven Immunsystems ist die Funktion der Interferone entscheidend für die Ausbildung der Krankheit oder die Eliminierung der Viren. In der vorgelegten Arbeit wird die zentrale Rolle des Phosphoproteins des Tollwutvirus (Rabies virus, Fam. *Rhabdoviridae*) als Modulator des Interferonsystems aufgeklärt.

Bisher waren die Mechanismen unbekannt, mit deren Hilfe das neurotrope Tollwutvirus der Erkennung durch das Immunsystem entgegenwirken kann. In dieser Arbeit konnte ich zeigen, dass das Tollwutvirus (Stamm SAD L16) sowohl die Produktion von Interferon a/b als auch die Effekte von Interferon a/b und Interferon g hemmen kann. Der verantwortliche virale Faktor ist in beiden Fällen das Phosphoprotein P. Das P Protein verhindert die Serin-Phosphorylierung und damit der Aktivierung der entscheidenden IFN Transkriptionsfaktoren IRF3 und IRF7 durch deren Kinasen TBK1 und IKKε. Nicht phosphorylierte IRFs sind nicht imstande zu dimerisieren und in den Zellkern zu gelangen. Darüber hinaus ist P in der Lage, IFN-vermittelte JAK-STAT Signalübertragungswege zu blockieren und damit die Expression von IFN-stimulierten Genen mit antiviraler und immunmodulierenden Funktionen zu verhindern. Die Hemmung der JAK-STAT Signalübertragung durch P erfolgt durch einen bisher einzigartigen Mechanismus, die spezifische Bindung der tyrosin-phosphorylierten STAT1 und STAT2 Isoformen und deren Retention im Zytoplasma. Die inhibitorische Aktivität des P Proteins auf die IFN Induktion und die JAK-STAT Signaltransduktion sind genetisch unabhängige Funktionen. Dies konnte durch ortsgerichtete Mutagenese und die Identifizierung von P Mutanten mit Defekten in jeweils einer der Funktionen bestätigt werden.

Die inhibitorischen Funktionen von P konnten darüber hinaus im Viruskontext bestätigt werden. Mit Hilfe der "reversen Genetik" konnte ein rekombinantes Tollwutvirus hergestellt werden (SAD ΔPLP), in dem die Expression des P Proteins durch die Translokation des P Gens an eine Promotor-distale Position wesentlich reduziert war

(SAD ΔPLP; Genomorganisation 3'-N-M-G-L-P-5'). Dieses Virus verursachte eine effiziente Induktion von IFN in infizierten Zellen sowie die Induktion von IFN-stimulierten Genen. Die in der Zellkultur bestätigte Sensitivität von SAD ΔLP gegenüber IFN wurde in der Zellkultur bestätigt und wird jetzt in Tierexperimenten, u.a. in wt und IFN Rezeptor-KO Mäusen, weiter analysiert, um die Relevanz der Funktionen von P *in vivo* zu bestätigen. Die vorliegende Arbeit trägt zum Verständnis der Immun-Antwort gegenüber Viren bei, insbesondere gegenüber neurotropen Viren wie dem Tollwutvirus. Viren mit modifizierten IFN Antagonisten wie hier beschrieben stellen darüber hinaus attraktive Kandidaten zur Entwicklung von attenuierten Lebendvakzinen und Vektoren dar.

7 REFERENCE LIST

Aaronson,D.S. and Horvath,C.M. (2002). A road map for those who don't know JAK-STAT. Science *296*, 1653-1655.

Ahmed,M. and Lyles,D.S. (1998). Effect of vesicular stomatitis virus matrix protein on transcription directed by host RNA polymerases I, II, and III. J Virol *72*, 8413-8419.

Ahmed,M., McKenzie,M.O., Puckett,S., Hojnacki,M., Poliquin,L., and Lyles,D.S. (2003). Ability of the matrix protein of vesicular stomatitis virus to suppress beta interferon gene expression is genetically correlated with the inhibition of host RNA and protein synthesis. J Virol *77*, 4646-4657.

Alcami,A. and Smith,G.L. (1996). Receptors for gamma-interferon encoded by poxviruses: implications for the unknown origin of vaccinia virus. Trends Microbiol. *4*, 321-326.

Andrejeva,J., Childs,K.S., Young,D.F., Carlos,T.S., Stock,N., Goodbourn,S., and Randall,R.E. (2004). The V proteins of paramyxoviruses bind the IFN-inducible RNA helicase, mda-5, and inhibit its activation of the IFN-beta promoter. Proc Natl Acad Sci U S A *101*, 17264-17269.

Andrejeva,J., Poole,E., Young,D.F., Goodbourn,S., and Randall,R.E. (2002). The p127 subunit (DDB1) of the UV-DNA damage repair binding protein is essential for the targeted degradation of STAT1 by the V protein of the paramyxovirus simian virus 5. J Virol *76*, 11379-11386.

Asselin-Paturel,C. and Trinchieri,G. (2005). Production of type I interferons: plasmacytoid dendritic cells and beyond. J Exp. Med. *202*, 461-465.

Baloul,L., Camelo,S., and Lafon,M. (2004). Up-regulation of Fas ligand (FasL) in the central nervous system: a mechanism of immune evasion by rabies virus. J Neurovirol. *10*, 372-382.

Baloul,L. and Lafon,M. (2003). Apoptosis and rabies virus neuroinvasion. Biochimie *85*, 777-788.

Basler,C.F., Mikulasova,A., Martinez-Sobrido,L., Paragas,J., Muhlberger,E., Bray,M., Klenk,H.D., Palese,P., and Garcia-Sastre,A. (2003). The Ebola virus VP35 protein inhibits activation of interferon regulatory factor 3. J Virol *77*, 7945-7956.

Basler,C.F., Wang,X., Muhlberger,E., Volchkov,V., Paragas,J., Klenk,H.D., Garcia-Sastre,A., and Palese,P. (2000). The Ebola virus VP35 protein functions as a type I IFN antagonist. Proc Natl Acad Sci U S A *97*, 12289-12294.

Blondel,D., Regad,T., Poisson,N., Pavie,B., Harper,F., Pandolfi,P.P., De The,H., and Chelbi-Alix,M.K. (2002). Rabies virus P and small P products interact directly with PML and reorganize PML nuclear bodies. Oncogene *21*, 7957-7970.

Bossert,B., Marozin,S., and Conzelmann,K.K. (2003). Nonstructural proteins NS1 and NS2 of bovine respiratory syncytial virus block activation of interferon regulatory factor 3. J Virol *77*, 8661-8668.

Brzózka,K., Finke,S., and Conzelmann,K.K. (2005). Identification of the rabies virus alpha/beta interferon antagonist: phosphoprotein P interferes with phosphorylation of interferon regulatory factor 3. J Virol *79*, 7673-7681.

Brzózka,K., Finke,S., and Conzelmann,K.K. (2006). Inhibition of Interferon Signaling by Rabies Virus Phosphoprotein P: Activation-Dependent Binding of STAT1 and STAT2. J Virol *80*, 2675-2683.

Buchholz,U.J., Finke,S., and Conzelmann,K.K. (1999). Generation of bovine respiratory syncytial virus (BRSV) from cDNA: BRSV NS2 is not essential for virus replication in tissue culture, and the human RSV leader region acts as a functional BRSV genome promoter. J Virol *73*, 251-259.

Burdeinick-Kerr,R. and Griffin,D.E. (2005). Gamma interferon-dependent, noncytolytic clearance of sindbis virus infection from neurons in vitro. J Virol *79*, 5374-5385.

Caillaud,A., Hovanessian,A.G., Levy,D.E., and Marie,I.J. (2005). Regulatory serine residues mediate phosphorylation-dependent and phosphorylation-independent activation of interferon regulatory factor 7. J Biol. Chem. *280*, 17671-17677.

Camelo,S., Lafage,M., and Lafon,M. (2000). Absence of the p55 Kd TNF-alpha receptor promotes survival in rabies virus acute encephalitis. J Neurovirol. *6*, 507-518.

Chenik,M., Chebli,K., and Blondel,D. (1995). Translation initiation at alternate in-frame AUG codons in the rabies virus phosphoprotein mRNA is mediated by a ribosomal leaky scanning mechanism. J Virol *69*, 707-712.

Chenik,M., Chebli,K., Gaudin,Y., and Blondel,D. (1994). In vivo interaction of rabies virus phosphoprotein (P) and nucleoprotein (N): existence of two N-binding sites on P protein. J Gen Virol *75 (Pt 11)*, 2889-2896.

Chenik,M., Schnell,M., Conzelmann,K.K., and Blondel,D. (1998). Mapping the interacting domains between the rabies virus polymerase and phosphoprotein. J Virol *72*, 1925-1930.

Civas,A., Genin,P., Morin,P., Lin,R., and Hiscott,J. (2005). Promoter organization of the interferon-A genes differentially affects virus-induced expression and responsiveness to TBK1 and IKKepsilon. J Biol. Chem.

Conzelmann,K.K. (2004). Reverse genetics of mononegavirales. Curr. Top. Microbiol. Immunol. *283*, 1-41.

Conzelmann,K.K. (2005). Transcriptional activation of alpha/beta interferon genes: interference by nonsegmented negative-strand RNA viruses. J Virol *79*, 5241-5248.

Deb,D.K., Sassano,A., Lekmine,F., Majchrzak,B., Verma,A., Kambhampati,S., Uddin,S., Rahman,A., Fish,E.N., and Platanias,L.C. (2003). Activation of protein kinase C delta by IFN-gamma. J Immunol. *171*, 267-273.

Dietzschold,B. (1993). Antibody-mediated clearance of viruses from the mammalian central nervous system. Trends Microbiol. *1*, 63-66.

Dietzschold,B., Kao,M., Zheng,Y.M., Chen,Z.Y., Maul,G., Fu,Z.F., Rupprecht,C.E., and Koprowski,H. (1992). Delineation of putative mechanisms involved in antibody-mediated clearance of rabies virus from the central nervous system. Proc Natl Acad Sci U S A *89*, 7252-7256.

Eriguchi,Y., Toriumi,H., and Kawai,A. (2002). Studies on the rabies virus RNA polymerase: 3. Two-dimensional electrophoretic analysis of the multiplicity of non-catalytic subunit (P protein). Microbiol. Immunol. *46*, 463-474.

Faber,M., Pulmanausahakul,R., Hodawadekar,S.S., Spitsin,S., McGettigan,J.P., Schnell,M.J., and Dietzschold,B. (2002). Overexpression of the rabies virus glycoprotein results in enhancement of apoptosis and antiviral immune response. J Virol *76*, 3374-3381.

Ferran,M.C. and Lucas-Lenard,J.M. (1997). The vesicular stomatitis virus matrix protein inhibits transcription from the human beta interferon promoter. J Virol *71*, 371-377.

Ferreon,J.C., Ferreon,A.C., Li,K., and Lemon,S.M. (2005). Molecular determinants of TRIF proteolysis mediated by the hepatitis C virus NS3/4A protease. J Biol. Chem. *280*, 20483-20492.

Finke,S., Brzózka,K., and Conzelmann,K.K. (2004). Tracking fluorescence-labeled rabies virus: enhanced green fluorescent protein-tagged phosphoprotein P supports virus gene expression and formation of infectious particles. J Virol *78*, 12333-12343.

Finke,S. and Conzelmann,K.K. (2003). Dissociation of rabies virus matrix protein functions in regulation of viral RNA synthesis and virus assembly. J Virol *77*, 12074-12082.

Finke,S. and Conzelmann,K.K. (2005). Replication strategies of rabies virus. Virus Res. *111*, 120-131.

Finke,S., Mueller-Waldeck,R., and Conzelmann,K.K. (2003). Rabies virus matrix protein regulates the balance of virus transcription and replication. J Gen Virol *84*, 1613-1621.

Fitzgerald,K.A., McWhirter,S.M., Faia,K.L., Rowe,D.C., Latz,E., Golenbock,D.T., Coyle,A.J., Liao,S.M., and Maniatis,T. (2003a). IKKepsilon and TBK1 are essential components of the IRF3 signaling pathway. Nat. Immunol. *4*, 491-496.

Fitzgerald,K.A., Rowe,D.C., Barnes,B.J., Caffrey,D.R., Visintin,A., Latz,E., Monks,B., Pitha,P.M., and Golenbock,D.T. (2003b). LPS-TLR4 signaling to IRF-3/7 and NF-kappaB involves the toll adapters TRAM and TRIF. J Exp. Med. *198*, 1043-1055.

Gigant,B., Iseni,F., Gaudin,Y., Knossow,M., and Blondel,D. (2000). Neither phosphorylation nor the amino-terminal part of rabies virus phosphoprotein is required for its oligomerization. J Gen Virol *81*, 1757-1761.

Griffin,D.E. (2003). Immune responses to RNA-virus infections of the CNS. Nat. Rev. Immunol. *3*, 493-502.

Gupta,A.K., Blondel,D., Choudhary,S., and Banerjee,A.K. (2000). The phosphoprotein of rabies virus is phosphorylated by a unique cellular protein kinase and specific isomers of protein kinase C. J Virol *74*, 91-98.

Hacker,H., Redecke,V., Blagoev,B., Kratchmarova,I., Hsu,L.C., Wang,G.G., Kamps,M.P., Raz,E., Wagner,H., Hacker,G., Mann,M., and Karin,M. (2006). Specificity in Toll-like receptor signalling through distinct effector functions of TRAF3 and TRAF6. Nature *439*, 204-207.

Hemachudha,T., Laothamatas,J., and Rupprecht,C.E. (2002). Human rabies: a disease of complex neuropathogenetic mechanisms and diagnostic challenges. Lancet Neurol. *1*, 101-109.

Hengel,H., Koszinowski,U.H., and Conzelmann,K.K. (2005). Viruses know it all: new insights into IFN networks. Trends Immunol. *26*, 396-401.

Honda,K., Ohba,Y., Yanai,H., Negishi,H., Mizutani,T., Takaoka,A., Taya,C., and Taniguchi,T. (2005a). Spatiotemporal regulation of MyD88-IRF-7 signalling for robust type-I interferon induction. Nature *434*, 1035-1040.

Honda,K., Yanai,H., Mizutani,T., Negishi,H., Shimada,N., Suzuki,N., Ohba,Y., Takaoka,A., Yeh,W.C., and Taniguchi,T. (2004). Role of a transductional-transcriptional processor complex involving MyD88 and IRF-7 in Toll-like receptor signaling. Proc Natl Acad Sci U S A *101*, 15416-15421.

Honda,K., Yanai,H., Negishi,H., Asagiri,M., Sato,M., Mizutani,T., Shimada,N., Ohba,Y., Takaoka,A., Yoshida,N., and Taniguchi,T. (2005b). IRF-7 is the master regulator of type-I interferon-dependent immune responses. Nature *434*, 772-777.

Hooper,D.C., Morimoto,K., Bette,M., Weihe,E., Koprowski,H., and Dietzschold,B. (1998). Collaboration of antibody and inflammation in clearance of rabies virus from the central nervous system. J Virol *72*, 3711-3719.

Huynh,Q.K., Kishore,N., Mathialagan,S., Donnelly,A.M., and Tripp,C.S. (2002). Kinetic mechanisms of IkappaB-related kinases (IKK) inducible IKK and TBK-1 differ from IKK-1/IKK-2 heterodimer. J Biol. Chem. *277*, 12550-12558.

Ilangumaran,S., Ramanathan,S., and Rottapel,R. (2004). Regulation of the immune system by SOCS family adaptor proteins. Semin. Immunol. *16*, 351-365.

Jackson,A.C., Warrell,M.J., Rupprecht,C.E., Ertl,H.C., Dietzschold,B., O'Reilly,M., Leach,R.P., Fu,Z.F., Wunner,W.H., Bleck,T.P., and Wilde,H. (2003). Management of rabies in humans. Clin. Infect. Dis. *36*, 60-63.

Jacob,Y., Badrane,H., Ceccaldi,P.E., and Tordo,N. (2000). Cytoplasmic dynein LC8 interacts with lyssavirus phosphoprotein. J Virol *74*, 10217-10222.

Jacob,Y., Real,E., and Tordo,N. (2001). Functional interaction map of lyssavirus phosphoprotein: identification of the minimal transcription domains. J Virol *75*, 9613-9622.

Katze,M.G., He,Y., and Gale,M., Jr. (2002). Viruses and interferon: a fight for supremacy. Nat. Rev. Immunol. *2*, 675-687.

Kawai,T., Sato,S., Ishii,K.J., Coban,C., Hemmi,H., Yamamoto,M., Terai,K., Matsuda,M., Inoue,J., Uematsu,S., Takeuchi,O., and Akira,S. (2004). Interferon-alpha induction through Toll-like receptors involves a direct interaction of IRF7 with MyD88 and TRAF6. Nat. Immunol. *5*, 1061-1068.

Kawai,T., Takahashi,K., Sato,S., Coban,C., Kumar,H., Kato,H., Ishii,K.J., Takeuchi,O., and Akira,S. (2005). IPS-1, an adaptor triggering RIG-I- and Mda5-mediated type I interferon induction. Nat. Immunol. *6*, 981-988.

Kinjyo,I., Hanada,T., Inagaki-Ohara,K., Mori,H., Aki,D., Ohishi,M., Yoshida,H., Kubo,M., and Yoshimura,A. (2002). SOCS1/JAB is a negative regulator of LPS-induced macrophage activation. Immunity *17*, 583-591.

Kishore,N., Huynh,Q.K., Mathialagan,S., Hall,T., Rouw,S., Creely,D., Lange,G., Caroll,J., Reitz,B., Donnelly,A., Boddupalli,H., Combs,R.G., Kretzmer,K., and Tripp,C.S. (2002). IKK-i and TBK-1 are enzymatically distinct from the homologous enzyme IKK-2: comparative analysis of recombinant human IKK-i, TBK-1, and IKK-2. J Biol. Chem. *277*, 13840-13847.

Kobayashi,K., Hernandez,L.D., Galan,J.E., Janeway,C.A., Jr., Medzhitov,R., and Flavell,R.A. (2002). IRAK-M is a negative regulator of Toll-like receptor signaling. Cell *110*, 191-202.

Lafon,M. (2005). Modulation of the immune response in the nervous system by rabies virus. Curr. Top. Microbiol. Immunol. *289*, 239-258.

Larsen,L. and Ropke,C. (2002). Suppressors of cytokine signalling: SOCS. APMIS *110*, 833-844.

Le May,N., Dubaele,S., Proietti,D.S., Billecocq,A., Bouloy,M., and Egly,J.M. (2004). TFIIH transcription factor, a target for the Rift Valley hemorrhagic fever virus. Cell *116*, 541-550.

Lentz,T.L., Burrage,T.G., Smith,A.L., Crick,J., and Tignor,G.H. (1982). Is the acetylcholine receptor a rabies virus receptor? Science *215*, 182-184.

Li,K., Foy,E., Ferreon,J.C., Nakamura,M., Ferreon,A.C., Ikeda,M., Ray,S.C., Gale,M., Jr., and Lemon,S.M. (2005). Immune evasion by hepatitis C virus NS3/4A protease-mediated cleavage of the Toll-like receptor 3 adaptor protein TRIF. Proc Natl Acad Sci U S A *102*, 2992-2997.

Liew,F.Y., Xu,D., Brint,E.K., and O'Neill,L.A. (2005). Negative regulation of toll-like receptor-mediated immune responses. Nat. Rev. Immunol. *5*, 446-458.

Lin,R., Heylbroeck,C., Pitha,P.M., and Hiscott,J. (1998). Virus-dependent phosphorylation of the IRF-3 transcription factor regulates nuclear translocation, transactivation potential, and proteasome-mediated degradation. Mol. Cell Biol. *18*, 2986-2996.

Lin,R., Mamane,Y., and Hiscott,J. (1999). Structural and functional analysis of interferon regulatory factor 3: localization of the transactivation and autoinhibitory domains. Mol. Cell Biol. *19*, 2465-2474.

Lin,R., Mamane,Y., and Hiscott,J. (2000). Multiple regulatory domains control IRF-7 activity in response to virus infection. J Biol. Chem. *275*, 34320-34327.

Mansell,A., Smith,R., Doyle,S.L., Gray,P., Fenner,J.E., Crack,P.J., Nicholson,S.E., Hilton,D.J., O'Neill,L.A., and Hertzog,P.J. (2006). Suppressor of cytokine signaling 1 negatively regulates Toll-like receptor signaling by mediating Mal degradation. Nat. Immunol. *7*, 148-155.

Mavrakis,M., Iseni,F., Mazza,C., Schoehn,G., Ebel,C., Gentzel,M., Franz,T., and Ruigrok,R.W. (2003). Isolation and characterisation of the rabies virus N degrees-P complex produced in insect cells. Virology *305*, 406-414.

Mavrakis,M., McCarthy,A.A., Roche,S., Blondel,D., and Ruigrok,R.W. (2004). Structure and function of the C-terminal domain of the polymerase cofactor of rabies virus. J Mol. Biol. *343*, 819-831.

McKendry,R., John,J., Flavell,D., Muller,M., Kerr,I.M., and Stark,G.R. (1991). High-frequency mutagenesis of human cells and characterization of a mutant unresponsive to both alpha and gamma interferons. Proc Natl Acad Sci U S A *88*, 11455-11459.

Mebatsion,T. (2001). Extensive attenuation of rabies virus by simultaneously modifying the dynein light chain binding site in the P protein and replacing Arg333 in the G protein. J Virol *75*, 11496-11502.

Meyer,T. and Vinkemeier,U. (2004). Nucleocytoplasmic shuttling of STAT transcription factors. Eur. J Biochem. *271*, 4606-4612.

Meylan,E., Curran,J., Hofmann,K., Moradpour,D., Binder,M., Bartenschlager,R., and Tschopp,J. (2005). Cardif is an adaptor protein in the RIG-I antiviral pathway and is targeted by hepatitis C virus. Nature *437*, 1167-1172.

Mori,M., Yoneyama,M., Ito,T., Takahashi,K., Inagaki,F., and Fujita,T. (2004). Identification of Ser-386 of interferon regulatory factor 3 as critical target for inducible phosphorylation that determines activation. J Biol. Chem. *279*, 9698-9702.

Morimoto,K., Foley,H.D., McGettigan,J.P., Schnell,M.J., and Dietzschold,B. (2000). Reinvestigation of the role of the rabies virus glycoprotein in viral pathogenesis using a reverse genetics approach. J Neurovirol. *6*, 373-381.

Morimoto,K., Hooper,D.C., Spitsin,S., Koprowski,H., and Dietzschold,B. (1999). Pathogenicity of different rabies virus variants inversely correlates with apoptosis and rabies virus glycoprotein expression in infected primary neuron cultures. J Virol *73*, 510-518.

Najarro,P., Traktman,P., and Lewis,J.A. (2001). Vaccinia virus blocks gamma interferon signal transduction: viral VH1 phosphatase reverses Stat1 activation. J Virol *75*, 3185-3196.

Nakamichi,K., Inoue,S., Takasaki,T., Morimoto,K., and Kurane,I. (2004). Rabies virus stimulates nitric oxide production and CXC chemokine ligand 10 expression in macrophages through activation of extracellular signal-regulated kinases 1 and 2. J Virol *78*, 9376-9388.

Nakamichi,K., Saiki,M., Sawada,M., Takayama-Ito,M., Yamamuro,Y., Morimoto,K., and Kurane,I. (2005). Rabies virus-induced activation of mitogen-activated protein kinase and NF-kappaB signaling pathways regulates expression of CXC and CC chemokine ligands in microglia. J Virol *79*, 11801-11812.

Nisole,S., Stoye,J.P., and Saib,A. (2005). TRIM family proteins: retroviral restriction and antiviral defence. Nat. Rev. Microbiol. *3*, 799-808.

Oganesyan,G., Saha,S.K., Guo,B., He,J.Q., Shahangian,A., Zarnegar,B., Perry,A., and Cheng,G. (2006). Critical role of TRAF3 in the Toll-like receptor-dependent and -independent antiviral response. Nature *439*, 208-211.

Palosaari,H., Parisien,J.P., Rodriguez,J.J., Ulane,C.M., and Horvath,C.M. (2003). STAT protein interference and suppression of cytokine signal transduction by measles virus V protein. J Virol *77*, 7635-7644.

Parisien,J.P., Lau,J.F., and Horvath,C.M. (2002a). STAT2 acts as a host range determinant for species-specific paramyxovirus interferon antagonism and simian virus 5 replication. J Virol *76*, 6435-6441.

Parisien,J.P., Lau,J.F., Rodriguez,J.J., Ulane,C.M., and Horvath,C.M. (2002b). Selective STAT protein degradation induced by paramyxoviruses requires both STAT1 and STAT2 but is independent of alpha/beta interferon signal transduction. J Virol *76*, 4190-4198.

Perry,L.L. and Lodmell,D.L. (1991). Role of CD4+ and CD8+ T cells in murine resistance to street rabies virus. J Virol *65*, 3429-3434.

Platanias,L.C. (2005). Mechanisms of type-I- and type-II-interferon-mediated signalling. Nat. Rev. Immunol. *5*, 375-386.

Prehaud,C., Lay,S., Dietzschold,B., and Lafon,M. (2003). Glycoprotein of nonpathogenic rabies viruses is a key determinant of human cell apoptosis. J Virol *77*, 10537-10547.

Prehaud,C., Megret,F., Lafage,M., and Lafon,M. (2005). Virus Infection Switches TLR-3-Positive Human Neurons To Become Strong Producers of Beta Interferon. J Virol *79*, 12893-12904.

Qin,B.Y., Liu,C., Lam,S.S., Srinath,H., Delston,R., Correia,J.J., Derynck,R., and Lin,K. (2003). Crystal structure of IRF-3 reveals mechanism of autoinhibition and virus-induced phosphoactivation. Nat. Struct. Biol. *10*, 913-921.

Rasalingam,P., Rossiter,J.P., Mebatsion,T., and Jackson,A.C. (2005). Comparative pathogenesis of the SAD-L16 strain of rabies virus and a mutant modifying the dynein light chain binding site of the rabies virus phosphoprotein in young mice. Virus Res. *111*, 55-60.

Raux,H., Flamand,A., and Blondel,D. (2000). Interaction of the rabies virus P protein with the LC8 dynein light chain. J Virol *74*, 10212-10216.

Rodriguez,J.J., Cruz,C.D., and Horvath,C.M. (2004). Identification of the nuclear export signal and STAT-binding domains of the Nipah virus V protein reveals mechanisms underlying interferon evasion. J Virol *78*, 5358-5367.

Rodriguez,J.J. and Horvath,C.M. (2004). Host evasion by emerging paramyxoviruses: Hendra virus and Nipah virus v proteins inhibit interferon signaling. Viral Immunol. *17*, 210-219.

Rodriguez,J.J., Parisien,J.P., and Horvath,C.M. (2002). Nipah virus V protein evades alpha and gamma interferons by preventing STAT1 and STAT2 activation and nuclear accumulation. J Virol *76*, 11476-11483.

Rothenfusser,S., Goutagny,N., DiPerna,G., Gong,M., Monks,B.G., Schoenemeyer,A., Yamamoto,M., Akira,S., and Fitzgerald,K.A. (2005). The RNA helicase Lgp2 inhibits TLR-independent sensing of viral replication by retinoic acid-inducible gene-I. J Immunol. *175*, 5260-5268.

Rupprecht,C.E., Hanlon,C.A., and Hemachudha,T. (2002). Rabies re-examined. Lancet Infect. Dis. *2*, 327-343.

Samuel,C.E. (2001). Antiviral actions of interferons. Clin. Microbiol. Rev. *14*, 778-809, table.

Sarkar,S.N., Peters,K.L., Elco,C.P., Sakamoto,S., Pal,S., and Sen,G.C. (2004). Novel roles of TLR3 tyrosine phosphorylation and PI3 kinase in double-stranded RNA signaling. Nat. Struct. Mol. Biol. *11*, 1060-1067.

Sarkar,S.N. and Sen,G.C. (2004). Novel functions of proteins encoded by viral stress-inducible genes. Pharmacol. Ther. *103*, 245-259.

Sarmento,L., Li,X.Q., Howerth,E., Jackson,A.C., and Fu,Z.F. (2005). Glycoprotein-mediated induction of apoptosis limits the spread of attenuated rabies viruses in the central nervous system of mice. J Neurovirol. *11*, 571-581.

Sato,M., Suemori,H., Hata,N., Asagiri,M., Ogasawara,K., Nakao,K., Nakaya,T., Katsuki,M., Noguchi,S., Tanaka,N., and Taniguchi,T. (2000). Distinct and essential roles of transcription factors IRF-3 and IRF-7 in response to viruses for IFN-alpha/beta gene induction. Immunity *13*, 539-548.

Sato,S., Sugiyama,M., Yamamoto,M., Watanabe,Y., Kawai,T., Takeda,K., and Akira,S. (2003). Toll/IL-1 receptor domain-containing adaptor inducing IFN-beta (TRIF) associates with TNF receptor-associated factor 6 and TANK-binding kinase 1, and activates two distinct transcription factors, NF-kappa B and IFN-regulatory factor-3, in the Toll-like receptor signaling. J Immunol. *171*, 4304-4310.

Schlender,J., Hornung,V., Finke,S., Gunthner-Biller,M., Marozin,S., Brzózka,K., Moghim,S., Endres,S., Hartmann,G., and Conzelmann,K.K. (2005). Inhibition of toll-like receptor 7- and 9-mediated alpha/beta interferon production in human plasmacytoid dendritic cells by respiratory syncytial virus and measles virus. J Virol *79*, 5507-5515.

Schnell,M.J., Mebatsion,T., and Conzelmann,K.K. (1994). Infectious rabies viruses from cloned cDNA. EMBO J *13*, 4195-4203.

Servant,M.J., ten Oever,B., LePage,C., Conti,L., Gessani,S., Julkunen,I., Lin,R., and Hiscott,J. (2001). Identification of distinct signaling pathways leading to the phosphorylation of interferon regulatory factor 3. J Biol. Chem. *276*, 355-363.

Seth,R.B., Sun,L., Ea,C.K., and Chen,Z.J. (2005). Identification and characterization of MAVS, a mitochondrial antiviral signaling protein that activates NF-kappaB and IRF 3. Cell *122*, 669-682.

Sharma,S., tenOever,B.R., Grandvaux,N., Zhou,G.P., Lin,R., and Hiscott,J. (2003). Triggering the interferon antiviral response through an IKK-related pathway. Science *300*, 1148-1151.

Shaw,M.L., Garcia-Sastre,A., Palese,P., and Basler,C.F. (2004). Nipah virus V and W proteins have a common STAT1-binding domain yet inhibit STAT1 activation from the cytoplasmic and nuclear compartments, respectively. J Virol *78*, 5633-5641.

Shoji,Y., Inoue,S., Nakamichi,K., Kurane,I., Sakai,T., and Morimoto,K. (2004). Generation and characterization of P gene-deficient rabies virus. Virology *318*, 295-305.

Spann,K.M., Tran,K.C., Chi,B., Rabin,R.L., and Collins,P.L. (2004). Suppression of the induction of alpha, beta, and lambda interferons by the NS1 and NS2 proteins of human respiratory syncytial virus in human epithelial cells and macrophages [corrected]. J Virol *78*, 4363-4369.

Spann,K.M., Tran,K.C., and Collins,P.L. (2005). Effects of nonstructural proteins NS1 and NS2 of human respiratory syncytial virus on interferon regulatory factor 3, NF-kappaB, and proinflammatory cytokines. J Virol *79*, 5353-5362.

Spiegel,M., Pichlmair,A., Martinez-Sobrido,L., Cros,J., Garcia-Sastre,A., Haller,O., and Weber,F. (2005). Inhibition of Beta interferon induction by severe acute respiratory syndrome coronavirus suggests a two-step model for activation of interferon regulatory factor 3. J Virol *79*, 2079-2086.

Stack,J., Haga,I.R., Schroder,M., Bartlett,N.W., Maloney,G., Reading,P.C., Fitzgerald,K.A., Smith,G.L., and Bowie,A.G. (2005). Vaccinia virus protein A46R targets multiple Toll-like-interleukin-1 receptor adaptors and contributes to virulence. J Exp. Med. *201*, 1007-1018.

Su,X., Li,S., Meng,M., Qian,W., Xie,W., Chen,D., Zhai,Z., and Shu,H.B. (2006). TNF receptor-associated factor-1 (TRAF1) negatively regulates Toll/IL-1 receptor domain-containing adaptor inducing IFN-beta (TRIF)-mediated signaling. Eur. J Immunol. *36*, 199-206.

Takeuchi,K., Kadota,S.I., Takeda,M., Miyajima,N., and Nagata,K. (2003). Measles virus V protein blocks interferon (IFN)-alpha/beta but not IFN-gamma signaling by inhibiting STAT1 and STAT2 phosphorylation. FEBS Lett. *545*, 177-182.

tenOever,B.R., Sharma,S., Zou,W., Sun,Q., Grandvaux,N., Julkunen,I., Hemmi,H., Yamamoto,M., Akira,S., Yeh,W.C., Lin,R., and Hiscott,J. (2004). Activation of TBK1 and IKKvarepsilon kinases by vesicular stomatitis virus infection and the role of viral ribonucleoprotein in the development of interferon antiviral immunity. J Virol *78*, 10636-10649.

Thoulouze,M.I., Lafage,M., Schachner,M., Hartmann,U., Cremer,H., and Lafon,M. (1998). The neural cell adhesion molecule is a receptor for rabies virus. J Virol *72*, 7181-7190.

Tojima,Y., Fujimoto,A., Delhase,M., Chen,Y., Hatakeyama,S., Nakayama,K., Kaneko,Y., Nimura,Y., Motoyama,N., Ikeda,K., Karin,M., and Nakanishi,M. (2000). NAK is an IkappaB kinase-activating kinase. Nature *404*, 778-782.

Tuffereau,C., Benejean,J., Blondel,D., Kieffer,B., and Flamand,A. (1998). Low-affinity nerve-growth factor receptor (P75NTR) can serve as a receptor for rabies virus. EMBO J *17*, 7250-7259.

Tuffereau,C., Desmezieres,E., Benejean,J., Jallet,C., Flamand,A., Tordo,N., and Perrin,P. (2001). Interaction of lyssaviruses with the low-affinity nerve-growth factor receptor p75NTR. J Gen Virol *82*, 2861-2867.

Uddin,S., Sassano,A., Deb,D.K., Verma,A., Majchrzak,B., Rahman,A., Malik,A.B., Fish,E.N., and Platanias,L.C. (2002). Protein kinase C-delta (PKC-delta) is activated by type I interferons and mediates phosphorylation of Stat1 on serine 727. J Biol. Chem. *277*, 14408-14416.

Uematsu,S., Sato,S., Yamamoto,M., Hirotani,T., Kato,H., Takeshita,F., Matsuda,M., Coban,C., Ishii,K.J., Kawai,T., Takeuchi,O., and Akira,S. (2005). Interleukin-1 receptor-associated kinase-1 plays an essential role for Toll-like receptor (TLR)7- and TLR9-mediated interferon-{alpha} induction. J Exp. Med. *201*, 915-923.

Ulane,C.M., Kentsis,A., Cruz,C.D., Parisien,J.P., Schneider,K.L., and Horvath,C.M. (2005). Composition and assembly of STAT-targeting ubiquitin ligase complexes: paramyxovirus V protein carboxyl terminus is an oligomerization domain. J Virol *79*, 10180-10189.

Unterstab,G., Ludwig,S., Anton,A., Planz,O., Dauber,B., Krappmann,D., Heins,G., Ehrhardt,C., and Wolff,T. (2005). Viral targeting of the interferon-{beta}-inducing Traf family member-associated NF-{kappa}B activator (TANK)-binding kinase-1. Proc Natl Acad Sci U S A.

Vidy,A., Chelbi-Alix,M., and Blondel,D. (2005). Rabies virus P protein interacts with STAT1 and inhibits interferon signal transduction pathways. J Virol *79*, 14411-14420.

Vinkemeier,U. (2004). Getting the message across, STAT! Design principles of a molecular signaling circuit. J Cell Biol. *167*, 197-201.

Wald,D., Qin,J., Zhao,Z., Qian,Y., Naramura,M., Tian,L., Towne,J., Sims,J.E., Stark,G.R., and Li,X. (2003). SIGIRR, a negative regulator of Toll-like receptor-interleukin 1 receptor signaling. Nat. Immunol. *4*, 920-927.

Wang,Z.W., Sarmento,L., Wang,Y., Li,X.Q., Dhingra,V., Tseggai,T., Jiang,B., and Fu,Z.F. (2005). Attenuated Rabies Virus Activates, while Pathogenic Rabies Virus Evades, the Host Innate Immune Responses in the Central Nervous System. J Virol *79*, 12554-12565.

Warrell,M.J. and Warrell,D.A. (2004). Rabies and other lyssavirus diseases. Lancet *363*, 959-969.

Weber,F., Kochs,G., and Haller,O. (2004). Inverse interference: how viruses fight the interferon system. Viral Immunol. *17*, 498-515.

Xu,L.G., Wang,Y.Y., Han,K.J., Li,L.Y., Zhai,Z., and Shu,H.B. (2005). VISA is an adapter protein required for virus-triggered IFN-beta signaling. Mol. Cell *19*, 727-740.

Yamamoto,M., Sato,S., Hemmi,H., Hoshino,K., Kaisho,T., Sanjo,H., Takeuchi,O., Sugiyama,M., Okabe,M., Takeda,K., and Akira,S. (2003a). Role of adaptor TRIF in the MyD88-independent toll-like receptor signaling pathway. Science *301*, 640-643.

Yamamoto,M., Sato,S., Hemmi,H., Uematsu,S., Hoshino,K., Kaisho,T., Takeuchi,O., Takeda,K., and Akira,S. (2003b). TRAM is specifically involved in the Toll-like receptor 4-mediated MyD88-independent signaling pathway. Nat. Immunol. *4*, 1144-1150.

Yokota,S., Saito,H., Kubota,T., Yokosawa,N., Amano,K., and Fujii,N. (2003). Measles virus suppresses interferon-alpha signaling pathway: suppression of Jak1 phosphorylation and association of viral accessory proteins, C and V, with interferon-alpha receptor complex. Virology *306*, 135-146.

Yoneyama,M., Kikuchi,M., Matsumoto,K., Imaizumi,T., Miyagishi,M., Taira,K., Foy,E., Loo,Y.M., Gale,M., Jr., Akira,S., Yonehara,S., Kato,A., and Fujita,T. (2005). Shared and unique functions of the DExD/H-box helicases RIG-I, MDA5, and LGP2 in antiviral innate immunity. J Immunol. *175*, 2851-2858.

Yoneyama,M., Kikuchi,M., Natsukawa,T., Shinobu,N., Imaizumi,T., Miyagishi,M., Taira,K., Akira,S., and Fujita,T. (2004). The RNA helicase RIG-I has an essential function in double-stranded RNA-induced innate antiviral responses. Nat. Immunol. *5*, 730-737.

Yoneyama,M., Suhara,W., and Fujita,T. (2002). Control of IRF-3 activation by phosphorylation. J Interferon Cytokine Res. *22*, 73-76.

Yoneyama,M., Suhara,W., Fukuhara,Y., Fukuda,M., Nishida,E., and Fujita,T. (1998). Direct triggering of the type I interferon system by virus infection: activation of a transcription factor complex containing IRF-3 and CBP/p300. EMBO J *17*, 1087-1095.

Yuan,H., Puckett,S., and Lyles,D.S. (2001). Inhibition of host transcription by vesicular stomatitis virus involves a novel mechanism that is independent of phosphorylation of TATA-binding protein (TBP) or association of TBP with TBP-associated factor subunits. J Virol *75*, 4453-4458.

Yuan,H., Yoza,B.K., and Lyles,D.S. (1998). Inhibition of host RNA polymerase II-dependent transcription by vesicular stomatitis virus results from inactivation of TFIID. Virology *251*, 383-392.

Zimmermann,A., Trilling,M., Wagner,M., Wilborn,M., Bubic,I., Jonjic,S., Koszinowski,U., and Hengel,H. (2005). A cytomegaloviral protein reveals a dual role for STAT2 in IFN-{gamma} signaling and antiviral responses. J Exp. Med. *201*, 1543-1553.

8 APPENDIX:

8.1 Articles enclosed as a part of the cumulative doctoral thesis:

I. **Brzózka,K**., Finke,S., and Conzelmann,K.K. (2006). Inhibition of Interferon Signaling by Rabies Virus Phosphoprotein P: Activation-Dependent Binding of STAT1 and STAT2. J Virol *80*, 2675-2683.

II. **Brzózka,K**., Finke,S., and Conzelmann,K.K. (2005). Identification of the rabies virus alpha/beta interferon antagonist: phosphoprotein P interferes with phosphorylation of interferon regulatory factor 3. J Virol *79*, 7673-7681.

III. Schlender,J., Hornung,V., Finke,S., Gunthner-Biller,M., Marozin,S., **Brzózka,K**., Moghim,S., Endres,S., Hartmann,G., and Conzelmann,K.K. (2005). Inhibition of toll-like receptor 7- and 9-mediated alpha/beta interferon production in human plasmacytoid dendritic cells by respiratory syncytial virus and measles virus. J Virol *79*, 5507-5515.

IV. Finke,S., **Brzózka,K**., and Conzelmann,K.K. (2004). Tracking fluorescence-labeled rabies virus: enhanced green fluorescent protein-tagged phosphoprotein P supports virus gene expression and formation of infectious particles. J Virol *78*, 12333-12343.

8.2 Acknowledgements

I would like to sincerely thank my supervisor, prof. Karl Klaus Conzelmann, for his trust in my work and enormous support in hard times. I am grateful for the scientifical freedom I had, his big interest in my project and plenty of helpful discussions.

I particularly appreciate my PhD supervisor PD Dr. Bettina Kempkes, for critically reading the manuscript and representing me at the faculty.

I am grateful to all my lab members, for the atmosphere that they have created. And to personalize it a little bit, I am especially grateful to Stefan for his big help with confocal laser microscopy and starting the IFN project. My “lunch group” : Yvonne, Christian, Anika and Sergej for your company and refreshing breaks from the everyday lab life. Christine and Adrianne for their sense of humor and last but not least, I would like to truly thank Nadin for her patience and enormous help with the cloning, cell culture and all the other things I had to struggle with.

My special thanks goes to my friends. The Munich part, Maciek, Iwona, Guergana, Laura and others, for all the fun we had, all the evenings in my kitchen, that will stay in my memories as the best pub in Munich. And my polish part, Marta, Asia, Milosz and rest, for the phone calls reminding me of their presence in my life and ongoing support.

My great flat mates deserve a special paragraph: Mustafa, Paolo and Aysegül, but especially Lutz and Helene. Thanks to you and the great vibes you have been generating, I could call our apartment home for almost three years.

Dziękuję moim rodzicom i siostrze. To ich wsparcie i przewodnictwo przez wszystkie lata pozwoliło mi ukończyć doktorat. W dowód mojej dozgonnej wdzięczności za ich miłość, właśnie mojej rodzinie dedykuje tę pracę...

8.3 Curriculum Vitae

Personal information **Krzysztof Brzózka**

Date of birth: 28.12.1979
Place of birth: Sieradz, Poland
Nationality: polish

Education

07.2003 - 04.2006	doctoral studies at the Ludwig-Maximilians-University, Max von Pettenkofer Insitute & Genzentrum, Munich, Germany
04.2003	university graduation with a Master of Science degree in biotechnology
02.2002 - 08.2002	Socrates/Erasmus scholarship at the LMU, Munich, Germany
10.1998 - 04.2003	5-year biotechnology studies at the Jagiellonian University, Institute of Molecular Biology, Krakow, Poland
06.1998	high-school graduation and final secondary-school examination (das Abitur)
09.1994 - 06.1998	Queen Jadwiga Secondary School, Sieradz, Poland

Publications

Brzózka,K., Finke,S., and Conzelmann,K.K. (2006). Inhibition of Interferon Signaling by Rabies Virus Phosphoprotein P: Activation-Dependent Binding of STAT1 and STAT2. J Virol *80*, 2675-2683.

Brzózka,K., Finke,S., and Conzelmann,K.K. (2005). Identification of the rabies virus alpha/beta interferon antagonist: phosphoprotein P interferes with phosphorylation of interferon regulatory factor 3. J Virol *79*, 7673-7681.

Schlender,J., Hornung,V., Finke,S., Gunthner-Biller,M., Marozin,S., **Brzózka,K**., Moghim,S., Endres,S., Hartmann,G., and Conzelmann,K.K. (2005). Inhibition of toll-like receptor 7- and 9-mediated alpha/beta interferon production in human plasmacytoid dendritic cells by respiratory syncytial virus and measles virus. J Virol *79*, 5507-5515.

Finke,S., **Brzózka,K**., and Conzelmann,K.K. (2004). Tracking fluorescence-labeled rabies virus: enhanced green fluorescent protein-tagged phosphoprotein P supports virus gene expression and formation of infectious particles. J Virol *78*, 12333-12343.

Presentations

Oral presentations:

03.2006	German Society of Virology Annual Meeting in Munich
09.2005	SFB455 Retreat Hohenkammer
07.2005	IUMS 2005 San Francisco – Joint meeting of the 3 divisions of the International Union of Microbiological Societies
03.2005	German Society of Virology Annual Meeting in Hannover
03.2005	SFB455 Retreat Wildbad-Kreuth

Poster presentations:

03.2004	German Society of Virology Annual Meeting in Tübingen

Ehrenwörtliche Erklärung

Hiermit erkläre ich, dass ich die vorliegende Dissertation selbstständig und ohne unerlaubte Hilfe angefertigt habe. Ich habe weder anderweitig versucht, eine Dissertation einzureichen oder eine Doktorprüfung durchzuführen, noch habe ich diese Dissertation oder Teile derselben einer anderen Prüfungskommission vorgelegt.

Mein Beitrag zu den Publikationen:

1. Brzózka et al., 2006 : Die Experimente wurden von mir geplant, durchgeführt, und ausgewertet. Die Publikation wurde von mir geschrieben, S.F. und K.C. halfen bei der Ausformulierung.

2. Brzózka et al., 2005 : Die Fragestellung wurde von K.C. formuliert, die Experimente wurden von mir und K.C. geplant, und sind von mir durchgeführt worden, unter Einbeziehung von Reagenzien und Viren, die S.F. zur Verfügung stellte. Die Daten wurden von mir und K.C. analysiert. Die Publikation wurde von mir geschrieben und von K.C. redigiert.

3. Schlender et al., 2005 : Die Experimente wurden von J.S. und anderen geplant, ich habe zu der Durchführung der Experimente durch Bereitstellung von geeigneten Zellkulturen beigetragen sowie durch Mithilfe bei der Auswertung und Diskussion der Daten.

4. Finke et al., 2004 : S.F. hat die Experimente geplant und durchgeführt. Ich war an der Analyse der Daten und der Abfassung der Publikation beteiligt.

Krzysztof Brzózka

JOURNAL OF VIROLOGY, Mar. 2006, p. 2675–2683 Vol. 80, No. 6
0022-538X/06/$08.00+0 doi:10.1128/JVI.80.6.2675–2683.2006

Inhibition of Interferon Signaling by Rabies Virus Phosphoprotein P: Activation-Dependent Binding of STAT1 and STAT2

Krzysztof Brzózka, Stefan Finke, and Karl-Klaus Conzelmann*

Max von Pettenkofer Institute and Gene Center, Ludwig-Maximilians-University, D-81377 Munich, Germany

Received 27 October 2005/Accepted 21 December 2005

Rabies virus (RV) phosphoprotein P is an interferon (IFN) antagonist counteracting transcriptional activation of type I IFN (K. Brzózka, S. Finke, and K. K. Conzelmann, J. Virol 79:7673–7681, 2005). We here show that RV P in addition is responsible for preventing IFN-α/β- and IFN-γ-stimulated JAK-STAT signaling in RV-infected cells by the retention of activated STATs in the cytoplasm. Expression of IFN-stimulated response element- and gamma-activated sequence-controlled genes was severely impaired in cells infected with RV SAD L16 or in cells expressing RV P protein from transfected plasmids. In contrast, a recombinant RV expressing small amounts of P had lost the ability to interfere with JAK-STAT signaling. IFN-mediated tyrosine phosphorylation of STAT1 and STAT2 was not impaired in RV P-expressing cells; rather, a defect in STAT recycling was suggested by distinct accumulation of tyrosine-phosphorylated STATs in cell extracts. In the presence of P, activated STAT1 and STAT2 were unable to accumulate in the nucleus. Notably, STAT1 and STAT2 were coprecipitated with RV P only from extracts of cells previously stimulated with IFN-α or IFN-γ, whereas in nonstimulated cells no association of P with STATs was observed. This conditional, IFN activation-dependent binding of tyrosine-phosphorylated STATs by RV P is unique for a viral IFN antagonist. The 10 C-terminal residues of P are required for counteracting JAK-STAT signaling but not for inhibition of transcriptional activation of IFN-β, thus demonstrating two independent functions of RV P in counteracting the host's IFN response.

The interferon (IFN) systems represent powerful defense elements of higher organisms that integrate innate and adaptive immunity. Type I IFN (IFN-α/β) is produced in response to virus infection in most tell types, including neurons, and upon recognition of conserved exogenous pathogen-associated molecular patterns by several Toll-like receptors (2, 4, 14). Expression of IFN-γ is mostly confined to T cells and NK cells; however, some neurons can also produce IFN-γ (32).

IFN-α/β and IFN-γ act through binding to ubiquitous receptors, the IFN-α/β receptor (IFNAR) and the IFN-γ receptor (IFNGR), respectively, and activation of two variants of the Janus kinase-signal transducer and activator of transcription (JAK-STAT) pathway (44). IFN-α/β binding to IFNAR results in TYK2- and JAK1-mediated tyrosine phosphorylation of the latent transcription factors STAT1 and STAT2 and formation of a heteromeric complex (IFN-stimulated gene factor 3 [ISGF3]) containing STAT1, STAT2, and IFN regulatory factor 9 (IRF-9; p48). IFNGR signaling involves tyrosine phosphorylation of STAT1 by JAK1 and JAK2 and formation of STAT1 homodimers, known as gamma-activated factor. ISGF3 and gamma-activated factor drive the expression of two big sets of genes that are controlled by specific promoter sequences, the interferon stimulated response elements (ISRE) and the gamma-activated sequences (GAS), respectively (reviewed in references [1, 34, and 44]). Expression of interferon-stimulated genes (ISG) leads to establishment of a powerful antiviral status and supports the development of an adequate adaptive Th1-biased immune response.

IFN expression and IFN effector functions are therefore vital targets of viruses (14, 17, 20, 51). It turns out that even small viruses with a limited coding capacity, including nonsegmented negative-strand RNA viruses (order *Mononegavirales*), which comprise the important *Paramyxoviridae* and *Rhabdoviridae* families, have evolved multiple mechanisms to target different functions of the IFN networks (10, 13, 29). Members of the *Paramyxoviridae* family are well known for their effective "weapons of STAT destruction," represented, for example, by the nonessential V protein, which lead to depletion of STATs from virus-infected cells and thereby demolish the IFN JAK-STAT signaling pathway (18, 52).

In contrast, interference with IFN signaling has not been shown so far for members of the *Rhabdoviridae* family including the prototypic neurotropic rabies virus (RV) of the *Lyssavirus* genus. RV encodes merely five viral proteins, all of which are essential for virus amplification, namely the nucleoprotein (N), phosphoprotein (P), matrix protein (M), glycoprotein (G), and a large (L) RNA-dependent RNA polymerase (gene order: 3′-N-P-M-G-L-5′). We have previously identified the RV phosphoprotein P as an IFN-α/β antagonist preventing expression of IFN-β in RV-infected cells by interfering with the phosphorylation of the critical IFN transcription factor IRF-3 (5). Although RV P is essential for viral RNA synthesis, we could generate a recombinant IFN-β-inducing RV (SAD ΔPLP) by shifting the P gene to a promoter-distal position of the genome. The low levels of P expressed were sufficient to support viral RNA synthesis but not to block activation of IRF-3.

* Corresponding author. Mailing address: Max von Pettenkofer Institute and Gene Center, Feodor Lynen Str. 25, D-81377 Munich, Germany, Phone: 49 89 2180 76851. Fax: 49 89 2180 76899. E-mail: conzelma@lmb.uni-muenchen.de.

We show here, by analysis of SAD ΔPLP and wild-type (wt) RV and by expression of P from cDNA, that RV P is also effective in preventing IFN-α/β- and IFN-γ-mediated signaling and expression of ISGs. Inhibition of JAK-STAT signaling and IFN induction are two separate functions of RV P since a deletion mutant lacking the C-terminal 10 residues has lost the ability to counteract JAK-STAT signaling but retained activity in preventing IFN induction by TBK-1. The STAT inhibitory activity of RV involves a unique mechanism among viral IFN antagonists, in that it targets STAT1 and STAT2 exclusively after activation by IFN-α/β or IFN-γ. Such a purposive activity only on demand may stem from a limited coding capacity of the virus and the busy nature of P, allowing P to perform its many other functions in virus replication.

(This work represents part of the doctoral thesis of K. Brzózka in fulfillment of the requirements for a Ph.D. degree from L-M-University, Munich, Germany, 2006)

MATERIALS AND METHODS

Cells, viruses, and reagents. HEp-2 cells (ATCC CCL-23) were maintained in Dulbecco's modified Eagle's medium supplemented with 5% fetal calf serum and antibiotics. HEK 293 and U3A cells (25) were propagated in Dulbecco's modified Eagle's medium with 10% fetal calf serum, L-glutamine, and antibiotics, and BSR-T7/5 cells (7) were propagated in minimal essential medium supplemented with 10% newborn calf serum.

Recombinant RV SAD L16 (42) comprising the consensus sequence of the attenuated vaccine strain SAD B19 (11) was used as wt RV. Cloning and recovery of SAD ΔPLP was described previously (5). Mouse monoclonal antibodies to RV N (W239) were kindly provided by J. Cox (Tübingen, Germany), and monoclonal antibodies and polyclonal anti-P serum (9, 37) were provided by D. Blondel (Gif-sur-Yvette, France). Anti-STAT1 p84/p91 (sc-392), anti-STAT2 (sc-476), anti-ISGF-γ p48 (IRF-9) (sc-496), and anti-NFκB p65 (sc-109) antibodies were obtained from Santa Cruz Biotechnology; anti-pY701-STAT1 and anti-pS727-STAT1 were obtained from Cell Signaling; anti-pY689-STAT2 was obtained from Upstate Biotechnology; and anti-actin was obtained from Sigma. Cytokines were purchased from Sigma (tumor necrosis factor alpha [TNF-α]) and PBC Biomedical Lab (IFN-α A/D and human IFN-γ).

Plasmids and transfection. The plasmid encoding RV P (pCR3-RVP) was described previously (5). Similarly, the pCR3-RVPD288–297 expression vector was created by PCR using an alternative antisense primer, PΔ288–297NotI3′ (5′-ATGCGGCCGCTTACATGATTTTACTCAG-3′), leading to a deletion of the 10 C-terminal amino acids of P. The pCR3-Ig (where Ig is immunoglobulin) vector (6) was used to create an N-terminally Ig-tagged P fusion protein. PCR primers (5′-ATATGAATTCATGAGCAAGATCTTTGTCAATCC-3′ and 5′-ATATGCGGCCGCTTAGCAAGATGTATAGCGATTCAA-3′) were used for amplification of P cDNA and cloning into EcoRI/NotI restriction sites.

For reporter gene assays in virus-infected cells, 2×10^5 cells (HEp-2 or BSR-T7/5) were seeded in 24-well plates and infected at multiplicities of infection (MOIs) of 1 or 3. After 16 h, cells were transfected with 0.5 μg of pISRE-luc or 0.5 μg of pGAS-luc (Stratagene) per well using Lipofectamine 2000. In all experiments, 10 ng of pCMV-RL encoding *Renilla* luciferase were cotransfected as an internal control. Medium was changed 6 h later, and the cells were stimulated with either universal IFN type I (IFN-α A/D) or human IFN-γ. After an additional 24 h, cell extracts were prepared and subjected to the reporter gene assay using a Dual Luciferase Reporter system (Promega). Luciferase activity was measured in a Luminometer (Berthold) according to the supplier's instructions. For reporter gene assays using P cDNA transfection, 2×10^5 HEp-2 cells were seeded in 24-well plates, and after 16 h cells were transfected with 0.8 μg of DNA (0.4 μg of pISRE-luc or 0.4 μg of pGAS-luc cotransfected with 0.4 μg of empty vector or RV P expression construct) per well using Lipofectamine 2000. At 24 h posttransfection, the medium was changed, and cells were treated with the amounts of IFN indicated in the figures. At 24 h poststimulation, cell lysates were subjected to the ISRE and GAS reporter gene assays. The reporter gene assays for monitoring IFN-β promoter activity (p125luc) upon TBK-1 expression were performed as described previously (5).

Precipitation assays. HEK 293 cells were transfected using a calcium phosphate mammalian transfection kit (Stratagene), and U3A cells were transfected using Lipofectamine 2000 (Invitrogen). Precipitation was performed 48 h posttransfection. Briefly, cells were lysed in lysing buffer (50 mM NaCl, 150 mM Tris, 1 mM Na-vanadate, 1 mM EDTA, and protease inhibitor cocktail [Roche]), and after centrifugation (14,000 rpm for 10 min) protein A Sepharose (Amersham Biosciences) was used to pull down Ig-tagged complexes from the supernatant (2h at 4°C). After the incubation and washing steps, beads were resuspended in lysis buffer (62.5 mM Tris, 2% sodium dodecyl sulfate [SDS], 10% glycerol, 6 M urea, 5% β-mercaptoethanol, 0.01% bromophenol blue, 0.01% phenol red) and incubated at 95°C for 10 min in order to destroy bead-bound complexes.

Western blotting. Cell extracts were prepared by treatment with cell lysis buffer (62.5 mM Tris, 2% SDS, 10% glycerol, 6 M urea, 5% β-mercaptoethanol, 0.01% bromophenol blue, 0.01% phenol red). Proteins were resolved by 10% SDS-polyacrylamide gel electrophoresis and transferred to nitrocellulose membrane (Schleicher and Schuell) using a semidry blotter (Peq-Lab). Membranes were incubated overnight at 4°C with primary antibodies. Protein signals were visualized with horseradish peroxidase-conjugated secondary antibodies and an ECL system (Perkin Elmer).

Immunofluorescence microscopy. HEp-2 cells were seeded on glass coverslips and were infected with RV at an MOI of 1 or were transfected with plasmid cDNA using Lipofectamine 2000. The cells were fixed using 3% paraformaldehyde for 20 min at room temperature and were permeabilized in 0.5% Triton X-100 in phosphate-buffered saline (PBS). After incubation with primary antibodies (1:100 in PBS for 45 min at 37°C), the specimens were incubated with fluorescence-labeled secondary antibodies at a dilution of 1:200 in PBS for 1 h at 37°C (goat anti-rabbit Alexa Fluor 488 and anti-mouse tetramethylrhodamine, both from Molecular Probes). Nuclear chromatin was stained by adding TO-PRO-3-iodide (Molecular Probes) to the secondary antibodies (final concentration, 0.5 μM TO-PRO-3-iodide).

Confocal laser scanning microscopy was performed with a Zeiss LSM510 Meta laser system using a Zeiss Axiovert 200 microscope. Excitation of Alexa Fluor 488, tetramethylrhodamine, and TO-PRO-3-iodide occurred at wavelengths of 488 nm, 543 nm, and 633 nm, respectively. To avoid cross talk, the individual channels were scanned sequentially.

RESULTS

RV infection inhibits production of ISGs. RV is not able to replicate in cells activated by IFN-α/β or IFN-γ, i.e., in cells in which an antiviral state has been established (data not shown). We noticed, however, that IFN had no obvious effect on viral replication and gene expression when cells were treated after RV infection. This suggested that RV encodes proteins to interfere with the establishment of an antiviral state by IFN or to counteract the antiviral activity of ISGs.

To explore whether RV is able to interfere with the production of ISGs, HEp2 cells were infected at a MOI of 1 with RV SAD L16 for 18 h and were then transfected with plasmids encoding firefly luciferase under the control of ISRE or GAS sequences (pISRE-luc or pGAS-luc). At 6 h posttransfection, cells were treated with IFN-α or IFN-γ. Cell lysates were prepared 24 h after IFN stimulation and processed for luciferase assays and for Western blotting.

In mock-infected cells, stimulation with 1,000 U of IFN-α resulted in a more than 20-fold induction of luciferase activity from the ISRE plasmid, whereas in SAD L16-infected cells induction of luciferase activity was almost completely prevented. Indeed, luciferase activity was comparable to mock-infected nontreated cells (Fig. 1A). Similarly, IFN-γ stimulation of luciferase from the GAS-controlled plasmid was greatly impaired in RV-infected cells (Fig. 1B).

To check the expression of some individual ISGs upon IFN treatment, cell extracts were also analyzed by Western blotting with antibodies to IRF9, STAT1, and STAT2. In mock-infected cells, a conspicuous accumulation of these proteins, in particular, STAT2 and IRF9, was noticed already upon stimulation with 100 U of IFN-α (Fig. 1C) or 10 ng/ml IFN-γ (Fig. 1D). In contrast, in RV-infected cells the

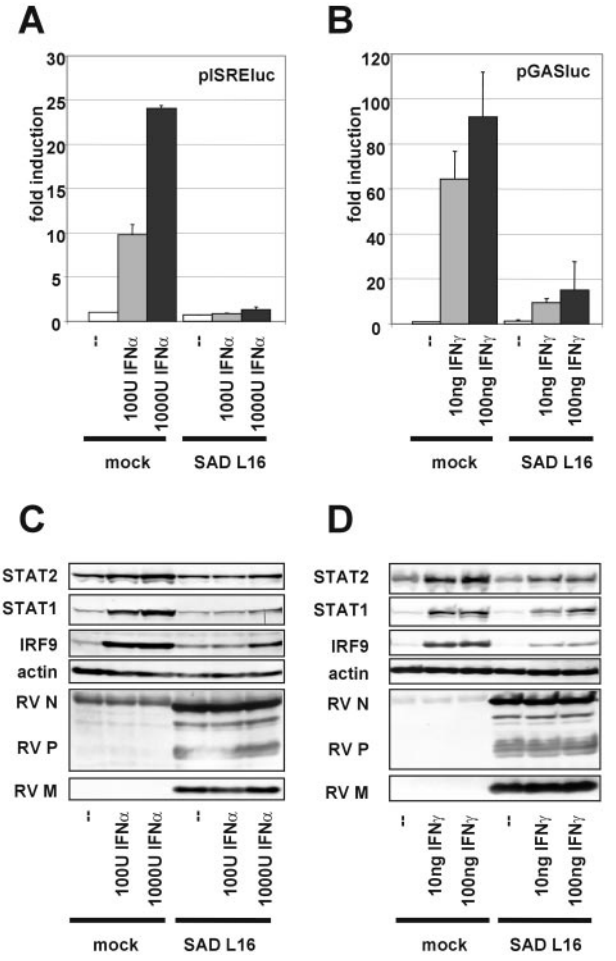

FIG. 1. RV inhibits induction of ISGs by IFN-α and IFN-γ. (A and B) HEp-2 cells were infected with RV SAD L16 (MOI of 1), transfected with pISRE-luc (A) or pGAS-luc (B) at 18 h postinfection, and IFN-α or IFN-γ was added at 6 h posttransfection. Twenty-four hours later firefly luciferase activities were measured and corrected to the *Renilla* luciferase activity from a cotransfected control plasmid to normalize for variations in the transfection efficiency. Transfection experiments were repeated at least three times and averages and error bars are shown. (C and D) Expression of individual ISGs STAT1, STAT2, and IRF9 was analyzed by Western blot analysis of extracts from HEp-2 cells infected at an MOI of 1 for 24 h and a subsequent 24-h stimulation with IFN-α (C) or IFN-γ (D). In contrast to mock-infected cells, RV-infected cells do not upregulate ISRE- or GAS-controlled luciferase or STAT1, STAT2, and IRF9 upon IFN stimulation.

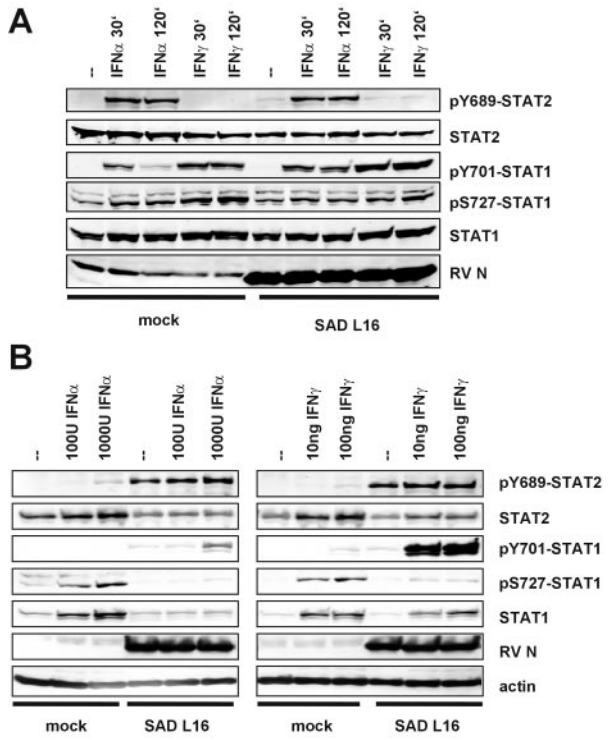

FIG. 2. RV infection does not prevent tyrosine phosphorylation of STAT1 and STAT2 (A) but leads to accumulation of tyrosine-phosphorylated STAT1 and STAT2 over time (B). Mock-infected and RV-infected HEp-2 cells (MOI of 1) were stimulated at 24 h postinfection with IFN-α or IFN-γ. After 30 or 120 min (A) cell extracts were processed for Western blotting and probed with phospho-specific antibodies as indicated. Tyrosine phosphorylation of STAT2 (pY689-STAT2) and STAT1 (pY701-STAT1) was similar in mock- and RV-infected IFN-stimulated cells, whereas serine phosphorylation of STAT1 (pS727-STAT1) by IFN was more effective in mock-infected cells. Tyrosine-phosphorylated STAT1 and STAT2 accumulate. As shown in panel B, at later stages after IFN stimulation (24 h poststimulation), abundant amounts of tyrosine-phosphorylated STATs are still detectable only in RV-infected cells but not in mock-infected cells, suggesting a defect in STAT recycling.

upregulation of STAT1, STAT2, and IRF9 was evidently impaired, confirming the luciferase reporter gene assays. Only at a high dose of 1,000 U of IFN-α was some increase of protein levels apparent, though levels remained below those of mock-infected IFN-stimulated cells. Notably, the basic levels of STAT1 and STAT2 were not reduced in RV-infected cells. This indicated that the observed inhibition of ISG expression by RV was not due to depletion of STATs.

STAT tyrosine phosphorylation is not affected. STATs are activated by Janus tyrosine kinases associated with the cytoplasmic domains of IFNAR and IFNGR. To analyze the phosphorylation status of STAT1 and STAT2 in RV-infected cells, Western blot experiments with phospho-specific STAT antibodies were performed. HEp-2 cells infected for 24 h with SAD L16 were treated with IFN, and cell extracts were prepared 30 min and 120 min after the IFN stimulation (Fig. 2A). As observed previously, the total levels of STAT1 and STAT2 were similar in mock- and virus-infected cells. As in mock-infected cells, tyrosine-phosphorylated STAT2 (pY689-STAT2) and STAT1 (pY701-STAT1) were readily detected in RV-infected cells at 30 min poststimulation with IFN-α. Similarly, IFN-γ stimulation resulted in comparable amounts of pY701-STAT1 in mock-infected and RV-infected cells at 30 min poststimulation (Fig. 2A). Thus, activation of STAT1 and STAT2 by tyrosine phosphorylation is not impaired in RV-infected cells.

To follow the long-term fate of phosphorylated STATs, cells were allowed to grow for 24 h following IFN treatment (Fig. 2B). At this late time point, only trace amounts of pY701-STAT1 and pY689-STAT2 were left in mock-infected cells treated with IFN-α, while total levels of STAT1 and STAT2 were increased as a result of IFN stimulation. In striking contrast, abundant amounts of pY689-STAT2 were present in

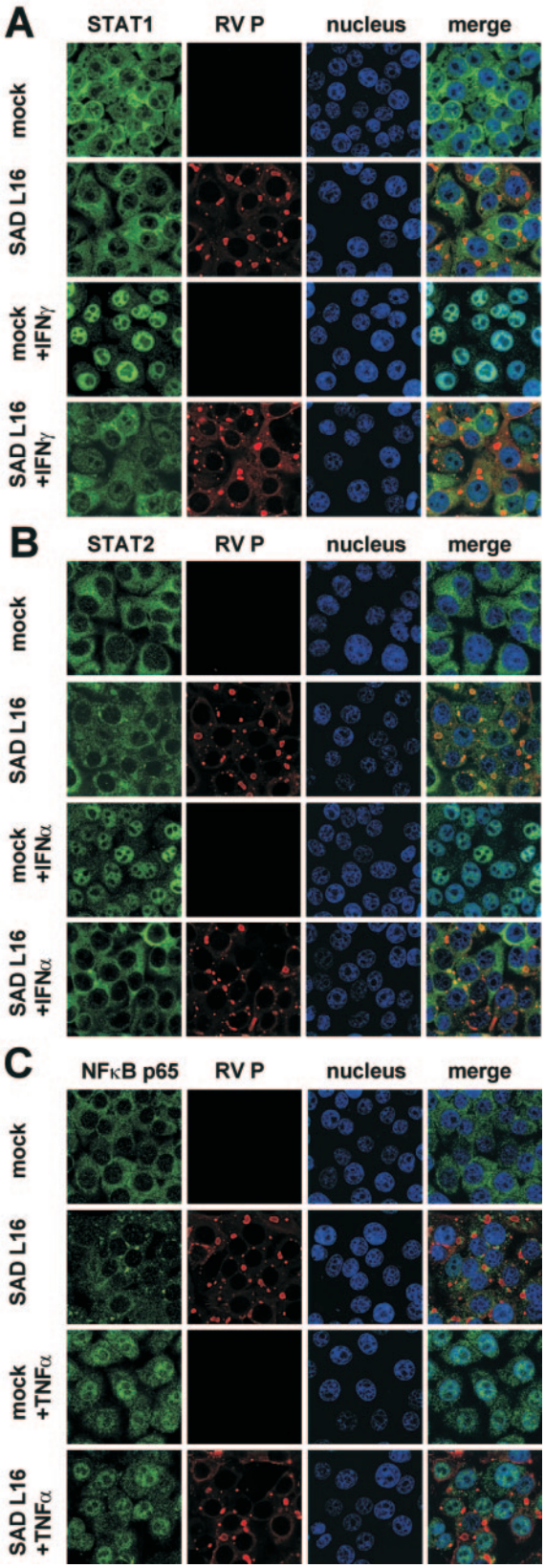

FIG. 3. RV infection prevents IFN-mediated translocation of STAT1 (A) and STAT2 (B) to the nucleus. RV-infected (MOI of 1) and mock-infected Hep-2 cells were stimulated with IFN-γ or IFN-α for 45 min at 24 h postinfection, fixed with 3% paraformaldehyde, and stained with STAT1 or STAT2 antibodies as indicated. The import of both STATs on IFN-treated cells is prevented in RV-infected cells, whereas import of NF-κB p65 on TNF-α-treated cells is not (C). Nuclei of cells were visualized by staining with TO-PRO-3 dye; RV P was visualized by using P-specific polyclonal mouse serum.

RV-infected cells at this late time point, as well as increased levels of pY701-STAT1 (Fig. 2B, left panel). In line with these findings, IFN-γ treatment resulted in the most pronounced accumulation of pY701-STAT1 and a less prominent accumulation of pY689-STAT2 in RV-infected cells during the 24-h period following IFN treatment. These results further confirmed that the initial tyrosine phosphorylation of STATs is unimpaired and pointed toward a defect in recycling of correctly activated STATs.

In contrast to tyrosine phosphorylation of STAT1, serine phosphorylation, which is not required for the transcriptional activity of STATs, appeared to be somewhat less efficient in RV-infected cells. Lower levels of pS727-STAT1 were observed both at early (Fig. 2A) and late time points after IFN stimulation (Fig. 2B).

RV prevents nuclear import of activated STAT1 and STAT2. As STATs were found to be correctly activated by tyrosine phosphorylation in RV-infected cells, we examined by confocal laser scanning microscopy the subcellular localization of STAT1 and STAT2 proteins after stimulation with IFN. For this purpose, HEp-2 cells were infected at an MOI of 1 for 24 h, stimulated for 45 min with 100 ng/ml of IFN-γ or 1,000 U/ml of IFN-α, and immunostained for STAT1 and STAT2, respectively. In noninfected HEp-2 cells, IFN-γ treatment led to a redistribution of STAT1 from the cytoplasm to the nucleus (Fig. 3A), whereas IFN-treated RV-infected cells maintained the phenotype of nontreated cells, with the major portion of STAT1 in the cytoplasm (Fig. 3A). Stimulation of noninfected cells with IFN-α led to an almost complete relocalization of STAT2 from the cytoplasm to the nucleus. This translocation was precluded when cells were previously infected with RV (Fig. 3B). To exclude the possibility that RV causes a general block of nuclear import or an increase in nuclear export, we investigated the nuclear localization of another transcription factor, NF-κB p65, on stimulation with TNF-α (Fig. 3C). In contrast to STAT1 and STAT2, nuclear accumulation of NF-κB p65 was not affected in RV-infected cells, indicating that RV specifically interferes with the nuclear import of STAT1 and STAT2 (see Discussion).

Failure of the RV SAD ΔPLP to interfere with JAK-STAT signaling. To identify the viral protein(s) responsible for interference with JAK-STAT signaling, we compared wt RV SAD L16 with the previously described SAD ΔPLP. Due to a change in the gene order from 3′-N-P-M-G-L-5′ to 3′-N-M-G-L-P-5′, SAD ΔPLP virus expresses very low amounts of P and is therefore unable to prevent activation of IRF-3 and IFN-β production (5). Reporter gene assays were therefore performed in BSR-T7/5 cells, which do not produce endogenous IFN on SAD ΔPLP infection. Cells infected at an MOI of 3 with SAD L16 and SAD ΔPLP virus for 18 h were transfected with pISRE-luc and stimulated with IFN-α, and luciferase activity was determined 24 h after stimulation. An approximately 60-

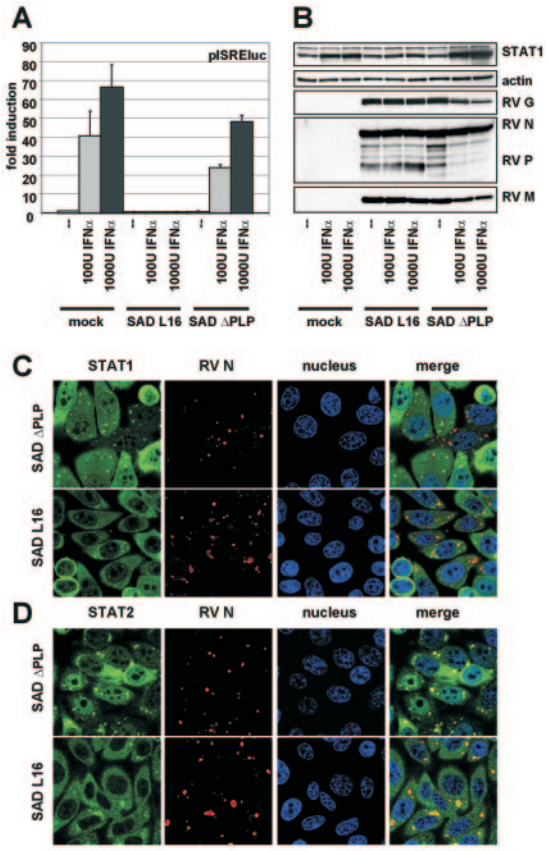

FIG. 4. SAD ΔPLP fails in inhibiting JAK-STAT signaling. (A) BSR-T7/5 cells infected at an MOI of 3 with wt RV SAD L16 and a mutant expressing low levels of P (SAD ΔPLP) were transfected with pISRE-luc and were stimulated with IFN-α 18 h postinfection. In contrast to wt RV, SAD ΔPLP is not able to abolished luciferase activities. (B) BSR T7/5 cells infected at an MOI of 1 with RV SAD L16 and SAD ΔPLP were treated with IFN-α at 24 h postinfection. Cell lysates were prepared 24 h after stimulation (48 h postinfection) and were analyzed by Western blotting. Accumulation of viral proteins in SAD ΔPLP-infected cells was decreased after IFN induction. (C) HEp-2 cells infected with SAD L16 or SAD ΔPLP at an MOI of 1 were immunostained for STAT1 and STAT2 24 h postinfection as described in the legend of Fig. 3. In contrast to wt SAD L16, SAD ΔPLP-infected HEp-2 cells allow nuclear accumulation of both STAT1 and STAT2. RV N was visualized using N-specific mouse monoclonal antibodies.

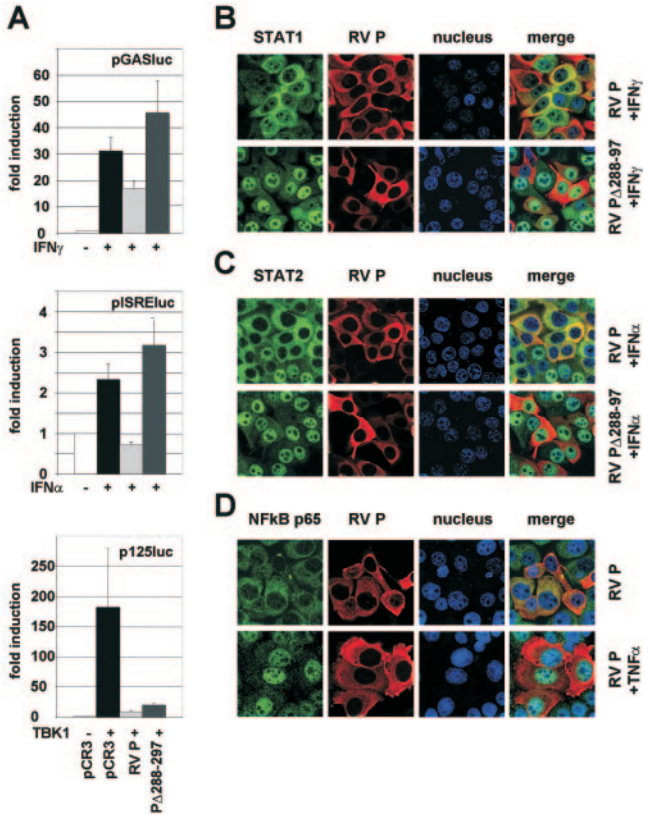

FIG. 5. Expression of P alone prevents STAT signaling. (A) pISRE-luc or pGAS-luc reporter constructs were cotransfected with plasmids encoding wt P (pCR3-RVP), a C-terminally truncated protein, PΔ288-297 (pCR3-RVPΔ288-297), or with empty vector (pCR3) into HEp-2 cells. After 24 h, IFN-α or IFN-γ was added, and luciferase activities were analyzed after an additional 24 h (top and middle panels). A reporter gene construct controlled by the IFN-β promoter (p125luc) was cotransfected with RV P and TBK-1 expression plasmids into HEK 293 cells as indicated. Luciferase activities were determined at 48 h posttransfection (lower panel). The average of at least two independent experiments is shown with error bars. (B to D) RV P prevents nuclear accumulation of STATs. HEp-2 cells were transfected with the indicated expression constructs. After 24 h cells were stimulated for 45 min and were subsequently stained for STAT1 (B), STAT2 (C), and NF-κB p65 (D) as described in the legend of Fig. 3. In contrast to PΔ288-297, expression of wt P prevents nuclear import of STAT1 and STAT2 by IFN but not of NF-κB p65 by TNF-α.

fold induction of luciferase activity was observed for mock-infected cells. While infection with wt RV completely abolished luciferase activity, SAD ΔPLP infection was not able to prevent IFN signaling (Fig. 4A), suggesting that the RV P protein is involved in or responsible for counteracting IFN signaling. Indeed, SAD ΔPLP showed an increased sensitivity to the antiviral effects of IFN. Treatment of virus-infected BSR T7/5 cells with IFN-α caused a clear and dose-dependent inhibitory effect of protein expression of SAD ΔPLP, in contrast to wt RV SAD L16 (Fig. 4B). Microscopic examination of STAT localization in HEp2 cells infected with SAD ΔPLP or SAD L16 further confirmed that SAD ΔPLP has a defect in preventing nuclear accumulation of STAT1 and STAT2 (Fig. 4C and D). Thus, it appears that insufficient levels of P protein expressed from SAD ΔPLP are responsible for the failure of this virus in preventing JAK-STAT signaling.

Rabies virus phosphoprotein P is responsible for interference with STAT functions. In order to clarify whether P alone is able to prevent ISG expression, HEp-2 cells were transfected with an empty vector (pCR3) or an RV P-encoding plasmid (pCR3-RVP), stimulated with IFN, and assayed for GAS- and ISRE-directed luciferase expression. Expression of RV P was sufficient to considerably reduce both IFN-γ- and IFN-α-induced luciferase activity (Fig. 5A, top and middle panels). In striking contrast to full-length P, a P deletion mutant lacking the 10 C-terminal residues (PΔ288-297) did not show an inhibitory effect on either GAS- or ISRE-driven reporter gene expression. Notably, however, PΔ288-297 has retained the ability to prevent TBK-1-mediated activation of IRF-3 and IFN-β induction. Compared to HEK 293 cells transfected with empty vector plasmids, cotransfection of both P-encoding plasmids

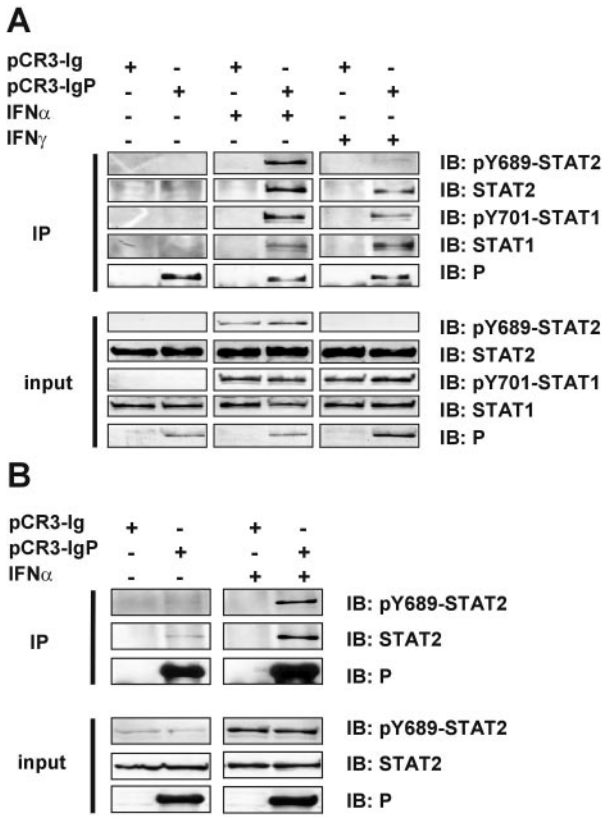

FIG. 6. RV P interacts with STATs in an IFN-dependent manner. (A) HEK 293 cells were transfected with constructs encoding Ig-tagged P (pCR3-IgP) or the Ig moiety alone (pCR3-Ig). Precipitation was performed using Sepharose A beads binding the Ig tag at 48 h postinfection from extracts of cells that were treated for 45 min with 1,000 U/ml IFN-α or 100 ng/ml IFN-γ or were not treated. Precipitates (IP) and 3% of cell extracts (input) were analyzed by Western blotting with the indicated antibodies. Only from IFN-treated cells were STATs coprecipitated with Ig-P. (B) The experiment shown in panel A was performed with U3A cells that lack STAT1. STAT2 is precipitated from IFN-treated cells independent of STAT1.

with a TBK-1-encoding plasmid reduced expression of luciferase from the IFN-β promoter (p125luc) considerably (Fig. 5A, bottom panel).

To verify the results from the reporter gene assays and to address the question of how expression of RV P and PΔ288-297 affect the nuclear import of STATs, transfected HEp-2 cells were treated with IFN and processed for confocal microscopy as described above. In cells expressing P, neither STAT1 nor STAT2 could accumulate in the nucleus upon IFN stimulation. In contrast, cells expressing even abundant PΔ288-297 showed efficient nuclear accumulation of STAT1 and STAT2 (Fig. 5B and C). As observed previously for RV-infected cells, nuclear import of NF-κB p65 was not impaired in P-expressing cells (Fig. 5D). Thus, RV P alone is sufficient to specifically and efficiently prevent STAT1 and STAT2 nuclear import and ISG induction by IFN JAK-STAT signaling.

Activation-dependent binding of STATs by RV P. To assay whether RV P is able to physically associate with STATs and thereby preclude their nuclear import, precipitation assays were performed using a P in which an Ig tag was fused to the N terminus of P (pCR3-IgP) or of PΔ288-297 (pCR3-Ig PΔ288-297). As we considered the possibility that activated STATs represent the targets of P (see Discussion), the experiments were designed in a way to include IFN-treated cells. HEK 293 cells were transfected with pCR3-IgP or a control plasmid expressing the Ig tag alone (pCR3-Ig) and were stimulated with 1,000 U/ml of IFN-α or 100 ng/ml of IFN-γ after 48 h for 45 min. Ig-containing complexes were precipitated from cell extracts using Sepharose A beads (Amersham Biosciences), and precipitates were analyzed by Western blotting.

Notably, neither STAT1 nor STAT2 was coprecipitated with IgP from nonstimulated cells (Fig. 6A, left panel). However, when cells were pretreated with IFN-α, both STAT1 and STAT2 molecules were effectively pulled down with IgP but not by the Ig control construct (Fig. 6A, middle panel). The presence of activated, tyrosine-phosphorylated STAT2 (pY689) and STAT1 (pY701) in the precipitates was confirmed by phosphospecific antibodies.

After treatment of cells with IFN-γ, pY701-STAT1 was readily detected in the cell extracts in contrast to pY689-STAT2 (Fig. 6A, right panel, input). Again, IgP coprecipitated STAT1 exclusively and effectively from stimulated cells. Furthermore, not only STAT1 (pY701-STAT1) was present in the IgP precipitates but also STAT2 (pY689-STAT2), although pY689-STAT2 was below the detection limit in the input cell extracts (Fig. 6A, lower panel). Coprecipitation of STATs with IgPΔ288-297 was not observed in either IFN-stimulated or nonstimulated cells (data not shown).

These experiments confirmed that RV P associated with STAT2 and/or STAT1 only after IFN activation; however, they did not reveal whether the interaction with STAT2 occurs via STAT1 or independently of STAT1. We therefore repeated the precipitation experiments with cell extracts of U3A cells that lack STAT1. IgP clearly coprecipitated pY689-STAT2 from cell extracts of IFN-α-stimulated U3A cells, as well as from nonstimulated cells, in which low amounts of pY689-STAT2 were already detectable (Fig. 6B). Again, no precipitation was observed with the C-terminally truncated IgPΔ288-297 (data not shown). Thus, full-length RV P is able to independently interact with pY-STAT1 and pY-STAT2 in IFN-stimulated cells.

DISCUSSION

In this work, we have demonstrated that RV has the ability to interrupt the IFN-stimulated JAK-STAT signaling pathways and thereby to prevent the detrimental effects of type I and type II IFN. This activity could be attributed entirely to the P protein. The mechanism by which RV P interrupts IFN JAK-STAT signaling involves a specific association of P with STAT1 and STAT2 exclusively after activation by IFN, which is unique for viral IFN antagonists.

The existence of RV proteins able to counteract IFN signaling was first suggested by the observation that treatment of cells previously infected with RV had no detectable effects on virus gene expression and infectious virus titers, whereas pretreatment of cells with IFN completely prohibits RV replication. The resistance of RV to both IFN-α/β and IFN-γ further pointed toward STAT1 as a target, since it is a common factor of the IFNAR and IFNGR/JAK-STAT pathways. In RV-in-

fected cells an almost complete inhibition of ISRE-controlled luciferase activity was observed, consistent with the later observation that RV P binds both STAT1 and STAT2. The observed residual leakiness of RV-infected cells for IFN-γ-stimulated and GAS-mediated reporter gene expression may be due to different reasons, e.g., activation of STAT3 in addition to STAT1 at the IFN-γ receptor (44).

Upon stimulation of the IFN receptors by IFN, STATs are phosphorylated by the receptor-associated Janus kinases at tyrosine residues 689 (STAT2) and 701 (STAT1) (19, 22, 23, 46). The STATs then dimerize through SH2-phosphotyrosine interactions, translocate to the nucleus, and bind to ISRE or GAS sequences. Additional phosphorylation of C-terminal Ser residues by kinases such as protein kinase C δ may improve the transcriptional activity of tyrosine-phosphorylated STATs by facilitating binding of nuclear factors, such as CBP/p300, but this is not a requirement for STAT transcriptional activity (12, 47). The analysis of STAT proteins with phospho-specific antibodies revealed that the critical tyrosine phosphorylation of STATs is not precluded in RV-infected cells. Rather, an accumulation of tyrosine-phosphorylated STATs was observed over time, whereas in mock-infected cells these molecules rapidly disappeared (Fig. 2B). In contrast to the initial tyrosine phosphorylation, however, the following serine phosphorylation of STATs appeared to be somewhat hampered in RV cells, as suggested by poor accumulation of pS727-STAT1 (Fig. 2B). These observations pointed toward an interference of RV P with a step following the initial receptor-mediated STAT activation.

Indeed, in spite of correct tyrosine phosphorylation, neither STAT1 nor STAT2 was able to accumulate in the nucleus of RV-infected cells. A very clear-cut alternative distribution was observed for STAT2. IFN-α treatment of mock-infected cells led to a rapid and almost complete relocalization of STAT2 from the cytoplasm to the nucleus, whereas in RV-infected or RV P-expressing and IFN-treated cells, virtually no STAT2 was detectable in the nucleus (Fig. 3 and 5). In case of STAT1, a readily detectable portion of the protein showed nuclear localization even in nonstimulated cells. This reflects the well-known shuttling of nonactivated STAT1 between the cytoplasm and nucleus (24, 28) and indicated that cycling of nonactivated STAT1 is not affected by RV P. Nevertheless, an efficient inhibition of IFN-triggered nuclear accumulation of STAT1 by RV was obvious, indicating that RV P retains activated STAT1 in the cytoplasm and prevents its nuclear import. It should be noted that pY-STAT1 is incapable of nuclear exit and has to be dephosphorylated first by nuclear phosphatases (26–28). Confocal live microscopy experiments involving photobleaching of cytoplasmic STAT1-GFP (where GFP is green fluorescent protein) revealed that the nuclear export rate of nonphosphorylated STAT1-GFP is not changed in the presence of RV P (not shown). The lack of nuclear import of activated STATs and of their dephosphorylation in the nucleus therefore explains the overall accumulation of pY-STATs over time in RV-infected cells.

Direct evidence for activation-dependent binding of STAT1 and STAT2 by P was obtained from precipitation assays with Ig-tagged P protein. Effective coprecipitation of both STATs with RV P was dependent on stimulation of cells with IFN. We were unable to detect substantial coprecipitation of STAT1 or STAT2 in nonstimulated HEK 293 cells, suggesting that nonphosphorylated STATs are not recognized, or only poorly recognized, and bound by P. After submission of this work, Vidy et al. published a report on binding of the RV P of the CVS strain to STAT1 (49). These authors were able to coprecipitate STAT1 from cell extracts using a glutathione transferase-P fusion construct. It was not revealed whether this represented activated or nonactivated STAT1. However, the observation that STAT1 and P coexpression was able to activate gene transcription in a yeast two-hybrid system indicates some basic association of P with STAT.

Only IFN stimulation, however, resulted in effective coprecipitation of both STAT1 and STAT2 in our hands. The presence of tyrosine-phosphorylated STATs in the precipitates strongly argues in favor of the idea that P binds exclusively to tyrosine-phosphorylated STATs, although we cannot formally exclude some coprecipitation of nonphosphorylated STATs via pY-STATs, due to the lack of antibodies that positively identify nonphosphorylated STATs. Recognition and precipitation of pY689-STAT2 by P appear to be very specific, as suggested by the precipitation of these molecules from cell extracts of IFN-γ-stimulated cells, in which they were not detectable by Western blotting or were present in very small amounts (53) among a bulk of nonphosphorylated STAT2 (Fig. 6A and B). We could further show that recognition of activated STAT2 is STAT1 independent, as shown by coprecipitation experiments using U3A cells that lack STAT1 (25) (Fig. 6B). Thus, RV P interacts with both STAT1 and STAT2 only upon activation, either directly or in a complex with other proteins, and this interaction explains the retention of activated STATs in the cytoplasm of infected cells.

The described conditional, activation-dependent targeting of STAT1 and STAT2 by RV P to interrupt IFN JAK-STAT signaling is unique among viruses. Constitutive targeting of bulk nonactivated STATs is a common strategy of the related paramyxoviruses and is due to the activities of their nonessential V proteins (for review see references 13, 14, 18, and 29). *Rubulavirus* V proteins assemble STAT-specific ubiquitin-ligase complexes from cellular components and target either STAT1 or STAT2 for proteasomal degradation (35, 48). The V proteins from other paramyxovirus genera do not lead to degradation of STATs. Henipaviruses, for example, in fact prevent phosphorylation of STATs and sequester STAT1 and STAT2 in high-molecular-mass complexes (39, 40). For Nipah virus it has been shown that the V, W, and P proteins, which are all encoded by the same viral gene and share an identical 407-amino-acid N-terminal region but have distinct C-terminal sequences, have anti-STAT function. This confirmed the finding that the common N-terminal domain is involved in the antagonist activity (38, 43). However, it was also found that activity of the P protein is not as strong as that of V or W, perhaps explaining why Nipah virus has evolved to express additionally two edited products (43). The V protein of measles virus was reported to copurify with STAT1, STAT2, STAT3, and IRF-9, to bind to the IFNAR, and to recruit STATs to viral inclusion bodies (33, 45).

We have here identified RV P as an inhibitor of IFN signaling and have previously shown that RV P is active in counteracting transcriptional induction of type I IFN (5). As demonstrated by PΔ288-297, these are independent functions of P. A

region within the 10 C-terminal amino acid residues of RV P is required for counteracting STAT signaling but not for inhibiting TBK-1. Interestingly, paramyxovirus V proteins also combine inhibitory activities in IFN signaling and in IFN induction (16) but with different targets in either function. Whereas V C-terminal domains bind and inhibit the double-stranded RNA receptor *mda-5* which relays signals to activation of IRF-3 and NF-kB (3), RV P acts farther downstream and specifically prevents phosphorylation of IRF-3 by TBK-1 (5). This finding stresses the importance for a virus of having means to target different steps within the powerful host IFN response. In particular, it is obvious that viral IFN antagonists are insufficient to prevent some early IFN synthesis or to prevent synthesis in certain tissue or cell types. Indeed, we have identified a variety of cell types in which active IFN is being expressed upon RV infection with SAD L16, though at lower magnitudes than the "IFN-inducing" SAD ΔPLP. In particular, and in striking contrast to measles virus and respiratory syncytial virus (41), RV SAD L16 is not able to prevent IFN induction in human plasmacytoid dendritic cells (unpublished data), which represent the major IFN producers in vivo. Consistent with these observations, IFN has been detected upon RV infection in vitro and in vivo (21, 30, 31, 36, 50). Since IFN-β and, in particular, IFN-γ have a major role in the noncytotoxic clearance of viruses from neurons and the central nervous system (8, 15), it is predicted that the ability of RV to counteract IFN-α/β and IFN-γ signaling is crucial for RV infection in vivo. Further experiments should be directed to further dissociate RV P functions in IFN induction and response. The use of recombinant RV with defined defects in either function should help to study the contribution of the innate immune response to the control of RV and to reveal a possible correlation of IFN antagonistic activities with viral pathogenicity. Viral antagonists targeting particular functions of the JAK-STAT pathways, such as RV P, may further help in studying details of STAT signaling.

ACKNOWLEDGMENTS

We thank J. Cox (FLI, Tübingen, Germany) and D. Blondel (CNRS, Gif-sur-Yvette, France) for providing RV antibodies, S. Goodbourn (St. George's University London, United Kingdom) for ISRE and GAS reporter gene plasmids, and I. Kerr (CR-UK, London, United Kingdom) for U3A cells. We are grateful to N. Hagendorf for perfect technical assistance.

This work was supported by the Deutsche Forschungsgemeinschaft through SFB 455, "Viral functions and immune modulation."

REFERENCES

1. **Aaronson, D. S., and C. M. Horvath.** 2002. A road map for those who don't know JAK-STAT. Science **296:**1653–1655.
2. **Akira, S., and K. Takeda.** 2004. Toll-like receptor signalling. Nat. Rev. Immunol. **4:**499–511.
3. **Andrejeva, J., K. S. Childs, D. F. Young, T. S. Carlos, N. Stock, S. Goodbourn, and R. E. Randall.** 2004. The V proteins of paramyxoviruses bind the IFN-inducible RNA helicase, mda-5, and inhibit its activation of the IFN-beta promoter. Proc. Natl. Acad. Sci. USA **101:**17264–17269.
4. **Bowie, A. G., and I. R. Haga.** 2005. The role of Toll-like receptors in the host response to viruses. Mol. Immunol. **42:**859–867.
5. **Brzozka, K., S. Finke, and K. K. Conzelmann.** 2005. Identification of the rabies virus alpha/beta interferon antagonist: phosphoprotein P interferes with phosphorylation of interferon regulatory factor 3. J. Virol. **79:**7673–7681.
6. **Bubeck, A., M. Wagner, Z. Ruzsics, M. Lotzerich, M. Iglesias, I. R. Singh, and U. H. Koszinowski.** 2004. Comprehensive mutational analysis of a herpesvirus gene in the viral genome context reveals a region essential for virus replication. J. Virol. **78:**8026–8035.
7. **Buchholz, U. J., S. Finke, and K. K. Conzelmann.** 1999. Generation of bovine respiratory syncytial virus (BRSV) from cDNA: BRSV NS2 is not essential for virus replication in tissue culture, and the human RSV leader region acts as a functional BRSV genome promoter. J. Virol. **73:**251–259.
8. **Burdeinick-Kerr, R., and D. E. Griffin.** 2005. Gamma interferon-dependent, noncytolytic clearance of Sindbis virus infection from neurons in vitro. J. Virol. **79:**5374–5385.
9. **Chenik, M., M. Schnell, K. K. Conzelmann, and D. Blondel.** 1998. Mapping the interacting domains between the rabies virus polymerase and phosphoprotein. J. Virol. **72:**1925–1930.
10. **Conzelmann, K. K.** 2005. Transcriptional activation of alpha/beta interferon genes: interference by nonsegmented negative-strand RNA viruses. J. Virol. **79:**5241–5248.
11. **Conzelmann, K. K., J. H. Cox, L. G. Schneider, and H. J. Thiel.** 1990. Molecular cloning and complete nucleotide sequence of the attenuated rabies virus SAD B19. Virology **175:**485–499.
12. **Deb, D. K., A. Sassano, F. Lekmine, B. Majchrzak, A. Verma, S. Kambhampati, S. Uddin, A. Rahman, E. N. Fish, and L. C. Platanias.** 2003. Activation of protein kinase C delta by IFN-gamma. J. Immunol. **171:**267–273.
13. **Garcia-Sastre, A.** 2004. Identification and characterization of viral antagonists of type I interferon in negative-strand RNA viruses. Curr. Top. Microbiol. Immunol. **283:**249–280.
14. **Goodbourn, S., L. Didcock, and R. E. Randall.** 2000. Interferons: cell signalling, immune modulation, antiviral response and virus countermeasures. J. Gen. Virol. **81:**2341–2364.
15. **Griffin, D. E.** 2003. Immune responses to RNA-virus infections of the CNS. Nat. Rev. Immunol. **3:**493–502.
16. **He, B., R. G. Paterson, N. Stock, J. E. Durbin, R. K. Durbin, S. Goodbourn, R. E. Randall, and R. A. Lamb.** 2002. Recovery of paramyxovirus simian virus 5 with a V protein lacking the conserved cysteine-rich domain: the multifunctional V protein blocks both interferon-beta induction and interferon signaling. Virology **303:**15–32.
17. **Hengel, H., U. H. Koszinowski, and K. K. Conzelmann.** 2005. Viruses know it all: new insights into IFN networks. Trends Immunol. **26:**396–401.
18. **Horvath, C. M.** 2004. Weapons of STAT destruction. Interferon evasion by paramyxovirus V protein. Eur. J. Biochem. **271:**4621–4628.
19. **Horvath, C. M., G. R. Stark, I. M. Kerr, and J. E. Darnell, Jr.** 1996. Interactions between STAT and non-STAT proteins in the interferon-stimulated gene factor 3 transcription complex. Mol. Cell. Biol. **16:**6957–6964.
20. **Katze, M. G., Y. He, and M. Gale, Jr.** 2002. Viruses and interferon: a fight for supremacy. Nat. Rev. Immunol. **2:**675–687.
21. **Lafon, M.** 2005. Modulation of the immune response in the nervous system by rabies virus. Curr. Top. Microbiol. Immunol. **289:**239–258.
22. **Lau, J. F., J. P. Parisien, and C. M. Horvath.** 2000. Interferon regulatory factor subcellular localization is determined by a bipartite nuclear localization signal in the DNA-binding domain and interaction with cytoplasmic retention factors. Proc. Natl. Acad. Sci. USA **97:**7278–7283.
23. **Li, X., S. Leung, I. M. Kerr, and G. R. Stark.** 1997. Functional subdomains of STAT2 required for preassociation with the alpha interferon receptor and for signaling. Mol. Cell. Biol. **17:**2048–2056.
24. **Marg, A., Y. Shan, T. Meyer, T. Meissner, M. Brandenburg, and U. Vinkemeier.** 2004. Nucleocytoplasmic shuttling by nucleoporins Nup153 and Nup214 and CRM1-dependent nuclear export control the subcellular distribution of latent Stat1. J. Cell Biol. **165:**823–833.
25. **McKendry, R., J. John, D. Flavell, M. Muller, I. M. Kerr, and G. R. Stark.** 1991. High-frequency mutagenesis of human cells and characterization of a mutant unresponsive to both alpha and gamma interferons. Proc. Natl. Acad. Sci. USA **88:**11455–11459.
26. **Meyer, T., L. Hendry, A. Begitt, S. John, and U. Vinkemeier.** 2004. A single residue modulates tyrosine dephosphorylation, oligomerization, and nuclear accumulation of STAT transcription factors. J. Biol. Chem. **279:**18998–19007.
27. **Meyer, T., A. Marg, P. Lemke, B. Wiesner, and U. Vinkemeier.** 2003. DNA binding controls inactivation and nuclear accumulation of the transcription factor Stat1. Genes Dev. **17:**1992–2005.
28. **Meyer, T., and U. Vinkemeier.** 2004. Nucleocytoplasmic shuttling of STAT transcription factors. Eur. J. Biochem. **271:**4606–4612.
29. **Nagai, Y., and A. Kato.** 2004. Accessory genes of the *Paramyxoviridae*, a large family of nonsegmented negative-strand RNA viruses, as a focus of active investigation by reverse genetics. Curr. Top. Microbiol. Immunol. **283:**197–248.
30. **Nakamichi, K., S. Inoue, T. Takasaki, K. Morimoto, and I. Kurane.** 2004. Rabies virus stimulates nitric oxide production and CXC chemokine ligand 10 expression in macrophages through activation of extracellular signal-regulated kinases 1 and 2. J. Virol. **78:**9376–9388.
31. **Nakamichi, K., M. Saiki, M. Sawada, M. Takayama-Ito, Y. Yamamuro, K. Morimoto, and I. Kurane.** 2005. Rabies virus-induced activation of mitogen-activated protein kinase and NF-κB signaling pathways regulates expression of CXC and CC chemokine ligands in microglia. J. Virol. **79:**11801–11812.
32. **Neumann, H., H. Schmidt, E. Wilharm, L. Behrens, and H. Wekerle.** 1997. Interferon gamma gene expression in sensory neurons: evidence for autocrine gene regulation. J. Exp. Med. **186:**2023–2031.
33. **Palosaari, H., J. P. Parisien, J. J. Rodriguez, C. M. Ulane, and C. M.**

Horvath. 2003. STAT protein interference and suppression of cytokine signal transduction by measles virus V protein. J. Virol. **77:**7635–7644.
34. **Platanias, L. C.** 2005. Mechanisms of type-I- and type-II-interferon-mediated signalling. Nat. Rev. Immunol. **5:**375–386.
35. **Precious, B., K. Childs, V. Fitzpatrick-Swallow, S. Goodbourn, and R. E. Randall.** 2005. Simian virus 5 V protein acts as an adaptor, linking DDB1 to STAT2, to facilitate the ubiquitination of STAT1. J. Virol. **79:**13434–13441.
36. **Prehaud, C., F. Megret, M. Lafage, and M. Lafon.** 2005. Virus infection switches TLR-3-positive human neurons to become strong producers of beta interferon. J. Virol. **79:**12893–12904.
37. **Raux, H., F. Iseni, F. Lafay, and D. Blondel.** 1997. Mapping of monoclonal antibody epitopes of the rabies virus P protein. J. Gen. Virol. **78:**119–124.
38. **Rodriguez, J. J., C. D. Cruz, and C. M. Horvath.** 2004. Identification of the nuclear export signal and STAT-binding domains of the Nipah virus V protein reveals mechanisms underlying interferon evasion. J. Virol. **78:**5358–5367.
39. **Rodriguez, J. J., J. P. Parisien, and C. M. Horvath.** 2002. Nipah virus V protein evades alpha and gamma interferons by preventing STAT1 and STAT2 activation and nuclear accumulation. J. Virol. **76:**11476–11483.
40. **Rodriguez, J. J., L. F. Wang, and C. M. Horvath.** 2003. Hendra virus V protein inhibits interferon signaling by preventing STAT1 and STAT2 nuclear accumulation. J. Virol. **77:**11842–11845.
41. **Schlender, J., V. Hornung, S. Finke, M. Gunthner-Biller, S. Marozin, K. Brzozka, S. Moghim, S. Endres, G. Hartmann, and K. K. Conzelmann.** 2005. Inhibition of Toll-like receptor 7- and 9-mediated alpha/beta interferon production in human plasmacytoid dendritic cells by respiratory syncytial virus and measles virus. J. Virol. **79:**5507–5515.
42. **Schnell, M. J., T. Mebatsion, and K. K. Conzelmann.** 1994. Infectious rabies viruses from cloned cDNA. EMBO J. **13:**4195–4203.
43. **Shaw, M. L., A. Garcia-Sastre, P. Palese, and C. F. Basler.** 2004. Nipah virus V and W proteins have a common STAT1-binding domain yet inhibit STAT1 activation from the cytoplasmic and nuclear compartments, respectively. J. Virol. **78:**5633–5641.
44. **Stark, G. R., I. M. Kerr, B. R. Williams, R. H. Silverman, and R. D. Schreiber.** 1998. How cells respond to interferons. Annu. Rev. Biochem. **67:**227–264.
45. **Takeuchi, K., S. I. Kadota, M. Takeda, N. Miyajima, and K. Nagata.** 2003. Measles virus V protein blocks interferon (IFN)-alpha/beta but not IFN-gamma signaling by inhibiting STAT1 and STAT2 phosphorylation. FEBS Lett. **545:**177–182.
46. **Uddin, S., A. Chamdin, and L. C. Platanias.** 1995. Interaction of the transcriptional activator Stat-2 with the type I interferon receptor. J Biol. Chem. **270:**24627–24630.
47. **Uddin, S., A. Sassano, D. K. Deb, A. Verma, B. Majchrzak, A. Rahman, A. B. Malik, E. N. Fish, and L. C. Platanias.** 2002. Protein kinase C-delta (PKC-delta) is activated by type I interferons and mediates phosphorylation of Stat1 on serine 727. J Biol. Chem. **277:**14408–14416.
48. **Ulane, C. M., A. Kentsis, C. D. Cruz, J. P. Parisien, K. L. Schneider, and C. M. Horvath.** 2005. Composition and assembly of STAT-targeting ubiquitin ligase complexes: paramyxovirus V protein carboxyl terminus is an oligomerization domain. J. Virol. **79:**10180–10189.
49. **Vidy, A., M. Chelbi-Alix, and D. Blondel.** 2005. Rabies virus P protein interacts with STAT1 and inhibits interferon signal transduction pathways. J. Virol. **79:**14411–14420.
50. **Wang, Z. W., L. Sarmento, Y. Wang, X. Q. Li, V. Dhingra, T. Tseggai, B. Jiang, and Z. F. Fu.** 2005. Attenuated rabies virus activates, while pathogenic rabies virus evades, the host innate immune responses in the central nervous system. J. Virol. **79:**12554–12565.
51. **Weber, F., G. Kochs, and O. Haller.** 2004. Inverse interference: how viruses fight the interferon system. Viral Immunol. **17:**498–515.
52. **Young, D. F., L. Didcock, S. Goodbourn, and R. E. Randall.** 2000. *Paramyxoviridae* use distinct virus-specific mechanisms to circumvent the interferon response. Virology **269:**383–390.
53. **Zimmermann, A., M. Trilling, M. Wagner, M. Wilborn, I. Bubic, S. Jonjic, U. Koszinowski, and H. Hengel.** 2005. A cytomegaloviral protein reveals a dual role for STAT2 in IFN-γ signaling and antiviral responses. J. Exp. Med. **201:**1543–1553.

JOURNAL OF VIROLOGY, June 2005, p. 7673–7681 Vol. 79, No. 12
0022-538X/05/$08.00+0 doi:10.1128/JVI.79.12.7673–7681.2005

Identification of the Rabies Virus Alpha/Beta Interferon Antagonist: Phosphoprotein P Interferes with Phosphorylation of Interferon Regulatory Factor 3

Krzysztof Brzózka, Stefan Finke, and Karl-Klaus Conzelmann*

Max-von-Pettenkofer Institute and Gene Center, Ludwig-Maximilians-University Munich, D-81377 Munich, Germany

Received 15 November 2004/Accepted 8 February 2005

Rabies virus (RV) of the *Rhabdoviridae* family grows in alpha/beta interferon (IFN)-competent cells, suggesting the existence of viral mechanisms preventing IFN gene expression. We here identify the viral phosphoprotein P as the responsible IFN antagonist. The critical involvement of P was first suggested by the observation that an RV expressing an enhanced green fluorescent protein (eGFP)-P fusion protein (SAD eGFP-P) (S. Finke, K. Brzózka, and K. K. Conzelmann, J. Virol. 78:12333–12343, 2004) was eliminated in IFN-competent HEp-2 cell cultures, in contrast to wild-type (wt) RV or an RV replicon lacking the genes for matrix protein and glycoprotein. SAD eGFP-P induced transcription of the IFN-β gene and expression of the IFN-responsive MxA and STAT-1 genes. Similarly, an RV expressing low levels of P, which was generated by moving the P gene to a promoter-distal gene position (SAD ΔPLP), lost the ability to prevent IFN induction. The analysis of RV mutants lacking expression of truncated P proteins P2, P3, or P4, which are expressed from internal AUG codons of the wt RV P open reading frame, further showed that full-length P is competent in suppressing IFN-β gene expression. In contrast to wt RV, the IFN-inducing SAD ΔPLP caused S386 phosphorylation, dimerization, and transcriptional activity of IFN regulatory factor 3 (IRF-3). Phosphorylation of IRF-3 by TANK-binding kinase-1 expressed from transfected plasmids was abolished in wt RV-infected cells or by cotransfection of P-encoding plasmids. Thus, RV P is necessary and sufficient to prevent a critical IFN response in virus-infected cells by targeting activation of IRF-3 by an upstream kinase.

The alpha/beta interferon (IFN) system, comprising IFN-β and the IFN-α family, represents a crucial defense element of higher organisms that activates both innate and adaptive immunity (for reviews, see references 2, 3, 26, and 35). IFN expression is tightly controlled by latent transcription factors, which are activated upon recognition of intruding viruses by cytoplasmic receptors that sense viral double-stranded RNA (dsRNA) such as retinoic acid-inducible gene I (RIG-I) (58) or through Toll-like receptors sensing exogenous ligands (2). The key factor for initiating an IFN response is interferon regulatory factor 3 (IRF-3), which is constitutively expressed in the cytoplasm of most cell types. Latent IRF-3 is activated by phosphorylation at C-terminal serine residues and then can form dimers that are recruited to the IFN-β enhancer as part of a protein complex that includes the transcription factors ATF-2/c-Jun and NF-κB and coactivators p300/CBP (38, 57, 59). As shown recently, the critical IRF-3 phosphorylation step is executed by kinases of the IKK family, i.e., TANK-binding kinase 1 (TBK-1) which is constitutively expressed, and the inducible IKK-i (22, 30, 41, 49).

Binding of the secreted early IFNs, predominantly IFN-β, to the IFN-α receptor in an autocrine or paracrine fashion activates JAK/STAT-mediated signal transduction pathways that culminate in the expression of a huge set of IFN-stimulated genes (ISGs). Among these is IRF-7, which is activated like IRF-3 and which allows transcription of the "late" IFN-α genes. Several of the ISGs encode enzymes with antiviral function, such as Mx proteins, 2′-5′ oligoadenylate synthetase, PKR, or factors that inhibit cell growth and promote apoptosis, thereby restricting viral spread. Moreover, IFN signaling stimulates mechanisms of the adaptive immune response, including expression of major histocompatibility complex, activation of NK cells, maturation of dendritic cells, and promotion of the T-helper cell response toward the Th1 type.

For members of most virus groups, including negative-strand RNA viruses, specific antagonists of IFN have been identified during the past years. These may interfere with IFN gene induction, IFN signaling, or the activity of ISGs (for recent reviews, see references 3 and 24). Members of the *Paramyxovirinae* subfamily encode small nonessential proteins, such as V and C, which are expressed from the phosphoprotein (P) gene through alternative translation initiation and mRNA editing. V and C proteins interfere with IFN JAK/STAT signaling, rendering the viruses IFN resistant. IFN resistance of respiratory syncytial virus (RSV) of the *Pneumovirinae* subfamily of paramyxoviruses, genus *Pneumovirus*, is mediated by the concerted action of two nonstructural proteins, NS1 and NS2. In this case, however, IFN signaling and expression of IFN-stimulated genes are not significantly affected (7, 47). Intriguingly, both the NS proteins of RSV (8, 50) and the V proteins of *Paramyxovirinae* (44) were recently also shown to be involved in inhibiting IFN induction, but with different targets, since NS proteins prevent activation of IRF-3 (8), whereas V proteins affect activation of NF-κB and IRF-3 (44).

In contrast to paramyxoviruses, members of the *Rhabdoviridae* such as rabies virus (RV) or vesicular stomatitis virus

* Corresponding author. Mailing address: Max-von-Pettenkofer Institute & Gene Center, Feodor-Lynen-Str. 25, D-81377 Munich, Germany. Phone: 49 89 2180 76851. Fax: 49 89 2180 76899. E-mail: conzelma@lmb.uni-muenchen.de.

(VSV) are sensitive to exogenous IFN and therefore must prevent IFN induction. For VSV, the lack of IFN induction was correlated with the activity of the viral matrix (M) protein, which causes a general shutoff of host-directed gene expression (1, 18). Compared to VSV, RV is more slowly growing and much less cytopathic, and a general cell shutoff is not observed, allowing expression of host cell genes throughout infection. We therefore reasoned that RV must encode specific mechanisms for preventing IFN induction.

The RV genome comprises five genes, encoding nucleoprotein (N), phosphoprotein (P), matrix protein (M), glycoprotein (G), and polymerase (L) in the order 3′-N-P-M-G-L-5′. The M and G proteins are predominantly involved in formation of the viral envelope. The N, P, and L proteins are components of the viral ribonucleoprotein, and each of them is essential for accomplishing RNA synthesis (13). The P protein is phosphorylated by cellular kinases (27) and is present in homo-oligomers. It associates both with the L protein to function as a noncatalytic cofactor for RNA polymerization and with the N protein to support specific and proper RNA encapsidation in a chaperone-like way (11, 12, 33). In addition to full-length P (P1), amino-terminally truncated products (P2, P3, and P4) which are translated from internal in-frame AUG initiation codons by a leaky scanning mechanism have been found in infected cells and in purified RV (10). The RV P gene contains a second open reading frame (ORF), termed C in analogy to similar ORFs in VSV P genes. Whereas VSV C proteins have been shown to be expressed (51), the existence of an RV C ORF product is unclear.

We here provide evidence that the P protein of RV, in addition to its above-described functions in RNA synthesis, is responsible for inhibition of IFN induction in RV-infected cells. Replicating RV and full-length P1 expressed from transfected plasmids interfered with phosphorylation of IRF-3 by the upstream kinase TBK-1 such that dimerization of IRF-3 and transcriptional activity was prevented. Although P is crucially required for viral RNA synthesis, it was possible to generate replicating infectious RV that could not prevent IFN induction and that therefore was not viable in IFN-competent cells and tissues. This was achieved by reducing the expression of P to levels sufficient for virus replication but insufficient for blocking IRF-3 activation. Such viruses are particularly interesting for development of live vaccines and oncolytic virus vectors.

MATERIALS AND METHODS

Cells and viruses. Vero (African green monkey kidney) and HEp-2 (human laryngeal epidermoid carcinoma) cells were maintained in Dulbecco's modified Eagle's medium supplemented with 5% fetal calf serum and antibiotics. HEK 293 (human embryonic kidney), 2fTGH, and U3A cells (40) were propagated in Dulbecco's modified Eagle's medium with 10% fetal calf serum, L-glutamine, and antibiotics. U3A cells were incubated in the presence of 250 μg/ml hygromycin. The BSR T7/5 cell clone, which constitutively expresses bacteriophage T7 polymerase (9), was used for RV rescue from cDNA as described previously (20).

Recombinant RV SAD L16 (48), comprising the sequence of the attenuated vaccine strain SAD B19 (14), was used as wild-type (wt) RV. SAD eGFP-P is a recombinant virus encoding an eGFP-P fusion protein (enhanced green fluorescent protein [eGFP] fused to the N terminus of P) instead of the authentic P (19). SAD VB GFP is a recombinant virus containing an extra eGFP gene between the G and L genes. NPgrL virus is a recombinant RV in which the matrix (M)- and glycoprotein (G)-encoding genes are replaced by reporter genes encoding eGFP and DsRed (red fluorescent protein from *Discosoma* sp.) (21).

cDNA constructs. Mutations in the P protein-coding sequences were introduced into the P expression plasmid pTIT-P (20) by using the Chameleon mutagenesis kit (Stratagene) according to the suppliers instructions.

For replacement of the P ORF of the full-length cDNA clone pSAD L16 (48), a pSADΔPsap subclone was generated, in which the coding region of the P gene was replaced by a linker comprising restriction enzyme sites in the following order: SapI-KpnI-NheI-KpnI-SapI. After SapI digestion, ATG and TAA overhangs at the stop and start codons of P allow insertion of SapI-digested PCR products amplified from mutated P-encoding plasmids (primers SADPatg [5′-GACAGAGCTCTTCGATGAGCAAGATCTTTGTCAA-3′] and SADPtaa [5′-TCTCTCGCTCTTCATTAGCAAGATGTATAGCGATCC-3′]) without causing alterations outside the P ORF. In a second cloning step, the plasmids were cut in the N and M genes, and a DNA fragment containing the modified P ORF was inserted in the full-length pSAD L16.

A cDNA full-length clone encoding an additional copy of the RV P gene downstream of the L gene (pSAD PLP; gene order, 3′-N-P-M-G-L-P-5′) was generated by insertion of an N/P gene border copy downstream of the L ORF, followed by a copy of the P-coding sequence. From pSAD PLP, the original P ORF was deleted by replacement of a region spanning from the N to the L gene with the corresponding DNA fragment from pSADΔPsap to generate SAD ΔPLP (gene order, 3′-N-M-G-L-P-5′). The sequences of all constructs are available from the authors upon request. Vaccinia virus-free rescue of recombinant RV from the cDNAs was performed as described previously (20) by transfection of 10 μg of full-length cDNA and plasmids pTIT-N (5 μg), pTIT-P (2.5 μg), and pTIT-L (2.5 μg) in 10^6 BSR T7/5 cells grown in 8-cm^2 culture dishes.

To generate a cytomegalovirus (CMV) promoter-controlled P expression plasmid, pCR3-P, the P ORF was amplified from pTIT-P by PCR (primers P1Acc65I [5′-TATAGGTACCATGAGCAAGATCTTT-3′] and P1NotI3 [5′-ATATGCGGCCGCTTAGCAAGATGTATAGCGATTCAA-3′]) and was inserted in the plasmid pCR3 (Invitrogen). The P gene of bovine respiratory syncytial virus (BRSV) was excised from pTIT P_{RSV} (9) and was also inserted in pCR3, resulting in pCR3-P_{RSV}.

Transfection. For reporter gene assays with infected cells, 1×10^6 Vero cells were seeded in 21-cm^2 cell culture dishes. After 16 h, 8 μg of the reporter plasmid p125luc, p55C1Bluc, p55A2luc (60) (kindly provided by Takashi Fujita, Tokyo), or pAP1luc (Stratagene) was transfected using Lipofectamine 2000 transfection reagent (Invitrogen). As an internal control, 20 ng of pCMV-RL (renilla luciferase) was cotransfected in all experiments. After 6 h the transfected cells were split and infected with viruses at a multiplicity of infection (MOI) of 3 or stimulated with 5×10^3 units of tumor necrosis factor alpha (Sigma) when indicated. After a further 48 h, cell extracts were prepared and subjected to the reporter gene assay. For transfection of HEK293 cells, the calcium phosphate precipitation method (mammalian transfection kit; Stratagene) was used. Cells were seeded into 12-well plates at 4×10^5 cells/well and were transfected after 16 h with 1 μg of p125luc or p55C1Bluc, 2 μg of fl-TBK-1, 0.1 μg of pCMV-RL, and 2 μg of pCR3 vector. For Western blot analyses, HEK293 cells were transfected in six-well plates (1.2×10^6 cells/well) with 3 μg of fl-TBK-1, 6 μg of pCR3-RVP, or empty vector as indicated. After 24 h, cell extracts were prepared and were analyzed by nondenaturing polyacrylamide gel electrophoresis (PAGE) or sodium dodecyl sulfate (SDS)-PAGE and Western blotting.

Luciferase assay. Cell lysates were prepared at the indicated time points and subjected to reporter gene assay using the dual luciferase reporter system (Promega). Luciferase activity was measured in a luminometer (Berthold) according to the supplier's instructions.

Western blots and antibodies. For native PAGE, cell extracts from infected or transfected cell cultures were prepared as described previously (31), and 1.5×10^6 cells were lysed in 100 μl lysis buffer. After centrifugation (14,000 rpm, 4°C, 10 min), 10 μl of the lysate was loaded on the gel. For SDS-PAGE, cells were lysed in cell lysis buffer (62.5 mM Tris, 2% SDS, 10% glycerol, 6 M urea, 5% β-mercaptoethanol, 0.01% bromophenol blue, 0.01% phenol red) at the indicated time points and loaded onto an SDS-10% polyacrylamide gel. Proteins were transferred to a nitrocellulose membrane (Schleicher & Schuell) with a semidry transfer apparatus (OWL Scientific). After incubation with blocking solution (2.5% dry milk and 0.05% Tween 20 in phosphate-buffered saline) at room temperature for 1 h, membranes were incubated overnight with the respective antibodies. The MxA antibody M134 (23) and the mouse polyclonal anti-P serum were kindly provided by Otto Haller and Georg Kochs, Freiburg, and Danielle Blondel, Gif-sur-Yvette, respectively. Primary antibodies to STAT-1 (Cell Signaling), actin (Sigma), IRF-3 (Santa Cruz Biotechnology), IRF-3 Ser386 (phosphorylated) (IBL) were purchased. Secondary antibodies were conjugated with peroxidase, and Western Lightning chemiluminescence reagent (Perkin-Elmer) was used for detection.

RNA analysis. Total RNA from infected cells was isolated with the RNeasy minikit (QIAGEN) according to the manufacturer's instructions. In RNA preparations for reverse transcription-PCR (RT-PCR) analysis, an additional on column DNase digestion was performed according to the supplier's instructions.

Northern blotting and hybridizations with [α-^{32}P]dCTP-labeled cDNAs were performed as described previously (15). Hybridization signals were quantitated by phosphorimaging (Molecular Dynamics Storm). IFN-β-specific RT-PCR was performed on 1 μg RNA isolated after 18 h postinfection (p.i.) with the primers hIFN-β+ (5′-CTCCTCCAAATTGCTCTCCTGTTGTG-3′) and hIFN-β− (5′-AAGATGTTCTGGAGCATCTCATAGATG-3′). As a control, β-actin-specific RT-PCR was performed using the primers βactin+ (5′-GGCATCGTGATGG ACTCC-3′) and βactin2− (5′ CCGCCAGACAGCACTGTGTTGGCGTA-3′).

RESULTS

An RV expressing an eGFP-P fusion protein induces IFN. Infection of interferon-competent cell lines such as HEp-2 with the RV SAD L16 does not result in interferon induction. To identify the responsible viral factors, we screened a series of recombinant RV mutants derived from strain SAD L16 (48) for their ability to suppress IFN induction in HEp-2 cells. Due to the sensitivity of SAD L16 to IFN (47), a more severe attenuation of growth in HEp-2 cells compared to IFN-incompetent BSR T7/5 cells served as a first criterion for the possibility of IFN production. An RV in which eGFP was fused to the N terminus of the P protein, SAD eGFP-P (19) (Fig. 1A), fulfilled this criterion, whereas another RV mutant, expressing eGFP from an extra gene inserted between G and L, did not. In BSR cells, SAD eGFP-P reached titers of 10^6 focus-forming units/ml after 3 days of infection at an MOI of 0,01, whereas HEp-2 cells virtually did not support virus amplification. Microscopic examination revealed initial eGFP-P expression in SAD eGFP-P-infected HEp-2 cells; however, accumulation of viral N and eGFP-P proteins was observed only in BSR cell cultures (Fig. 1B), suggesting induction of IFN by SAD eGFP-P. Notably, infection of HEp-2 cells with an RV lacking both the M and G genes, SAD NPgrL, (21) led to effective expression of the viral N and P proteins (Fig. 1B), demonstrating that the M protein is not required for virus replication in HEp-2 cells.

To confirm that growth restriction of SAD eGFP-P in HEp-2 cells is correlated to production of IFN, we checked the presence of IFN-β mRNAs by RT-PCR and the biological effects of IFN by demonstrating expression of ISGs. IFN-β RNA was detectable in SAD eGFP-P-infected cells but not in SAD L16-infected cells at 24 h p.i. (Fig. 1C). In accordance with this finding, expression of the IFN-inducible MxA protein and an up-regulation of STAT-1 levels were observed only in SAD eGFP-infected HEp-2 cell cultures and not in cultures infected with wt RV or NPgrL (Fig. 1C). From these results it appeared that RV P gene products are important in preventing IFN production in RV-infected cells, whereas the viral M protein is not required.

Induction of IFN by an RV expressing low levels of P. To further support the notion that RV P is critical in preventing IFN production in virus-infected cells, a recombinant RV was engineered to express low levels of P. To this end, we took advantage of the typical stop-start mechanism of nonsegmented negative-strand RNA viruses yielding a transcription gradient. In SAD ΔPLP, the viral genome organization was changed such that the P gene was moved from the second to the most promoter-distal fifth position (genome organization NMGLP) (Fig. 2A). As a control, SAD PLP (gene order, NPMGLP) was generated, retaining the P gene in its original position but containing an extra P copy downstream of L like in SAD ΔPLP. Viable virus was rescued from both cDNA constructs. As revealed by Northern hybridization, much less P

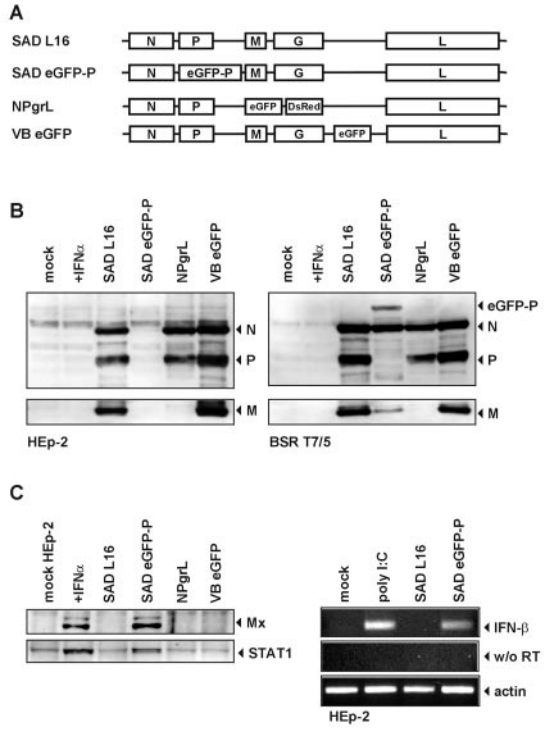

FIG. 1. SAD eGFP-P induces IFN-β gene expression. (A) Genome organization of wt SAD L16; SAD eGFP-P, expressing a P protein with an N-terminal eGFP-moiety; NPgrL virus, with M and G genes replaced with eGFP and DsRed genes; and SAD VB eGFP, containing an extra eGFP gene. (B) Whole-cell extracts of BSR T7/5 and HEp-2 cells were harvested at 48 h p.i. (MOI of 1) and analyzed by Western blotting for expression of the viral N, P, and M proteins. In contrast to infection of BSR cells (right panel), SAD eGFP-P produced low levels of N and eGFP-P protein in HEp-2 cells (left panel). (C) SAD eGFP-P infection of HEp-2 cells induces transcription of IFN-β mRNA as shown by RT-PCR (right panel). and up-regulation of MxA and STAT1 proteins as shown by Western blotting (left panel).

mRNA was transcribed in SAD ΔPLP-infected cells than in SAD L16- or SAD PLP-infected cells. In contrast, the amounts of N mRNAs were more similar for all viruses (Fig. 2B). Also, the amount of P protein was greatly lower in SAD ΔPLP-infected cells than in cells infected with the control viruses, as shown by Western blot analyses (Fig. 2B). A decelerated accumulation of other virus proteins such as N, M, and G and of viral RNAs further indicated that the reduced levels of P protein were limiting RNA synthesis of SAD ΔPLP.

Concordantly, growth of SAD ΔPLP in BSR cell cultures lagged behind that of SAD L16 and SAD PLP; however, final infectious titers of 10^7 focus-forming units/ml at 3 days p.i. were only 10-fold lower than those of wt RV (Fig. 2D). Compared to SAD eGFP-P, however, SAD ΔPLP yielded 10-fold-higher titers, indicating an RNA synthesis more severely affected by the eGFP-P fusion protein.

To investigate the effect of reduced P levels on the production of IFN, HEp-2 cells were infected in parallel with SAD L16, SAD PLP, SAD ΔPLP, and SAD eGFP-P as a positive control for IFN induction. Whereas SAD L16 and SAD PLP rapidly amplified to titers of greater than 10^6 after 3 days of infection, SAD ΔPLP and SAD eGFP-P were not able to productively grow in HEp-2 cells (Fig. 2E). RT-PCR and

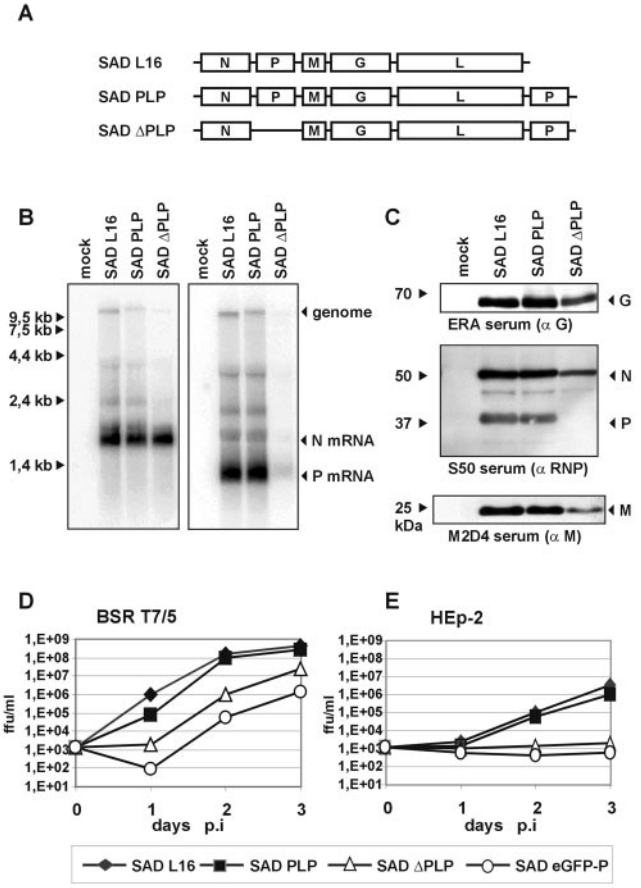

FIG. 2. The level of P protein is crucial for growth of RV in IFN-competent cells. (A) Genome organization of recombinant RV. SAD PLP carries an extra copy of the P gene downstream of L (gene order, 3′-N-P-M-G-L-P-5′). In SAD ΔPLP, the P gene downstream of N in SAD PLP was deleted, resulting in a virus with a single P gene copy downstream of L (gene order, 3′-N-M-G-L-P-5′). (B) Northern blot hybridization with N and P gene-specific cDNA of RNA from BSR T7/5 cells infected for 24 h at an MOI of 1 with the indicated viruses. SAD ΔPLP virus produces lower levels of P mRNA than SAD L16. (C) Expression of RV N, P, M, and G proteins was analyzed in Western blots of cell extracts from BSR T7/5 at 24 h p.i. at an MOI of 1. (D and E) Single-step growth curves were performed on BSR T7/5 cells (D) and on HEp-2 cells (E) after infection with the indicated viruses at an MOI of 0.01. ffu, focus-forming units.

Western blot analyses of ISGs confirmed that this failure was correlated with the presence of IFN-β mRNAs (Fig. 3A) and with stimulation of MxA and STAT-1 expression. In contrast to those of SAD L16, proteins of SAD ΔPLP were hardly detectable in HEp-2 cells at 48 h p.i. (Fig. 3B). The inability of SAD ΔPLP to inhibit IFN expression is therefore correlated to a reduction of P levels below a critical threshold. To further demonstrate that the IFN-induced establishment of an antiviral state is responsible for the observed growth restriction of SAD ΔPLP, 2fTGH cells and a mutant of 2fTGH, U3A, which lack STAT-1 and therefore do not respond to IFN (40), were infected in parallel. Whereas SAD L16 replicated effectively in both cell lines, accumulation of SAD ΔPLP proteins was observed only in the nonresponding U3A cells (Fig. 3C).

IFN-antagonistic activity of full-length P (P1). In addition to full-length P encoded by the P ORF (P1), N-terminally truncated forms of the P protein can be expressed from the RV P gene, due to ribosomal leaky scanning and internal translation initiation (10). Since the IFN-inducing phenotype of SAD eGFP-P could be due to the lack of truncated P products from the eGFP-P fusion gene, it was important to show IFN-antagonistic activity of the full-length P1. To generate an RV encoding only full-length P1, SAD P1xxx, the first three internal methionine codons of the SAD P ORF (codons 20, 53, and 83), which could serve for translation of P2, P3, and P4, respectively, were changed to isoleucine codons by site-directed mutagenesis. In addition, constructs expressing P1 along with one of the truncated P products (SAD P12xx, P1x3x, and P1xx4) were generated. In another construct, SAD PΔC, the methionine initiation codon of the internal C ORF of the SAD P gene was destroyed by a T384C base pair exchange, leaving the P protein sequence unchanged (Fig. 4A).

All mutant cDNAs could be rescued into viable virus displaying the predicted protein expression pattern. Only full-length P1 was detectable in cells infected with SAD P1xxx, and P1 along with P2 was detectable in SAD P12xx-infected cells. A slightly increased expression of P3 and P4 was observed for SAD P1x3x and SAD P1xx4, respectively, consistent with increased translation initiation at downstream methionine codons when upstream initiation codons are missing (Fig. 4B). The growth kinetics of the mutants in BSR cells, including SAD PΔC, did not greatly differ from that of SAD L16, although the triple mutant SAD P1xxx tended to lag behind at

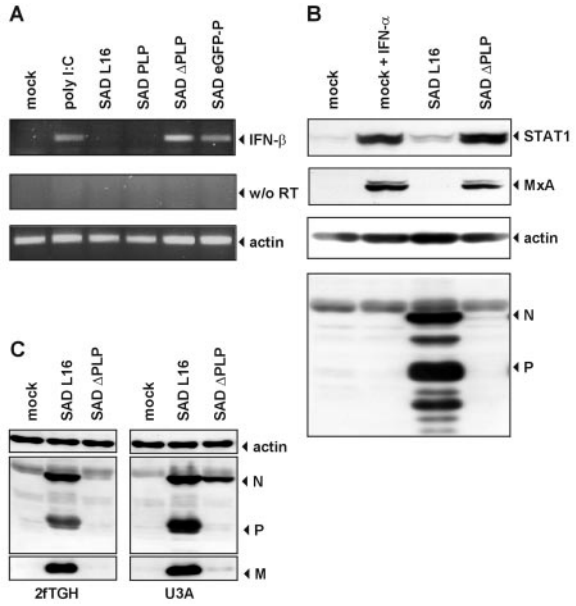

FIG. 3. The level of P protein is crucial for IFN-β gene expression. (A) SAD ΔPLP effectively induces transcription of IFN-β mRNA in HEp-2 cells as shown by RT-PCR. Mock-infected cells were stimulated by poly(I · C) transfection. RNA was isolated 20 h after infection at an MOI of 1. For RT-PCR, primers specific for IFN-β or β-actin (as a loading control) were used. (B) SAD ΔPLP infection induces an antiviral response and up-regulates expression of MxA and STAT1 as shown by Western blotting at 48 h p.i. Only in wt SAD L16-infected cells were abundant amounts of RV N and P proteins detected.(C) Infection (MOI of 1) with SAD ΔPLP of U3A cells lacking STAT-1 leads to accumulation of viral proteins, in contrast to the case for the parental STAT-1-containing 2fTGH cells.

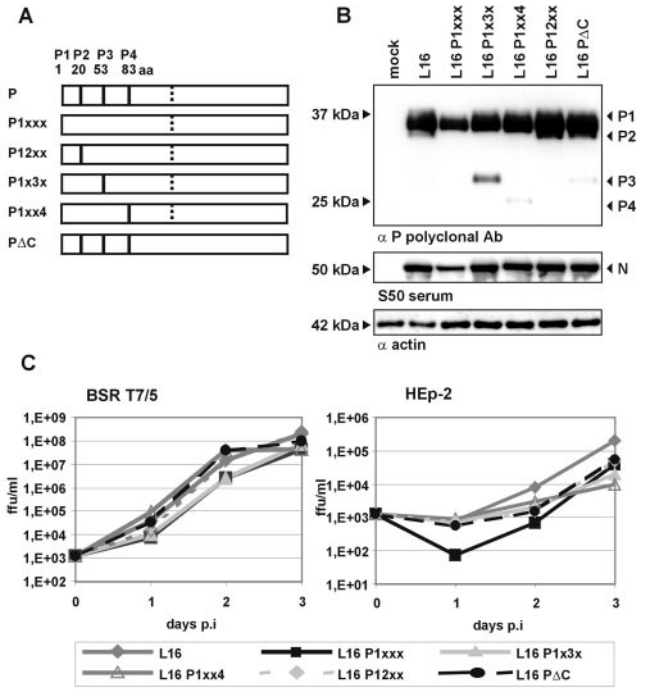

FIG. 4. Mutation of internal AUG start codons does not abrogate IFN-antagonistic activity of P. (A) Schematic representation of mutations introduced into the P protein. Solid vertical bars represent authentic methionine codons. Lack of the bar indicates substitution with isoleucine codons. Dotted vertical bars represent the AUG codon of the hypothetical C of P ORF + 1. In SAD PΔC, the AUG codon was mutated to ACG. (B) Protein synthesis of RV encoding mutated P proteins. BSR T7/5 cells were infected with the indicated viruses at an MOI of 1. Cell extracts were analyzed by Western blotting at 24 h p.i. P and N proteins were detected by mouse polyclonal anti-P serum and rabbit polyclonal serum S50, respectively. (C) Single-step growth curves of RVs lacking short forms of P protein on BSR T7/5 and HEp-2 cells infected at an MOI of 0.01. RV SAD P1xxx, lacking P2, P3, and P4, grew productively in HEp-2 cells.

early time points of infection. This indicates some attenuating effect of the mutations introduced into P. However, the virus reached comparable infectious titers at 3 days p.i. (Fig. 4C). Most importantly, all mutants were able to grow productively in the IFN-competent HEp-2 cells. Some lag phase was observed again for SAD P1xxx; however, the virus caught up and was amplified to titers similar to those of other P mutants. Thus, the full-length P1 expressed from SAD P1xxx is active in preventing IFN induction to an extent that is sufficient to permit virus growth in HEp-2 cells.

RV prevents phosphorylation of IRF-3 by TBK-1. Induction of the IFN-β promoter is known to require the binding of transcription factors NF-κB, IRF-3, and AP-1 (dimers of ATF-2 or heterodimers of ATF-2/c-Jun), which are activated in response to virus infection. To address the mechanisms utilized by RV to prevent IFN induction, we first made use of reporter gene assays in which a plasmid-encoded luciferase gene is controlled by the entire IFN-β promoter (p125luc) or by individual regulatory elements responsive to AP-1 (pAP1luc), NF-κB (p55A2luc), or IRF-3 (p55C1Bluc). Infection of Vero cells with SAD L16 had very little effect on luciferase expression from p125luc- and p55C1Bluc-driven reporter plasmids, containing the native IFN-β promoter and the IRF-3-responsive element, respectively, compared to mock infection of cells. However, infection with SAD ΔPLP resulted in 25- and 5-fold increases of luciferase activity from p125luc and p55C1Bluc, respectively. This indicated that RV P is able to inhibit transcriptional activity of IRF-3. In contrast, an inhibition of NF-κB or AP-1 was not apparent. Whereas SAD L16 caused similar three- to fourfold increases of luciferase activity from p55A2luc and pAP1luc, an even less effective stimulation was observed in SAD ΔPLP-infected cells (Fig. 5A).

To further address the failure of IRF-3-dependent transcription in RV-infected cells, we analyzed the activation status of IRF-3. C-terminal phosphorylation of IRF-3 by TBK-1 or the inducible IKK-i is a prerequisite for IRF-3 dimerization, nuclear import, association with CBP/p300 coactivators, and activation of IFN-β gene transcription. The IRF-3 status in extracts from virus-infected HEp-2 cells was analyzed by native PAGE. In contrast to mock- and SAD L16-infected cells, in which only monomeric IRF-3 was detectable, a prominent band of IRF-3 dimers appeared in cells infected with SAD ΔPLP (Fig. 5B). Western blotting with a serum specific for S386-phospho-IRF-3 confirmed that only the IRF-3 dimers were phosphorylated at S386, which is known as a target residue for TBK-1 phosphorylation (42). Thus, RV has the ability to selectively block the IRF-3 phosphorylation whereas SAD ΔPLP does not, because of insufficient expression of P protein.

To verify that RV P is able to directly inhibit TBK-1-mediated IRF-3 phosphorylation, we expressed the authentic P gene and P1xxx from transfected plasmids and investigated the effect on TBK-1-stimulated expression of luciferase from the IFN-β promoter in p125luc. As a control for the specificity of inhibition, a plasmid encoding the P protein of BRSV was used. Transfection of a TBK-1-encoding plasmid into cells transfected in addition with vector lacking an insert, or with the BRSV P-encoding plasmid, stimulated luciferase activity 40- to 50-fold. Cotransfection of pRV-P and pRV-P1xxx, however, abolished luciferase activity from p125 almost completely (Fig. 6A, left panel). Similarly, transfection of P abolished TBK-1-mediated expression of luciferase from p55C1Bluc containing only the IRF-3-responsive elements. This occurred in a dose-dependent manner, as evidenced by cotransfection of TBK-1 with decreasing amounts of P-encoding plasmids (Fig. 6A, right panel). The inability of TBK-1 to stimulate luciferase expression from p125luc and p55C1Bluc in the presence of RV P was correlated with the lack of IRF-3 phosphorylation, as visualized in Western blot experiments with cell extracts from transfected 293 cells (Fig. 6B). Whereas expression of TBK-1 resulted in appearance of S386-phosphorylated IRF-3 dimers, phosphorylation and dimerization of IRF-3 were not detectable in cells cotransfected with TBK-1- and P-encoding plasmids. In summary, these data show that RV P prevents IFN induction in virus-infected cells by obstructing phosphorylation of IRF-3 through its kinase, TBK-1.

DISCUSSION

In this study we present evidence that the phosphoprotein P of RV is an IFN antagonist preventing transcription of IFN-β in virus-infected cells. Viruses with reduced P expression such as SAD ΔPLP cannot sufficiently interfere with IFN-β transcription in HEp-2 cells. A critical IFN response is therefore

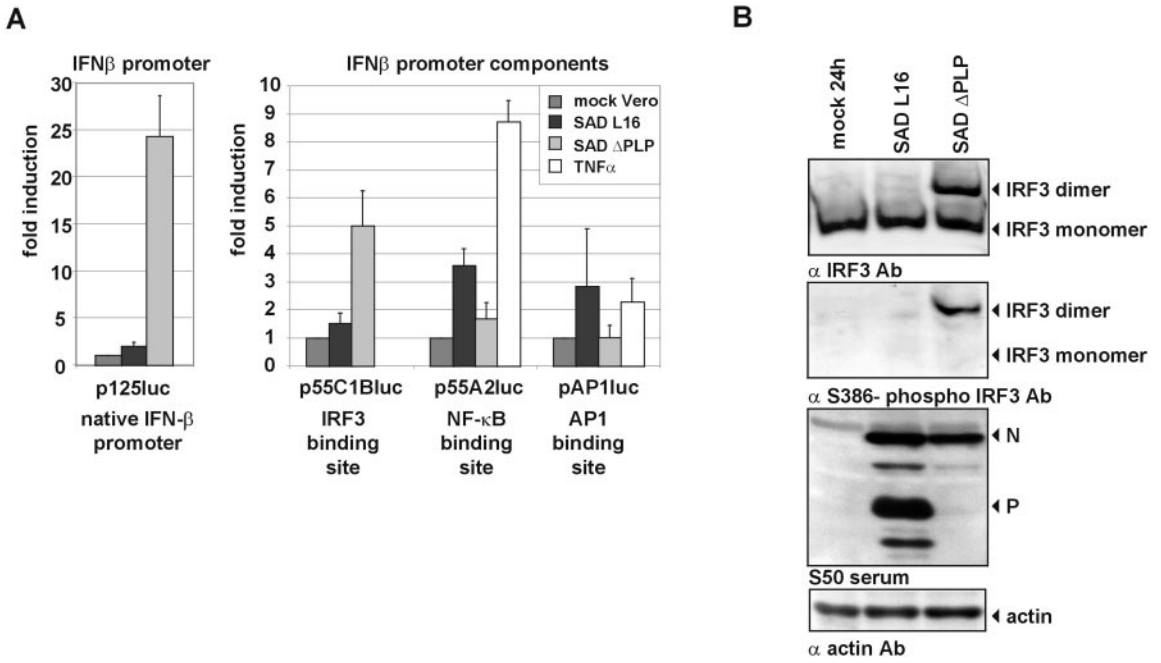

FIG. 5. Rabies virus targets the IRF-3 activation pathway. (A) Vero cells were transfected with reporter plasmid p125luc, p55C1Bluc, p55A2luc, or pAP1luc and infected at an MOI of 3 with SAD L16 or SAD ΔPLP. Cell lysates were analyzed using the dual luciferase reporter system (Promega) for luciferase activity at 48 h p.i. In contrast to SAD ΔPLP, SAD L16 is able to prevent expression of firefly luciferase from plasmids containing the IFN-β promoter (p125luc) and the IRF-3 binding site (p55C1Bluc). In contrast to IRF-3, the activities of NF-κB and AP-1 are not further stimulated in SAD ΔPLP-infected cells compared to SAD L16-infected cells. Incubation of cells with tumor necrosis factor alpha was used as a positive control. Error bars indicate standard deviations. (B) Dimerization and Ser386 phosphorylation of IRF-3 in SAD ΔPLP-infected cells. HEp-2 cells were infected at an MOI of 1 and cell extracts were analyzed at 24 h p.i. by native PAGE and Western blotting. In contrast to SAD ΔPLP, wt SAD L16 prevents IRF-3 dimerization and phosphorylation on Ser386. The same cell lysates were analyzed by SDS-PAGE for expression of viral N and P proteins.

activated, which prohibits productive virus replication. A substantial contribution of the M protein to IFN escape of RV, as observed for VSV (1), could be excluded, since RV replicons encoding N, P, and L did not induce an IFN response. IFN induction by SAD ΔPLP was correlated with the activation of the critical transcription factor IRF-3, whereas the activities of NF-κB and AP-1 were unchanged, demonstrating that the IRF-3 activation pathway is specifically blocked in RV-infected cells.

Activation of IRF-3 in virus-infected cells depends on the recognition of viruses by cytosolic receptors and on signal transduction pathways leading from recognition to activation of IRF-3. Recently, the RNA helicase RIG-I was identified as key in sensing viral dsRNA of Newcastle disease virus and in subsequent activation of IRF-3 and NF-κB (58). Downstream signaling by RIG-I required an active helicase function and caspase recruitment domains (58), suggesting the involvement of caspase recruitment domain-containing adapter proteins that relay signals to the IRF-3 kinase TBK-1 or IKK-i.

To circumvent IFN, viruses must either avoid their recognition and eliciting of an alert or target steps of the excited signaling pathways. Recognition of influenza A virus RNA and thus activation of IRF-3 are prevented by the viral NS1 protein, which has a pronounced dsRNA binding activity and thereby makes the critical virus pattern inaccessible to dsRNA receptors (16, 53). Although no direct RNA binding activity has been reported for RV P, it is an important structural component of the RV RNP and serves as a chaperone for proper encapsidation of RNA into N protein. Accordingly, it could be speculated that a critical level of RV P may be important for proper masking of viral RNAs in the RNA complex. Although it is formally not excluded that P may improve such camouflage, the fact that P is active at a downstream step of the IRF-3 activation pathway (see below) argues in favor of recognition of cytoplasmic RV RNPs by sensing molecules such as RIG-I, activation of the pathway, and a downstream inhibition at the step of IRF-3 phosphorylation. Indeed, activation of IRF-3 by replicating RNP complexes of VSV has been demonstrated recently (54).

Signaling pathways triggered by recognition of cytosolic virus and of dsRNA and lipopolysaccharide by Toll-like receptors 3 and 4, respectively, lead to activation of IRF-3 by two IKK-related kinases, TBK-1 and IKK-i (22, 30, 41, 49). The constitutively expressed TBK-1 may be the more important kinase for IRF-3 activation, since the IFN response of TBK-1 knockout mice is severely affected (30, 41). Activation of cytoplasmic IRF-3 involves phosphorylation of multiple serine residues at the C terminus of the protein which allow dimerization of IRF-3, accumulation in the nucleus, and binding of DNA in a complex including transcription factors ATF-2/c-Jun (AP-1) and NF-κB and coactivators CBP/p300 (38, 39, 45, 52, 57, 59). Evidence is accumulating that the phosphorylation status of the Ser386 residue critically determines the transcriptional activity of IRF-3, since TBK-1 can phosphorylate Ser386 and IRF-3 phosphorylated at Ser386 is observed exclusively within dimers. Moreover, mutation at Ser386 abolishes the dimerization potential of IRF-3 (42). In RV-infected cells,

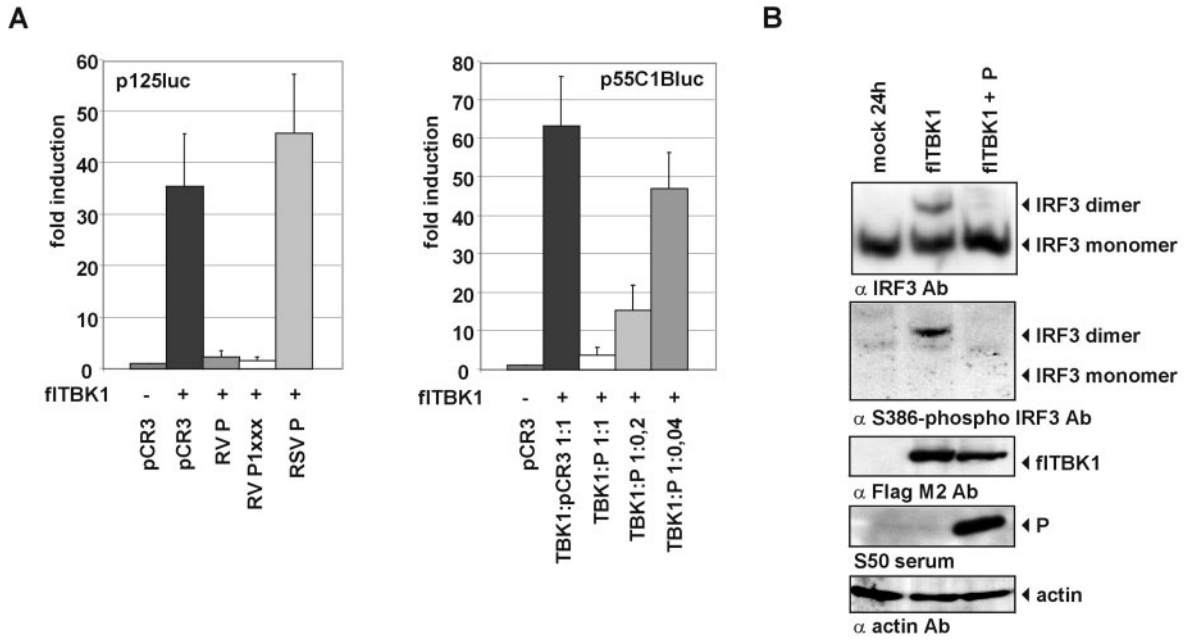

FIG. 6. Expression of P is sufficient to prevent TBK-1-mediated IFN-β induction. (A) HEK 293 cells were transfected with expression plasmids encoding the indicated genes and reporter plasmids harboring the firefly luciferase gene under control of the IFN-β promoter and renilla luciferase controlled by the CMV promoter. Luciferase activities were determined at 48 h posttransfection. Cotransfection of P or of P1xxx with TBK-1 inhibited activation of the IFN-β promoter almost completely. The P protein of BRSV (RSV P) was used as a control that is not able to inhibit TBK-1-mediated activation of the p125luc reporter plasmid (left panel). The inhibition of TBK-1-mediated activation of IRF-3 by RV P is dose dependent as revealed by luciferase expression from p55C1Bluc (right panel). Error bars indicate standard deviations. (B) Expression of RV P inhibits TBK-1-mediated dimerization of endogenous IRF-3 and phosphorylation of IRF-3 at Ser386. Cell extracts were harvested at 24 h posttransfection of TBK-1 or TBK-1 and P-encoding plasmids and were analyzed by native PAGE and Western blotting. Expression of Flag-tagged TBK-1 (fl-TBK1), RV P, and β-actin was confirmed by SDS-PAGE and Western blot analysis of the same lysates.

IRF-3 is not activated, as demonstrated by reporter gene analyses using plasmids controlled by the IFN-β promoter (p125luc) or the IRF-3 binding part of the IFN-β promoter (p55C1Bluc). The lack of transcriptional activity correlates with the absence of Ser386-phosphorylated IRF-3 and of IRF-3 dimers. In contrast, in SAD ΔPLP-infected cells, IRF-3-dependent expression of reporter genes was possible, and Ser386-phosphorylated IRF-3 was readily detectable (Fig. 5). As predicted, S386 phosphorylation was observed only in IRF-3 dimers and not in monomers.

How the activity of TBK-1 by TRIF or by putative adapters of the cytosolic IFN-inducing pathway is regulated is not known. However, overexpression of TBK-1 in cells is sufficient for IRF-3 activation (22). We have utilized this feature to demonstrate that the IFN-inhibitory activity of RV involves a downstream target of the IRF-3 activation pathway. In addition, this assay revealed that RV P alone is sufficient for inhibiting IRF-3 activation. As a control, the phosphoprotein P of BRSV was used, which has comparable functions in RNA synthesis and encapsidation of viral RNA. As we have shown previously, the BRSV nonstructural proteins NS1 and NS2 are critical for preventing IRF-3 activation (8), and therefore a corresponding activity of the RSV P protein appeared unlikely. In contrast to BRSV P, or empty vector, transfection of expression plasmids comprising the SAD L16 P ORF led to a drastic reduction of TBK-1-mediated transcriptional activity. The same effect was observed after expression of pP1xxx, in which the initiation codons of P2, P3, and P4 were deleted, confirming activity of full-length P. Further evidence that P alone is responsible for the phenotype observed in RV-infected cells was obtained by investigating the IRF-3 phosphorylation and dimerization status after overexpression of TBK-1 in the presence of P. These experiments confirmed that P precludes the critical S386 phosphorylation of IRF-3 by TBK-1 such that dimerization and transcriptional activity are prevented. Further experiments are needed to reveal the molecular mechanisms involved in blocking IRF-3 phosphorylation. From preliminary experiments it appears that a direct and strong interaction of P with either TBK-1 or IRF-3 is unlikely, since coimmunoprecipitations have been unsuccessful so far. Distinct colocalization of P and TBK-1 or IRF-3 in virus-infected cells has also not been observed, suggesting indirect mechanisms.

Activation of IRF-3 is a key step in initiating an antiviral innate and adaptive immune response and is apparently nonredundant in most tissues. The identification of proteins from negative-strand RNA viruses that interfere with IRF-3 activation is therefore not surprising. In most cases, small accessory proteins which are not strictly required for virus replication and which have "luxury functions" (34) are active as IFN antagonists. As first shown for influenza A virus, the NS1 protein hides viral dsRNA that could serve as a trigger for IRF-3 activation and IFN induction (53). However, RNA binding-deficient mutants still have some IRF-3-inhibiting capacity, suggesting additional activities (16). For the influenza B virus NS1 C terminus, an activity independent of RNA binding has been demonstrated, supporting the idea that influenza virus NS1 holoproteins combine multiple activities in inhibiting

IRF-3 (17). *Pneumovirus* NS1 and NS2 proteins, which are encoded by two extra genes, and *Paramyxovirinae* V and C proteins, which are encoded on P genes, are active in preventing both IFN response (reviewed in reference 24) and IFN induction (29, 36, 44). Whereas the RSV NS proteins are involved in targeting the IRF-3 pathway (8), V and C proteins appear to prevent activation of both IRF-3 and NF-κB (29, 36, 44), suggesting that they target different steps of the pathway.

The present work identifies an essential rhabdovirus protein as a specific IFN antagonist blocking activation of IRF-3. Interestingly, the Ebola virus VP35, which corresponds to the P protein of other *Mononegavirales* with respect to RNA synthesis and RNA encapsidation, has previously been shown to interfere with IFN induction and IRF-3 activation when expressed from transfected plasmids (4, 5, 28). This suggests that *Filoviridae* target a similar or more upstream target of the pathway.

Our data further indicate that the full-length RV P is active in preventing IFN induction. A recombinant virus expressing a P gene in which three internal methionine codons that in the wt P serve for internal translation initiation were exchanged for isoleucine codons (SAD P1xxx) was viable in BSR cells. Therefore, the N-terminally truncated P products are not essential for virus replication, as indicated previously by the viability of SAD eGFP-P (19). A slower growth of SAD P1xxx compared to wt RV may indicate that the functions of the P1xxx protein in RNA synthesis and assembly are somehow affected by the three Met-Ile mutations. Importantly, SAD P1xxx was able to grow in HEp-2 cells, showing that expression of P1xxx is sufficient to counteract IFN in virus-infected cells. On the other hand, this does not mean that the truncated P products may not aid P in blocking IRF-3 activation. The major difference from full-length P is that they do not possess the N-terminal L binding site (12), but oligomerization and binding to N should be possible (11). In addition, the binding domains for dynein light chain-1 (LC-8) (32, 43, 46) and the IFN-induced promyelocytic leukemia protein are retained (6). Expression experiments are under way to determine the activity of curtailed P proteins fragments to identify the minimal domains of P able to counteract IRF-3 activation.

A more demanding task will be the dissociation of P functions and the identification of mutations that eliminate the IFN-antagonistic function of P without significantly impairing its essential roles in virus RNA synthesis and assembly. The IFN-inducing SAD ΔPLP virus still expresses the authentic P gene, although at much lower levels. The low levels of P do not greatly limit gene expression, replication, and growth in BSR cells (Fig. 2D), but they are not sufficient to inhibit induction of an IFN response. In case of SAD eGFP-P, both reduced levels of the P fusion protein (Fig. 1B) and the impediment of P functions by the N-terminal eGFP moiety may be responsible for the limited growth and the inability to prevent IFN induction. Indeed, from previous experiments involving complementation of P-deficient RV, it appears that the eGFP-P fusion protein has severe defects in mRNA synthesis, while virus formation is well supported. In contrast, a protein in which eGFP was fused to the C terminus of P, P-eGFP, supported transcription well but had defects in virus assembly (19).

The possibility of generating recombinant RVs that are not able to prevent an IFN response in infected hosts, such as SAD ΔPLP, holds promise for the development of safe, attenuated live vaccines. Since alpha/beta IFN is able to foster the development of an adaptive immune response (for a review, see reference 55), such viruses should induce a potent adaptive immune response. Indeed, a potent adjuvant function of virus-induced early IFN in vivo is suggested by the high immunogenicity of viruses lacking critical IFN antagonists, such as influenza virus (25) or BRSV (56). Another approach in which the identification and knockdown of rhabdovirus IFN antagonists are important is oncolytic virotherapy (for a recent review, see reference 37). In contrast to nonmalignant tissue, many tumors are nonresponsive to IFN. Viruses that both induce the production of IFN and are susceptible to its antiviral effects should therefore preferentially replicate in malignant tissue and may serve as a basis for development of promising therapeutics.

ACKNOWLEDGMENTS

We thank Nadin Hagendorf for perfect technical assistance and S. Marozin for TBK-1 cDNA. The reporter plasmids p125luc, p55C1Bluc, and p55A2luc were a generous gift of Takashi Fujita, Tokyo, Japan. The MxA antibody M134 and the mouse polyclonal anti-P serum were kindly provided by Otto Haller and Georg Kochs, Freiburg, and Danielle Blondel, Gif-sur-Yvette, respectively.

This work was supported by the Deutsche Forschungsgemeinschaft through SFB 455, "Viral functions and immune modulation" project A3, and FI 941/1-1.

REFERENCES

1. **Ahmed, M., M. O. McKenzie, S. Puckett, M. Hojnacki, L. Poliquin, and D. S. Lyles.** 2003. Ability of the matrix protein of vesicular stomatitis virus to suppress beta interferon gene expression is genetically correlated with the inhibition of host RNA and protein synthesis. J. Virol. **77:**4646–4657.
2. **Akira, S., and K. Takeda.** 2004. Toll-like receptor signalling. Nat. Rev. Immunol. **4:**499–511.
3. **Basler, C. F., and A. Garcia-Sastre.** 2002. Viruses and the type I interferon antiviral system: induction and evasion. Int. Rev. Immunol. **21:**305–337.
4. **Basler, C. F., A. Mikulasova, L. Martinez-Sobrido, J. Paragas, E. Muhlberger, M. Bray, H. D. Klenk, P. Palese, and A. Garcia-Sastre.** 2003. The Ebola virus VP35 protein inhibits activation of interferon regulatory factor 3. J. Virol. **77:**7945–7956.
5. **Basler, C. F., X. Wang, E. Muhlberger, V. Volchkov, J. Paragas, H. D. Klenk, A. Garcia-Sastre, and P. Palese.** 2000. The Ebola virus VP35 protein functions as a type I IFN antagonist. Proc. Natl. Acad. Sci. USA **97:**12289–12294.
6. **Blondel, D., T. Regad, N. Poisson, B. Pavie, F. Harper, P. P. Pandolfi, H. De The, and M. K. Chelbi-Alix.** 2002. Rabies virus P and small P products interact directly with PML and reorganize PML nuclear bodies. Oncogene **21:**7957–7970.
7. **Bossert, B., and K. K. Conzelmann.** 2002. Respiratory syncytial virus (RSV) nonstructural (NS) proteins as host range determinants: a chimeric bovine RSV with NS genes from human RSV is attenuated in interferon-competent bovine cells. J. Virol. **76:**4287–4293.
8. **Bossert, B., S. Marozin, and K. K. Conzelmann.** 2003. Nonstructural proteins NS1 and NS2 of bovine respiratory syncytial virus block activation of interferon regulatory factor 3. J. Virol. **77:**8661–8668.
9. **Buchholz, U. J., S. Finke, and K. K. Conzelmann.** 1999. Generation of bovine respiratory syncytial virus (BRSV) from cDNA: BRSV NS2 is not essential for virus replication in tissue culture, and the human RSV leader region acts as a functional BRSV genome promoter. J. Virol. **73:**251–259.
10. **Chenik, M., K. Chebli, and D. Blondel.** 1995. Translation initiation at alternate in-frame AUG codons in the rabies virus phosphoprotein mRNA is mediated by a ribosomal leaky scanning mechanism. J. Virol. **69:**707–712.
11. **Chenik, M., K. Chebli, Y. Gaudin, and D. Blondel.** 1994. In vivo interaction of rabies virus phosphoprotein (P) and nucleoprotein (N): existence of two N-binding sites on P protein. J. Gen. Virol. **75:**2889–2896.
12. **Chenik, M., M. Schnell, K. K. Conzelmann, and D. Blondel.** 1998. Mapping the interacting domains between the rabies virus polymerase and phosphoprotein. J. Virol. **72:**1925–1930.
13. **Conzelmann, K. K.** 1998. Nonsegmented negative-strand RNA viruses: genetics and manipulation of viral genomes. Annu. Rev. Genet. **32:**123–162.
14. **Conzelmann, K. K., J. H. Cox, L. G. Schneider, and H. J. Thiel.** 1990. Molecular cloning and complete nucleotide sequence of the attenuated rabies virus SAD B19. Virology **175:**485–499.
15. **Conzelmann, K. K., J. H. Cox, and H. J. Thiel.** 1991. An L (polymerase)-deficient rabies virus defective interfering particle RNA is replicated and transcribed by heterologous helper virus L proteins. Virology **184:**655–663.

16. **Donelan, N. R., C. F. Basler, and A. Garcia-Sastre.** 2003. A recombinant influenza A virus expressing an RNA-binding-defective NS1 protein induces high levels of beta interferon and is attenuated in mice. J. Virol. **77:**13257–13266.
17. **Donelan, N. R., B. Dauber, X. Wang, C. F. Basler, T. Wolff, and A. Garcia-Sastre.** 2004. The N- and C-terminal domains of the NS1 protein of influenza B virus can independently inhibit IRF-3 and beta interferon promoter activation. J. Virol. **78:**11574–11582.
18. **Ferran, M. C., and J. M. Lucas-Lenard.** 1997. The vesicular stomatitis virus matrix protein inhibits transcription from the human beta interferon promoter. J. Virol. **71:**371–377.
19. **Finke, S., K. Brzózka, and K. K. Conzelmann.** 2004. Tracking fluorescence-labeled rabies virus: enhanced green fluorescent protein-tagged phosphoprotein p supports virus gene expression and formation of infectious particles. J. Virol. **78:**12333–12343.
20. **Finke, S., and K. K. Conzelmann.** 1999. Virus promoters determine interference by defective RNAs: selective amplification of mini-RNA vectors and rescue from cDNA by a 3′ copy-back ambisense rabies virus. J. Virol. **73:** 3818–3825.
21. **Finke, S., R. Mueller-Waldeck, and K. K. Conzelmann.** 2003. Rabies virus matrix protein regulates the balance of virus transcription and replication. J. Gen. Virol. **84:**1613–1621.
22. **Fitzgerald, K. A., S. M. McWhirter, K. L. Faia, D. C. Rowe, E. Latz, D. T. Golenbock, A. J. Coyle, S. M. Liao, and T. Maniatis.** 2003. IKKepsilon and TBK1 are essential components of the IRF3 signaling pathway. Nat. Immunol. **4:**491–496.
23. **Flohr, F., S. Schneider-Schaulies, O. Haller, and G. Kochs.** 1999. The central interactive region of human MxA GTPase is involved in GTPase activation and interaction with viral target structures. FEBS Lett. **463:**24–28.
24. **Garcia-Sastre, A.** 2004. Identification and characterization of viral antagonists of type I interferon in negative-strand RNA viruses. Curr. Top. Microbiol. Immunol. **283:**249–280.
25. **Garcia-Sastre, A., A. Egorov, D. Matassov, S. Brandt, D. E. Levy, J. E. Durbin, P. Palese, and T. Muster.** 1998. Influenza A virus lacking the NS1 gene replicates in interferon-deficient systems. Virology **252:**324–330.
26. **Goodbourn, S., L. Didcock, and R. E. Randall.** 2000. Interferons: cell signalling, immune modulation, antiviral response and virus countermeasures. J. Gen. Virol. **81:**2341–2364.
27. **Gupta, A. K., D. Blondel, S. Choudhary, and A. K. Banerjee.** 2000. The phosphoprotein of rabies virus is phosphorylated by a unique cellular protein kinase and specific isomers of protein kinase C. J. Virol. **74:**91–98.
28. **Hartman, A. L., J. S. Towner, and S. T. Nichol.** 2004. A C-terminal basic amino acid motif of Zaire Ebola virus VP35 is essential for type I interferon antagonism and displays high identity with the RNA-binding domain of another interferon antagonist, the NS1 protein of influenza A virus. Virology **328:**177–184.
29. **He, B., R. G. Paterson, N. Stock, J. E. Durbin, R. K. Durbin, S. Goodbourn, R. E. Randall, and R. A. Lamb.** 2002. Recovery of paramyxovirus simian virus 5 with a V protein lacking the conserved cysteine-rich domain: the multifunctional V protein blocks both interferon-beta induction and interferon signaling. Virology **303:**15–32.
30. **Hemmi, H., O. Takeuchi, S. Sato, M. Yamamoto, T. Kaisho, H. Sanjo, T. Kawai, K. Hoshino, K. Takeda, and S. Akira.** 2004. The roles of two IkappaB kinase-related kinases in lipopolysaccharide and double stranded RNA signaling and viral infection. J. Exp. Med. **199:**1641–1650.
31. **Iwamura, T., M. Yoneyama, K. Yamaguchi, W. Suhara, W. Mori, K. Shiota, Y. Okabe, H. Namiki, and T. Fujita.** 2001. Induction of IRF-3/-7 kinase and NF-kappaB in response to double-stranded RNA and virus infection: common and unique pathways. Genes Cells **6:**375–388.
32. **Jacob, Y., H. Badrane, P. E. Ceccaldi, and N. Tordo.** 2000. Cytoplasmic dynein LC8 interacts with lyssavirus phosphoprotein. J. Virol. **74:**10217–10222.
33. **Jacob, Y., E. Real, and N. Tordo.** 2001. Functional interaction map of lyssavirus phosphoprotein: identification of the minimal transcription domains. J. Virol. **75:**9613–9622.
34. **Kato, A., K. Kiyotani, Y. Sakai, T. Yoshida, and Y. Nagai.** 1997. The paramyxovirus, Sendai virus, V protein encodes a luxury function required for viral pathogenesis. EMBO J. **16:**578–587.
35. **Katze, M. G., Y. He, and M. Gale, Jr.** 2002. Viruses and interferon: a fight for supremacy. Nat. Rev. Immunol. **2:**675–687.
36. **Komatsu, T., K. Takeuchi, J. Yokoo, and B. Gotoh.** 2004. C and V proteins of Sendai virus target signaling pathways leading to IRF-3 activation for the negative regulation of interferon-beta production. Virology **325:**137–148.
37. **Lichty, B. D., A. T. Power, D. F. Stojdl, and J. C. Bell.** 2004. Vesicular stomatitis virus: re-inventing the bullet. Trends Mol. Med. **10:**210–216.
38. **Lin, R., C. Heylbroeck, P. M. Pitha, and J. Hiscott.** 1998. Virus-dependent phosphorylation of the IRF-3 transcription factor regulates nuclear translocation, transactivation potential, and proteasome-mediated degradation. Mol. Cell. Biol. **18:**2986–2996.
39. **Lin, R., Y. Mamane, and J. Hiscott.** 1999. Structural and functional analysis of interferon regulatory factor 3: localization of the transactivation and autoinhibitory domains. Mol. Cell. Biol. **19:**2465–2474.
40. **McKendry, R., J. John, D. Flavell, M. Muller, I. M. Kerr, and G. R. Stark.** 1991. High-frequency mutagenesis of human cells and characterization of a mutant unresponsive to both alpha and gamma interferons. Proc. Natl. Acad. Sci. USA **88:**11455–11459.
41. **McWhirter, S. M., K. A. Fitzgerald, J. Rosains, D. C. Rowe, D. T. Golenbock, and T. Maniatis.** 2004. IFN-regulatory factor 3-dependent gene expression is defective in Tbk1-deficient mouse embryonic fibroblasts. Proc. Natl. Acad. Sci. USA **101:**233–238.
42. **Mori, M., M. Yoneyama, T. Ito, K. Takahashi, F. Inagaki, and T. Fujita.** 2004. Identification of Ser-386 of interferon regulatory factor 3 as critical target for inducible phosphorylation that determines activation. J. Biol. Chem. **279:**9698–9702.
43. **Poisson, N., E. Real, Y. Gaudin, M. C. Vaney, S. King, Y. Jacob, N. Tordo, and D. Blondel.** 2001. Molecular basis for the interaction between rabies virus phosphoprotein P and the dynein light chain LC8: dissociation of dynein-binding properties and transcriptional functionality of P. J. Gen. Virol. **82:**2691–2696.
44. **Poole, E., B. He, R. A. Lamb, R. E. Randall, and S. Goodbourn.** 2002. The V proteins of simian virus 5 and other paramyxoviruses inhibit induction of interferon-beta. Virology **303:**33–46.
45. **Qin, B. Y., C. Liu, S. S. Lam, H. Srinath, R. Delston, J. J. Correia, R. Derynck, and K. Lin.** 2003. Crystal structure of IRF-3 reveals mechanism of autoinhibition and virus-induced phosphoactivation. Nat. Struct. Biol. **10:** 913–921.
46. **Raux, H., A. Flamand, and D. Blondel.** 2000. Interaction of the rabies virus P protein with the LC8 dynein light chain. J. Virol. **74:**10212–10216.
47. **Schlender, J., B. Bossert, U. Buchholz, and K. K. Conzelmann.** 2000. Bovine respiratory syncytial virus nonstructural proteins NS1 and NS2 cooperatively antagonize alpha/beta interferon-induced antiviral response. J. Virol. **74:** 8234–8242.
48. **Schnell, M. J., T. Mebatsion, and K. K. Conzelmann.** 1994. Infectious rabies viruses from cloned cDNA. EMBO J. **13:**4195–4203.
49. **Sharma, S., B. R. tenOever, N. Grandvaux, G. P. Zhou, R. Lin, and J. Hiscott.** 2003. Triggering the interferon antiviral response through an IKK-related pathway. Science **300:**1148–1151.
50. **Spann, K. M., K. C. Tran, B. Chi, R. L. Rabin, and P. L. Collins.** 2004. Suppression of the induction of alpha, beta, and lambda interferons by the NS1 and NS2 proteins of human respiratory syncytial virus in human epithelial cells and macrophages. J. Virol. **78:**4363–4369. (Erratum, **78:**6705.)
51. **Spiropoulou, C. F., and S. T. Nichol.** 1993. A small highly basic protein is encoded in overlapping frame within the P gene of vesicular stomatitis virus. J. Virol. **67:**3103–3110.
52. **Takahasi, K., N. N. Suzuki, M. Horiuchi, M. Mori, W. Suhara, Y. Okabe, Y. Fukuhara, H. Terasawa, S. Akira, T. Fujita, and F. Inagaki.** 2003. X-ray crystal structure of IRF-3 and its functional implications. Nat. Struct. Biol. **10:**922–927.
53. **Talon, J., C. M. Horvath, R. Polley, C. F. Basler, T. Muster, P. Palese, and A. Garcia-Sastre.** 2000. Activation of interferon regulatory factor 3 is inhibited by the influenza A virus NS1 protein. J. Virol. **74:**7989–7996.
54. **tenOever, B. R., S. Sharma, W. Zou, Q. Sun, N. Grandvaux, I. Julkunen, H. Hemmi, M. Yamamoto, S. Akira, W. C. Yeh, R. Lin, and J. Hiscott.** 2004. Activation of TBK1 and IKKvarepsilon kinases by vesicular stomatitis virus infection and the role of viral ribonucleoprotein in the development of interferon antiviral immunity. J. Virol. **78:**10636–10649.
55. **Tough, D. F.** 2004. Type I interferon as a link between innate and adaptive immunity through dendritic cell stimulation. Leuk. Lymphoma **45:**257–264.
56. **Valarcher, J. F., J. Furze, S. Wyld, R. Cook, K. K. Conzelmann, and G. Taylor.** 2003. Role of alpha/beta interferons in the attenuation and immunogenicity of recombinant bovine respiratory syncytial viruses lacking NS proteins. J. Virol. **77:**8426–8439.
57. **Wathelet, M. G., C. H. Lin, B. S. Parekh, L. V. Ronco, P. M. Howley, and T. Maniatis.** 1998. Virus infection induces the assembly of coordinately activated transcription factors on the IFN-beta enhancer in vivo. Mol. Cell **1:** 507–518.
58. **Yoneyama, M., M. Kikuchi, T. Natsukawa, N. Shinobu, T. Imaizumi, M. Miyagishi, K. Taira, S. Akira, and T. Fujita.** 2004. The RNA helicase RIG-I has an essential function in double-stranded RNA-induced innate antiviral responses. Nat. Immunol. **5:**730–737.
59. **Yoneyama, M., W. Suhara, Y. Fukuhara, M. Fukuda, E. Nishida, and T. Fujita.** 1998. Direct triggering of the type I interferon system by virus infection: activation of a transcription factor complex containing IRF-3 and CBP/p300. EMBO J. **17:**1087–1095.
60. **Yoneyama, M., W. Suhara, Y. Fukuhara, M. Sato, K. Ozato, and T. Fujita.** 1996. Autocrine amplification of type I interferon gene expression mediated by interferon stimulated gene factor 3 (ISGF3). J. Biochem. (Tokyo) **120:** 160–169.

JOURNAL OF VIROLOGY, May 2005, p. 5507–5515 Vol. 79, No. 9
0022-538X/05/$08.00+0 doi:10.1128/JVI.79.9.5507–5515.2005

Inhibition of Toll-Like Receptor 7- and 9-Mediated Alpha/Beta Interferon Production in Human Plasmacytoid Dendritic Cells by Respiratory Syncytial Virus and Measles Virus

Jörg Schlender,[1]† Veit Hornung,[2]† Stefan Finke,[1] Margit Günthner-Biller,[2] Sabrina Marozin,[1] Krzysztof Brzózka,[1] Sharareh Moghim,[1] Stefan Endres,[2] Gunther Hartmann,[2] and Karl-Klaus Conzelmann[1]*

Max von Pettenkofer Institute and Gene Center[1] and Division of Clinical Pharmacology, Department of Internal Medicine,[2] Ludwig-Maximilians-Universität München, Munich, Germany

Received 2 November 2004/Accepted 27 December 2004

Human plasmacytoid dendritic cells (PDC) are key sentinels alerting both innate and adaptive immune responses through production of huge amounts of alpha/beta interferon (IFN). IFN induction in PDC is triggered by outside-in signal transduction pathways through Toll-like receptor 7 (TLR7) and TLR9 as well as by recognition of cytosolic virus-specific patterns. TLR7 and TLR9 ligands include single-stranded RNA and CpG-rich DNA, respectively, as well as synthetic derivatives thereof which are being evaluated as therapeutic immune modulators promoting Th1 immune responses. Here, we identify the first viruses able to block IFN production by PDC. Both TLR-dependent and -independent IFN responses are abolished in human PDC infected with clinical isolates of respiratory syncytial virus (RSV), RSV strain A2, and measles virus Schwarz, in contrast to RSV strain Long, which we previously identified as a potent IFN inducer in human PDC (Hornung et al., J. Immunol. 173:5935–5943, 2004). Notably, IFN synthesis of PDC activated by the TLR7 and TLR9 agonists resiquimod (R848) and CpG oligodeoxynucleotide 2216 is switched off by subsequent infection by RSV A2 and measles virus. The capacity of RSV and measles virus of human PDC to shut down IFN production should contribute to the characteristic features of these viruses, such as Th2-biased immune pathology, immune suppression, and superinfection.

Successful defense against invading pathogens involves rapid recognition of conserved danger signals through members of the Toll-like receptor (TLR) protein family (1) and induction of cytokines that activate both innate and adaptive immunity. A principal effector integrating early antiviral and immunostimulatory activities is the alpha/beta interferon (IFN) system, including the group of IFN-α isotypes and IFN-β (21). Although most types of cells can produce IFN through recognition of cytosolic double-stranded RNA (1a, 36, 44), or upon stimulation of TLR3 and TLR4 through double-stranded RNA or lipopolysaccharide, respectively (1), the vast amount of IFN upon entry of bacterial and viral pathogens is produced by a specialized cell population, plasmacytoid dendritic cells (PDC) (2, 6). Transcriptional induction of IFN genes is controlled by interferon regulatory factors (IRFs). IRF-3 mainly regulates IFN-β induction, whereas IRF-7 has the ability to activate IFN-α promoters (22, 25, 45). In contrast to other cell types, PDC constitutively express high levels of IRF-7 such that expression of IFN-α by PDC is independent of the IFN-α receptor-mediated positive feedback via IFN-β (3, 13, 16, 18), explaining in part the promptness of high-capacity IFN-α production.

The TLR repertoire of human PDC is composed of TLR7 and TLR9, both located in the endosomal membrane. As shown recently, TLR7 and TLR8 recognize viral single-stranded RNA (8, 12) as well as imidazoquinolines such as imiquimod and resiquimod (R848) and guanosine analogs (reviewed in references 1 and 42). In contrast, TLR9 recognizes bacterial or viral DNA (1), including synthetic CpG oligodeoxynucleotides (ODN) (11). Indeed, recent work revealed IFN-α production in PDC after incubation with a variety of inactivated or live DNA and RNA viruses, including herpes simplex virus types 1 and 2 (16, 19, 23), murine cytomegalovirus (7), human immunodeficiency virus (46), influenza A virus (8, 24), Sendai virus (14, 16), and vesicular stomatitis virus (3, 24). For herpes simplex virus (19, 23), Influenza A virus (8, 24), and vesicular stomatitis virus (24), the critical involvement of MyD88 adaptor-dependent TLR9 and TLR7 signaling has been demonstrated.

In addition to perceiving external virus components through TLR7 and TLR9, human PDC have the means to sense cytosolic replicating RNA viruses. As we could show recently, respiratory syncytial virus (RSV) escapes from recognition by PDC TLRs (14). Nevertheless, infection with a particular laboratory strain of RSV (subtype A, strain Long), or cytosolic delivery of double-stranded RNA but not of poly(I:C) led to potent IFN-α induction in PDC in a TLR- and protein kinase R-independent manner (14).

The considerable repertoire of tools for sensing pathogens combined with a tremendous capacity to produce IFN make human PDC the key sentinels for exciting a generalized host alert upon infection. Indeed, activation of PDC by a variety of pathogens and synthetic TLR agonists profoundly shapes the host immune system by promoting Th1 immune responses and

* Corresponding author. Mailing address: Max-von-Pettenkofer Institute and Gene Center, Feodor-Lynen-Str. 25, D-81377 Munich, Germany. Phone: 49 89 2180 76851. Fax: 49 89 2180 76899. E-mail: conzelma@lmb.uni-muenchen.de.

† J.S. and V.H. contributed equally to this work.

suppressing Th2 immune responses (6, 11, 15, 42). This effect is exploited in the therapeutic use of TLR7 and TLR9 ligands, such as R848 and CpG ODN, which are promising as immunoprotective agents, vaccine adjuvants, and antiallergens (1, 11, 42).

It may therefore appear from the current literature that PDC are impeccable in sensing intruders. However, in view of the key role of human PDC in innate and adaptive immunity, natural viruses must have evolved tools to counteract IFN production by PDC. In order to identify such viruses, we scrutinized two negative-stranded RNA viruses of the *Paramyxoviridae* family, measles virus (MeV) and RSV, which were considered successful candidates because of their immunesuppressive features and Th2-biased immune response (10, 27, 35). Since RSV strain Long was previously identified as an efficient inducer of IFN in PDC (14), infection of different human cell types, including PDC, other immune cells, and fibroblast cell lines, was done as a control. Infection of PDC with RSV A2 and four primary RSV isolates from hospitalized children and the vaccine MeV Schwarz effectively and similarly repressed IFN expression. Most importantly, TLR7- and TLR9-dependent IFN-inducing pathways stimulated by R848 and CpG ODN were abolished by infection with MeV and RSV A2. Thus, these viruses can make PDC blind to other pathogens and therapeutic IFN stimuli.

MATERIALS AND METHODS

Virus and cell culture. IFN-free virus stocks of human RSV strains A2 (ATCC VR-1540) and Long (ATCC VR-26) were prepared by infection of 70 to 80% confluent Vero (American Type Culture Collection) cell layers at a multiplicity of 0.1 in Dulbecco's modified Eagle's medium (DMEM) (Gibco) in the absence of fetal calf serum (FCS) as described (34). The inoculum was removed after 1 h and cells were incubated in DMEM supplemented with 2.5% FCS at 37°C in a 5% CO_2 atmosphere. Virus was released by freezing and thawing the cell monolayers upon development of extensive cytopathic effects, followed by centrifugation at 3,500 rpm for 20 min at 4°C. Infectious virus titers were determined on Vero cells by endpoint dilution and counting of infected cell foci stained for indirect immunofluorescence with an RSV F-specific monoclonal antibody (Serotec).

Primary human RSV isolates from hospitalized children suffering from bronchiolitis or obstructive bronchitis were provided by H. Werchau, Bochum, Germany, and were first amplified by two passages on HEp2 cells (ATCC CCL-23) before preparation of IFN-free virus stocks on Vero cells as described above.

MeV strain Schwarz was obtained from a commercial batch (Ch.-B: W5663-2) of measles vaccine Meriéux (Pasteur Mérieux MSD, Leimen, Germany); 500 50% tissue culture infective doses were incubated with 2.5×10^6 Vero cells for 1 h in a 15-ml Falcon tube with 2.5 ml of DMEM without FCS. Cells were seeded in DMEM supplemented with 2.5% FCS at 37°C in a 5% CO_2 atmosphere until development of an extensive cytopathic effect. A virus stock for infection experiments was prepared from this first passage on Vero cells as described above for RSV.

For infection of epithelial cell lines HEp2, 293, and A549, 2.5×10^4 cells were seeded in DMEM with 10% FCS in 48-well plates and were grown for 16 h at 37°C and 5% CO_2. Cell numbers were then determined from three extra wells. FCS-containing medium was replaced by 200 μl of DMEM without FCS and containing the indicated viruses adjusted to a multiplicity of infection of 3. After 1 h of incubation virus-containing medium was removed and cells were washed and further incubated with DMEM plus 10% FCS. As a negative control for infection, cells were incubated in parallel with mock supernatant obtained from freeze-thaw cell lysates of noninfected Vero cells.

Isolation of human hematopoietic cells. Human peripheral blood mononuclear cells were prepared from whole blood of young healthy donors by Ficoll-Hypaque density gradient centrifugation (Biochrom, Berlin, Germany). PDC were isolated by magnetic activated cell sorting (MACS) using the BDCA-4 dendritic cell isolation kit from Miltenyi Biotec as described (14). Briefly, PDC were labeled with anti-BDCA-4 antibody coupled to colloidal paramagnetic microbeads and passed through a magnetic separation column once (LS column; Miltenyi Biotec). The purity of isolated PDC (lineage-negative, major histocompatibility complex class II-positive, CD123-positive) was between 75% and 100%. PDC from individual donors were used separately in all experiments and were not pooled. Contaminating cells represented mainly T cells.

Prior to isolation of monocytes and B cells, PDC were depleted by MACS (CS column; Miltenyi Biotec). B cells were isolated by MACS using the BDCA-1 dendritic cell isolation kit and B-cell isolation kit, respectively (both Miltenyi Biotec). Monocytes and T cells were isolated from buffy coats by Ficoll (Lymphoflot, Biotech, Dreieich) gradient centrifugation (33) at 1,500 rpm in a Heraeus Varifuge. T cells were separated from monocytes and B cells by plastic adherence for 1 h. A fraction of strongly adherent monocytes was separated from B cells by overnight incubation and rigorous washing three times. Remaining adherent monocytes were trypsinized and primary cultures of monocytes or T cells were grown in suspension in RPMI supplemented with 10% FCS at 37°C and 5% CO_2 atmosphere. The purity of primary cell cultures was determined by fluorescence-activated cell scanning (FACS) analysis using phycoerythrin-labeled monoclonal CD3 (Serotec), CD14 (Serotec), and CD19 (Serotec) antibodies. The purity of B cells, monocytes, and T cells was greater than 95%, 95%, and 80%, respectively. Viability was >95% as determined by trypan blue exclusion.

Prior to virus infection, T cells were activated by incubation with phytohemagglutinin (5 μg/ml, Sigma), while B cells and monocytes were activated by incubation with lipopolysaccharide (100 ng/ml, Sigma) in RPMI with 10% FCS at 37°C and 5% CO_2 for 16 h. For infection of 5×10^4 PDC or 10×10^4 B cells, T cells, or monocytes, cells were seeded in 100 μl of RPMI (Gibco) plus 10% FCS into 96-cluster-well plates; 100 μl of RPMI plus 10% FCS containing infectious virus adjusted to yield a multiplicity of infection of 3 was added, and cells were incubated at 37°C in a 5% CO_2 atmosphere.

TLR agonists. R848 was purchased from Invivogen (Toulouse, France). CpG ODN 2216 (5′-ggGGGA*CG*AT*CG*TCggggG-3′; lowercase letters are phosphorothioate linkage; capital letters are phosphodiester linkage 3′ of the base; italics are CpG dinucleotides) was kindly provided by Coley Pharmaceutical Group (Wellesley, Mass.). R848 or CpG ODN 2216 was added to PDC at the indicated time points at final concentrations of 2 μg/ml and 6 μg/ml, respectively.

Flow cytometry. Infection of epithelial cell lines and of primary hematopoietic cells was determined by cell surface staining of viral envelope proteins using 2.5×10^5 cells (except for PDC, where 2×10^4 cells were used), fixed for 5 min with 3% paraformaldehyde at room temperature. After washing with FACS buffer (phosphate-buffered saline containing 0.4% FCS and 0.02% NaN_3), staining for 30 min on ice was performed using the mouse monoclonal antibodies RSV-F (Serotec) and K83, recognizing MeV H (kindly provided by S. Schneider-Schaulies, Würzburg, Germany). As a negative control, mock-treated cells were stained in parallel. After washing, cells were incubated for 30 min with fluorescein isothiocyanate-labeled anti-mouse immunoglobulin antibody (Dianova) followed by washing and FACS analysis on a BD Biosciences (Heidelberg, Germany) FACSCalibur (excitation at 488 and 635 nm).

Detection of cytokines. For enzyme-linked immunosorbent assay (ELISA) detection of human interleukin-8 and IFN-α, the interleukin-8 kit and the IFN-α ELISA module set (detection range, 8 to 500 pg/ml) of Bender MedSystems (Graz, Austria) was used. The IFN-α module set ELISA detects most IFN-α isoforms but not IFN-β. ELISA for an individual experiment was performed in parallel with 20 μl of cell-free supernatant, each collected at indicated time points and stored at −20°C. Assays were performed according to the manufacturer's recommendations.

RESULTS

IFN production in virus-infected cell lines. We first compared two widely used RSV subtype A laboratory strains, A2 and Long, and the commercial MeV vaccine strain Schwarz (Mérieux) for their capacity to interfere with IFN-α induction in epithelial cells. Human A549, 293, and HEp-2 cells were equally well infected with RSV A2 and Long, as demonstrated by expression of the fusion (F) protein on the surface of infected cells (Fig. 1B). However, IFN-α production was significantly lower in RSV A2-infected cells at 12, 24, and 36 h postinfection (Fig. 1A). This is consistent with previous observations indicating that nonstructural proteins (NS) 1 and 2 of RSV A2 are able to counteract IFN induction in A549 cells (39). Among other IFN antagonistic activities (4, 31), the RSV

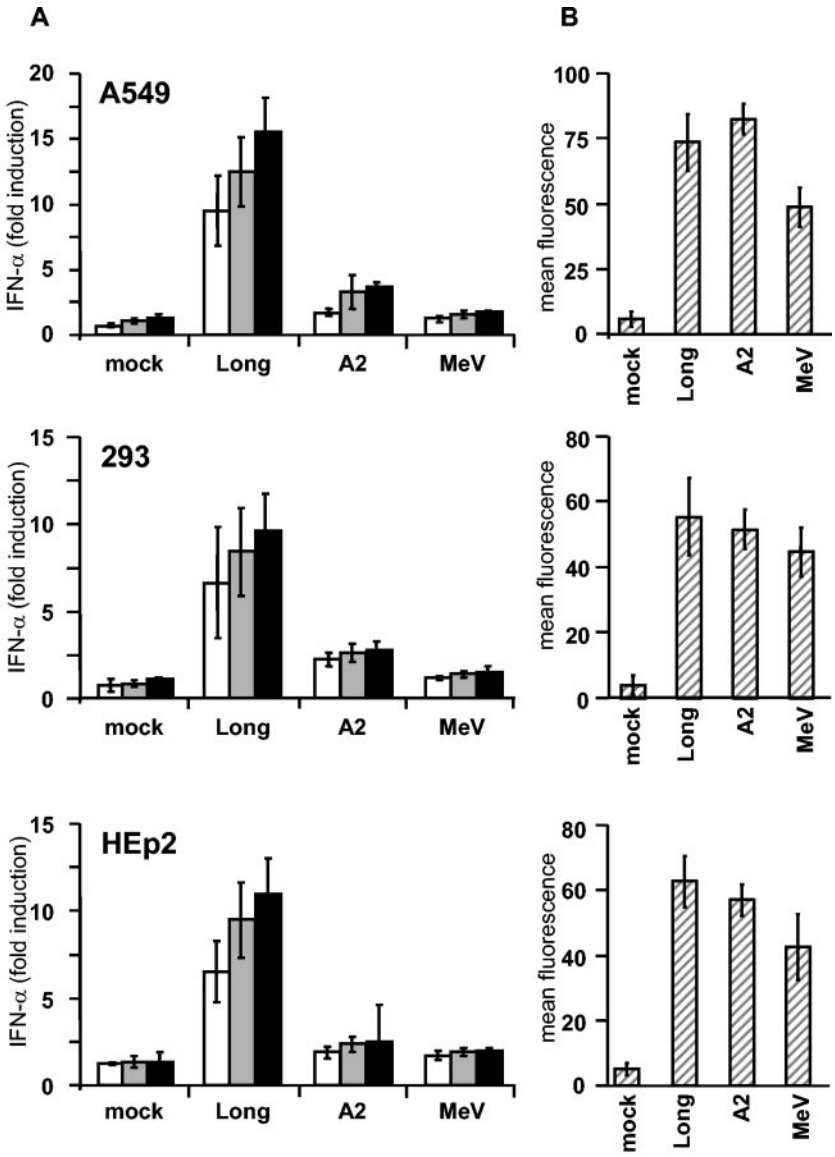

FIG. 1. MeV Schwarz and RSV strain A2 but not RSV strain Long are able to inhibit production of IFN-α in epithelial cell lines. (A) Human A549, 293, and HEp2 cells were infected with RSV A2, RSV Long, or the MeV vaccine strain Schwarz. After 12, 24, and 36 h (white, grey, and black bars, respectively) IFN-α secreted into the culture supernatants was determined by ELISA. Results are shown as induction compared to supernatants of mock-infected cells. (B) Cell surface expression of RSV fusion protein (F) and MeV hemagglutinin (H), determined 36 h postinfection by FACS with monoclonal antibodies, was used to verify productive virus infection. Error bars indicate the standard deviation in three independent experiments.

nonstructural (NS) proteins interfere with activation of the essential IFN transcription factor IRF-3 (5). In contrast to RSV A2, however, RSV Long induced approximately five times more IFN-α, suggesting that this virus has lost the ability to effectively counteract IRF-3 activation in virus-infected cells. Similar to RSV A2, infection by MeV Schwarz did not lead to IFN-α induction considerably exceeding that of mock-infected cells, confirming potent IFN-antagonistic activity described for measles virus (29).

IFN production in hematopoietic cells. To investigate virus-dependent IFN induction in abundant primary cells of the human immune system, we isolated T cells, B cells, and monocytes from the peripheral blood of individual healthy donors. Nonactivated cells were virtually not permissive for infection with either RSV strain or MeV. Only after activation of T cells with phytohemagglutinin and of B cells or monocytes with lipopolysaccharide could infection be demonstrated by appearance of the RSV fusion protein (F) and of MeV hemagglutinin (H) protein on the surface of cells by FACS (Fig. 2B). In the hematopoietic cells, a less effective expression of F protein by RSV Long compared to A2 indicated some growth restriction of this strain. Nevertheless, and similar to the experiments with the epithelial cell lines, RSV Long caused substantial IFN-α production in T and B cells and in monocytes, whereas RSV A2 and MeV completely suppressed IFN production (Fig. 2A). Notably, cells infected with the latter viruses produced even

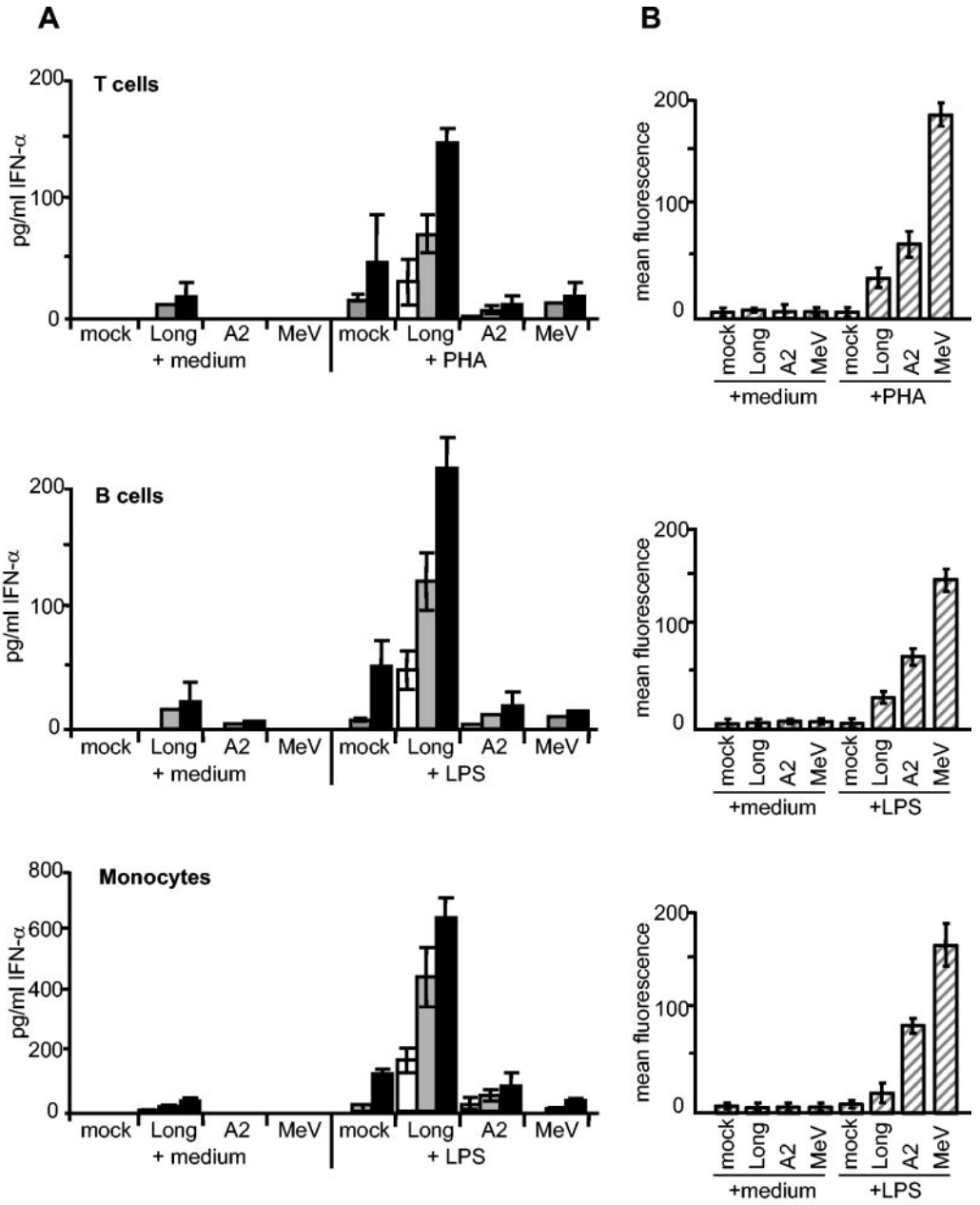

FIG. 2. MeV and RSV A2 but not RSV Long inhibit production of IFN-α in primary human hematopoietic cells. (A) Freshly isolated T cells, B cells, and monocytes were either incubated with medium or activated by addition of lipopolysaccharide (LPS) or phytohemagglutinin (PHA) for 16 h, followed by virus infection or incubation with mock supernatant. After 24, 36, and 48 h (white, grey, and black bars, respectively), the amount of IFN-α in supernatants was determined by ELISA. (B) Cell surface expression of RSV F protein and MeV H protein determined by FACS at 48 h postinfection as described for Fig. 1. Error bars indicate the standard deviation of mean in experiments using primary cells from three (T cells), six (B cells), or seven (monocytes) individual donors.

less IFN-α than mock-infected and lipopolysaccharide- or phytohemagglutinin-activated cells, suggesting an inhibition of TLR4-mediated IFN production.

IFN response of human PDC. To examine whether RSV and measles virus may also interfere with the activity of PDC, aliquots of 5×10^4 freshly isolated BDCA-4-positive peripheral blood PDC were incubated with virus-containing cell culture supernatants at a multiplicity of infection of 3. As expected from previous work (14), RSV Long was able to infect PDC, though with a small number of cells displaying moderate levels of newly synthesized F protein on the surface at 72 h postinfection (Fig. 3C). Infection by RSV A2 was less restricted, as indicated by highly increased numbers of F-stained cells and a threefold-increased mean F fluorescence intensity. Productive MeV infection of PDC was demonstrated by the fast appearance of cells staining for the H protein, their number reaching more than 90% within 72 h of infection (Fig. 3C).

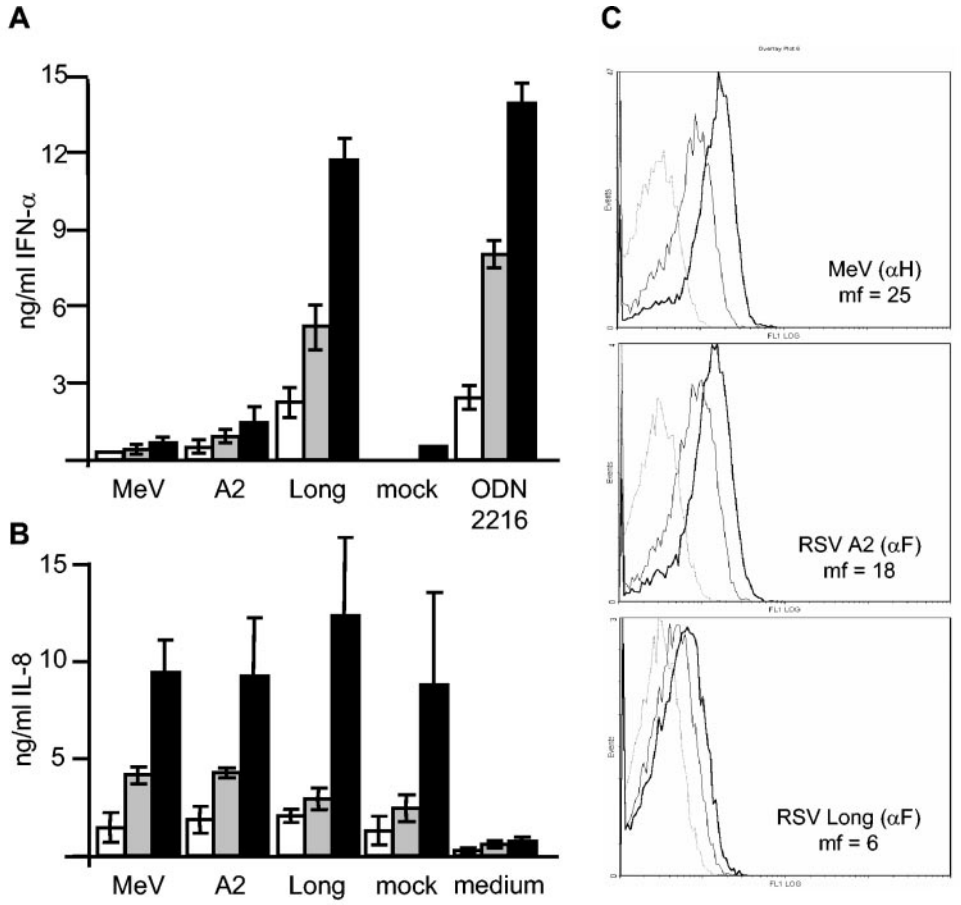

FIG. 3. MeV and RSV A2 but not RSV Long inhibit production of IFN-α in infected PDC. Freshly isolated PDC were infected with the indicated viruses and treated with mock supernatant or supernatant containing 4 μg/ml of ODN2216. After 12, 24, and 36 h (white, grey, and black bars, respectively), secreted IFN-α (A) and interleukin-8 (B) were determined by ELISA. Error bars in indicate the standard deviation of mean of four experiments using PDC from six individual donors (A) or three donors (B). Infection of PDC was assayed by FACS monitoring of cell surface expression of RSV F and MeV H protein at 36 h (thin line) and 72 h (bold line) postinfection. For a negative control (dotted line), mock-infected cells were incubated for 72 h.

As a positive control for IFN-α production, PDC were treated with 4 μg of CpG ODN 2216, which strongly activates PDC through TLR9 binding (20)/ml. Supernatants from virus-infected, mock-infected, and ODN-treated PDC were assayed 12, 24, and 36 h later for IFN-α production by ELISA. Both CpG ODN 2216-treated and RSV Long-infected PDC produced huge and comparable amounts of IFN-α, with concentrations reaching 13.8 ng/ml and 11.6 ng/ml at 36 h, respectively (Fig. 3A). However, in PDC infected with RSV A2 or measles virus, IFN-α production was suppressed. In particular, MeV infection allowed not much more IFN to be produced than in mock-infected cells. Importantly, infection with the different viruses had no obvious effect on production of interleukin-8, which is NF-κB dependent (18, 28). Treatment of PDC with supernatants from either mock-infected or virus-infected cell cultures led to a similar and approximately 10-fold increase of interleukin-8 compared to PDC treated with fresh medium (Fig. 3B). These data confirm the viability of virus-infected PDC and indicate that RSV NS proteins block IRF-3 and IRF-7 activation in PDC, whereas the activity of the NF-κB and AP-1 transcription factors is not affected, as was demonstrated previously for epithelial cells (5). Similarly, the major target of MeV appears to be the IRF rather than the NF-κB activation pathway.

To confirm that natural RSV shares the ability of A2 to prevent IFN-α induction in PDC, four clinical RSV isolates from children hospitalized with bronchiolitis or obstructive bronchitis were included in the assay. All four isolates were able to infect PDC similarly to RSV A2 (Fig. 4C) and suppressed IFN-α production equally well (Fig. 4A), while they did not suppress production of interleukin-8 (Fig. 4B). Thus, infection of human PDC and potent inhibition of IFN-α induction are intrinsic features of clinical human RSV isolates. RSV A2 but not RSV Long has fully retained this important wild-type phenotype.

Inhibition of TLR7 and TLR9 signaling. As shown previously, RSV Long and bovine RSV expressing the F protein from human RSV Long (34) escape detection by TLRs on PDC (14). Recognition of double-stranded RNA generated by replicating virus in the cytoplasm by cytosolic receptors such as RIG-I and related RNA helicases (1a, 44) is therefore responsible for the observed potent IFN-α expression. Since RSV A2 and MeV infection of PDC suppresses IFN-α production, it is suggested that these viruses interfere with the pathway leading

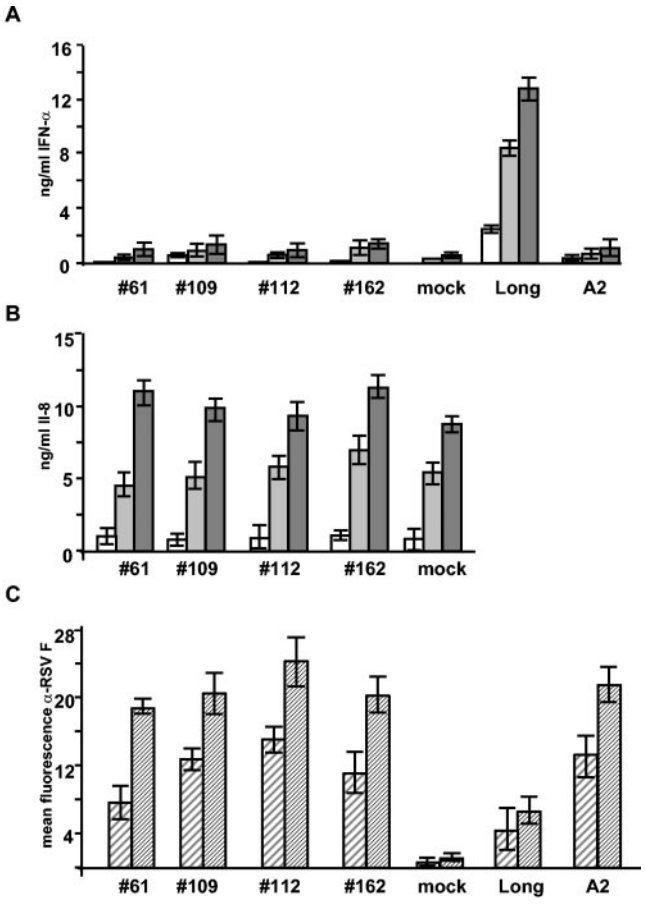

FIG. 4. Clinical RSV isolates from hospitalized children counteract IFN-α production in infected PDC. PDC were infected with the indicated clinical RSV isolates or RSV Long or incubated with mock supernatant. After 12, 24, and 36 h (white, light grey, and dark grey bars, respectively), secreted IFN-α (A) and interleukin-8 (B) were determined by ELISA. Error bars show the standard deviation of the mean of four experiments using PDC from individual donors. (C) Expression of RSV F on the surface of PDC as determined by FACS (mean fluorescence) after 36 h (grey) and 72 h (black) of incubation.

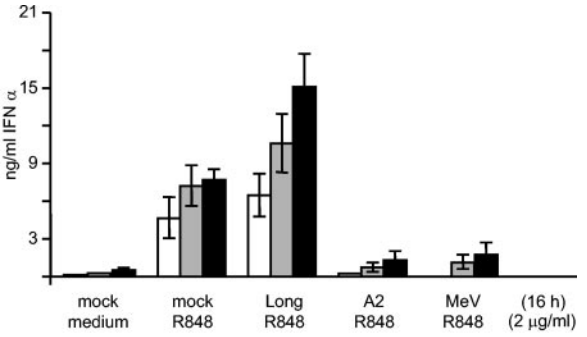

FIG. 5. RSV A2 and MeV infection precludes IFN production mediated by the TLR7 agonist R848. Human PDC were mock infected or infected with the indicated viruses for 16 h, followed by addition of fresh medium or medium containing 2 μg/ml of R848. IFN-α production was determined at 12, 24, and 36 h post-R848 treatment (white, grey, and black bars, respectively). Error bars indicate the standard deviation of the mean in three experiments using PDC from five individual donors.

from recognition of cytosolic viral double-stranded RNA to activation of IRF-3.

To assess whether RSV A2 and MeV are also able to interfere with the TLR-dependent IFN-α-inducing pathways, we measured the effect of virus infection on TLR7 and TLR9 signaling upon stimulation with known TLR agonists. First, the response to the TRL7 ligand R848 (resiquimod) was investigated. Stimulation of mock-infected PDC with 2 μg of R848 per ml led to production of up to 9 ng/ml IFN-α (Fig. 5). Even higher amounts, up to 15 ng/ml, of IFN were produced in PDC infected with RSV Long. Since similarly high IFN-α levels were previously observed in the absence of R848 in RSV Long-infected cells (see Fig. 3), a synergistic effect of the IFN-inducing virus and R848 stimulation was not evident. In striking contrast to the situation with RSV Long, R848 treatment of PDC infected with RSV A2 and MeV did not result in production of considerable amounts of IFN-α. Thus, RSV A2 and MeV are able to antagonize TLR7-mediated IFN induction pathways.

To study the effects of virus infection on TLR9 signaling, ODN 2216, which is the most potent IFN-inducing CpG ODN available so far, was used (18). Incubation of mock-infected PDC with 6 μg/ml ODN 2216 stimulated secretion of large amounts of IFN-α, reaching more than 15 ng/ml at 36 h (Fig. 6A). In cells previously infected with RSV Long, similar amounts of IFN were produced. An additive activation of IFN-α by ODN 2216 and the IFN-inducing RSV Long was indicated by even higher IFN production at 12 h postinfection. In striking contrast, IFN secretion was almost completely abolished in cells infected with RSV A2 or measles virus (Fig. 6A). Thus, RSV A2 and measles virus are able to prevent CpG-mediated activation of IFN through TLR9.

To assess the capacity of the viruses to shut down TLR9 signaling pathways previously activated by CpG, PDC were first stimulated by incubation with ODN 2216 for 6 h or 24 h. The cells were washed and incubated with supernatants from noninfected (mock) and virus-infected cell cultures (multiplicity of infection of 3). In mock-infected PDC, the 6-h ODN incubation period resulted in secretion of 2, 4, and 13 ng/ml IFN at 12, 24, and 36 h, respectively (Fig. 6B, upper panel). Whereas infection with RSV Long caused slightly increased levels of IFN-α, infection with RSV A2 and measles virus strongly diminished IFN-α secretion turned on during the 6-h ODN incubation period. Indeed, values were only slightly greater than previously observed for nonstimulated and mock-infected PDC (e.g., Fig. 6A). Moreover, virus infection was able to considerably reduce IFN production even after a 24-h ODN 2216 stimulation. Compared to mock- and RSV Long-infected PDC, a reduction of IFN-α levels to less than 50% was observed in RSV A2-infected PDC at all time points monitored (Fig. 6B, lower panel). These results show that previously activated operational TLR9 signaling can be shut down by both RSV A2 and measles virus.

DISCUSSION

In summary, we provide the first evidence that viruses can counteract IFN production by human PDC in vitro. Most remarkably, this applies to all IFN-inducing pathways so far known to be active in PDC, including those triggered by cyto-

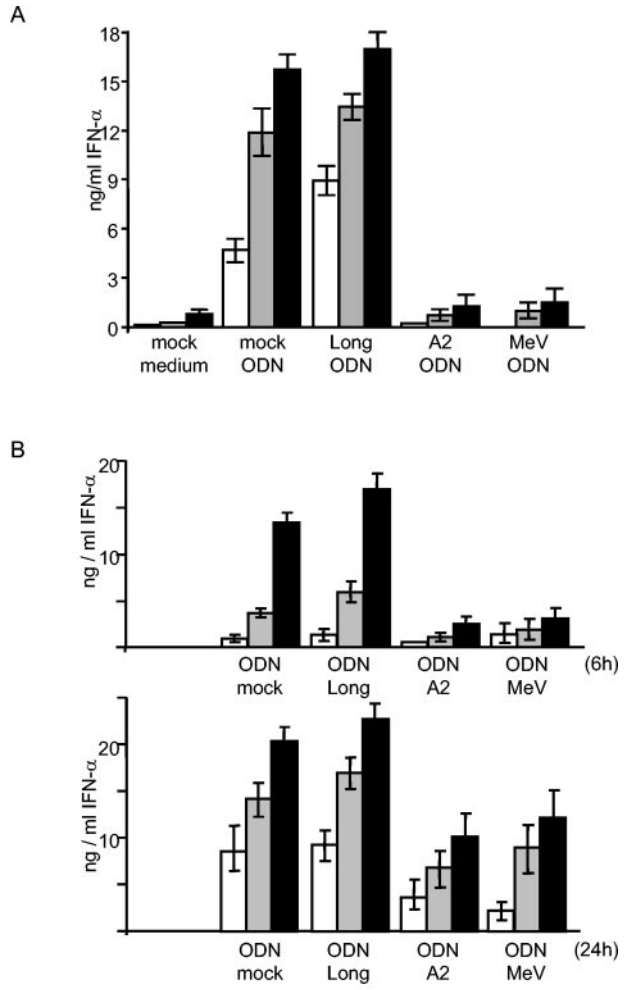

FIG. 6. MeV and RSV A2 abolishes ODN-induced IFN-α production of PDC. (A) PDC were infected with the indicated viruses for 16 h, followed by stimulation with 6 μg/ml ODN2216. IFN production after 12, 24, and 36 h (white, grey, and black bars, respectively) was measured by ELISA. Error bars indicate the standard deviation of the mean in three experiments using PDC from five individual donors. (B) Human PDC were first stimulated by addition of ODN 2216 for 6 h (upper panel) or 24 h (lower panel). Then, the medium was removed and the cells were infected with the indicated viruses at a multiplicity of infection of 3 or mock infected. The effect of the 6-h ODN 2216 stimulus is almost completely abolished by MeV and RSV A2, and infection after the long 24-h stimulus is still sufficient to diminish IFN production by approximately 40% and 50%, respectively. Error bars indicate the standard deviation in experiments using PDC from four individual donors.

plasmic recognition of viral replication, probably through molecules sensing viral double-stranded RNA, such as RIG-I and related DexD/H box RNA helicases like MDA5 (1a, 44), as well as those activated by outside-in signaling through TLR7 and TLR9 (40). In vivo, therefore, RSV and measles virus should not only avoid an immediate IFN alert caused by themselves but also be able to prevent or diminish an IFN and immune response triggered by coinfecting unrelated pathogens, including single-stranded RNA viruses, DNA viruses, and bacteria. Consequently, infection by RSV and measles virus should make hosts more permissive to other pathogens. In addition, an antagonistic effect on the effectiveness of synthetic TLR agonists such as CpG ODN and R848 administered as immune adjuvants can be predicted.

Intriguingly, deaths from measles are largely due to an increased susceptibility to secondary bacterial and viral infections, attributed to a prolonged state of immune suppression (27, 35). One mechanism contributing to immune suppression is contact-mediated inhibition of T-cell proliferation by measles virus surface proteins (32). The present findings that human PDC are highly permissive for infection with measles virus in vitro and fail to produce IFN upon different TLR stimuli may further explain how measles virus facilitates bacterial superinfections in vivo and encumbers the development of an adequate immune response. Of note in this respect is the typical strong Th2 bias in measles (27). Since IFN-α drives the immune response towards Th1, shutdown of the major human IFN-producing cells by measles virus may considerably contribute to this feature of measles pathology.

Unlike measles virus, which causes a generalized infection by targeting mainly cells of hematopoietic origin and therefore may reach a considerable portion of the PDC population, RSV infection remains restricted mainly to epithelial cells of the upper and lower respiratory tract. The finding that clinical RSV isolates have the capacity to prevent PDC IFN responses, however, strongly suggests that this feature is also vital for local infection of the respiratory tract by RSV. Notably, further immune-relevant features are shared by measles virus and RSV, including a pronounced in vitro contact inhibition of T cells by the viral surface proteins (33) and a Th2-biased immune response (10). Although bacterial superinfections in RSV infection appear to contribute little to the disease in humans, they are often described for infections of calves with bovine RSV (see the references in reference 33), a relevant animal model for human RSV.

In RSV-infected non-PDC cell types, induction of IFN-α and IFN-β is prevented by the activity of two unique proteins, the viral NS1 and NS2 proteins (5, 31, 39, 43). As we have shown recently, the NS1 and -2 proteins interfere with the activation of the essential IFN transcription factor IRF-3, while NF-κB and AP-1 activity is not affected (5). Both cytosolic double-stranded RNA-triggered and TLR3- and TLR4-dependent IFN induction pathways appear to merge in the phosphorylation of IRF-3 (and IRF-7, if present) by two homologous kinases, tank binding protein 1 (TBK-1), and the inducible inhibitor of kappa kinase, IKK-i (1, 9, 26, 38). IRF-3 activation through TLR3 and TLR4 involves the adapter TRIF, which has been shown to associate with TBK-1 and IKK-i (reviewed in reference 1). In contrast, TLR7 and TLR9 IFN signaling depends on MyD88 (8, 12, 17), which directly binds IRF-7 and TRAF6 but not IRF-3 (17).

The observation that RSV Long has lost the ability to counteract both TLR7- and TLR9-dependent and cytoplasmic IFN-inducing pathways while RSV A2 and all clinical RSV isolates have retained the full inhibitory set suggests molecular targets common to TLR-dependent and -independent IFN inducing pathways, namely, phosphorylation of the IRFs by the different IRF kinases. This is supported by our experiments with virus-infected B cells and monocytes stimulated by lipopolysaccharide (in order to render these cells permissive for virus infection), which indicate that RSV and measles virus not only

abolish the TLR7/9 MyD88-dependent signaling to IFN activation but might also counteract TRIF-dependent TLR4 signaling (see Fig. 2). As the NS proteins of RSV are critically involved in inhibiting IFN induction in non-PDC and the bovine RSV NS has been shown to prevent phosphorylation of IRF-3 (5), it will be interesting to determine whether these proteins are also involved in counteracting TLR-mediated IFN induction e.g., by preventing activation of IRF-7.

The situation with the IFN antagonists responsible for preventing IFN induction of wild-type measles virus (29) is less clear. As for other *Paramyxovirinae*, the V protein of measles virus interferes with IFN signaling through STAT (30), and a corresponding activity has been reported for the measles virus C protein (37). Since PDC are capable of producing IFN-α independently of the IFN-α receptor-mediated positive feedback via IFN-β (3, 13, 16, 18), these viral activities on IFN signaling are not sufficient to account for the observed effective IFN-α shutdown in PDC. It therefore remains to be clarified which measles virus factors interfere with IFN induction.

From the present experiment, it appears that measles virus and RSV have similar targets. Interestingly, measles virus strain Edmonston, which is closely related to strain Schwarz, has been shown to activate IRF-3 and to induce IFN in 293 cells (41). Comparison of the sequences of the strains might help to reveal the genetic basis for interference with IFN induction in fibroblasts and probably in PDC. Further analysis of the mechanisms used by RSV and measles virus to prevent IFN production in PDC will not only lead to recombinant vaccine viruses with abolished or reduced capacity to undermine the host immune response but may also help to develop tools to modulate the activities of therapeutic TLR ligands.

ACKNOWLEDGMENTS

We thank N. Hagendorf for perfect technical assistance. K83 antibody recognizing MeV H was provided by S. Schneider-Schaulies, Würzburg, Germany, and clinical RSV isolates by H. Werchau, Bochum, Germany.

This work was supported by the Deutsche Forschungsgemeinschaft through SFB 455 and SPP1089 Co260/1-1 and by the European Commission (5thFP-PRIOVAX-QLK2-CT-2002-81399). G.H. was supported by grants from the Deutsche Forschungsgemeinschaft, HA 2780/4-1 and SFB 571, the Mildred Scheel Stiftung 10-2074, the Friedrich-Baur-Stiftung, and the Human Science Foundation of Japan.

REFERENCES

1. **Akira, S., and K. Takeda.** 2004. Toll-like receptor signalling. Nat. Rev. Immunol. **4:**499–511.
1a. **Andrejeva, J., K. S. Childs, D. F. Young, T. S. Carlos, N. Stock, S. Goodbourn, and R. E. Randall.** 2004. The V proteins of paramyxoviruses bind the IFN-inducible RNA helicase, mda-5, and inhibit its activation of the IFN-β promoter. Proc. Natl. Acad. Sci. USA **101:**17264–17269.
2. **Asselin-Paturel, C., A. Boonstra, M. Dalod, I. Durand, N. Yessaad, C. Dezutter-Dambuyant, A. Vicari, A. O′Garra, C. Biron, F. Briere, and G. Trinchieri.** 2001. Mouse type I IFN-producing cells are immature APCs with plasmacytoid morphology. Nat. Immunol. **2:**1144–1150.
3. **Barchet, W., M. Cella, B. Odermatt, C. Asselin-Paturel, M. Colonna, and U. Kalinke.** 2002. Virus-induced interferon alpha production by a dendritic cell subset in the absence of feedback signaling in vivo. J. Exp. Med. **195:**507–516.
4. **Bossert, B., and K. K. Conzelmann.** 2002. Respiratory syncytial virus (RSV) nonstructural (NS) proteins as host range determinants: a chimeric bovine RSV with NS genes from human RSV is attenuated in interferon-competent bovine cells. J. Virol. **76:**4287–4293.
5. **Bossert, B., S. Marozin, and K. K. Conzelmann.** 2003. Nonstructural proteins NS1 and NS2 of bovine respiratory syncytial virus block activation of interferon regulatory factor 3. J. Virol. **77:**8661–8668.
6. **Cella, M., D. Jarrossay, F. Facchetti, O. Alebardi, H. Nakajima, A. Lanzavecchia, and M. Colonna.** 1999. Plasmacytoid monocytes migrate to inflamed lymph nodes and produce large amounts of type I interferon. Nat. Med. **5:**919–923.
7. **Dalod, M., T. Hamilton, R. Salomon, T. P. Salazar-Mather, S. C. Henry, J. D. Hamilton, and C. A. Biron.** 2003. Dendritic cell responses to early murine cytomegalovirus infection: subset functional specialization and differential regulation by interferon alpha/beta. J. Exp. Med. **197:**885–898.
8. **Diebold, S. S., T. Kaisho, H. Hemmi, S. Akira, and Reis E Sousa.** 2004. Innate antiviral responses by means of TLR7-mediated recognition of single-stranded RNA. Science **303:**1529–1531.
9. **Fitzgerald, K. A., S. M. McWhirter, K. L. Faia, D. C. Rowe, E. Latz, D. T. Golenbock, A. J. Coyle, S. M. Liao, and T. Maniatis.** 2003. IKKepsilon and TBK1 are essential components of the IRF3 signaling pathway. Nat. Immunol. **4:**491–496.
10. **Graham, B. S., J. A. Rutigliano, and T. R. Johnson.** 2002. Respiratory syncytial virus immunobiology and pathogenesis. Virology **297:**1–7.
11. **Hartmann, G., G. J. Weiner, and A. M. Krieg.** 1999. CpG DNA: a potent signal for growth, activation, and maturation of human dendritic cells. Proc. Natl. Acad. Sci. USA **96:**9305–9310.
12. **Heil, F., H. Hemmi, H. Hochrein, F. Ampenberger, C. Kirschning, S. Akira, G. Lipford, H. Wagner, and S. Bauer.** 2004. Species-specific recognition of single-stranded RNA via toll-like receptor 7 and 8. Science **303:**1526–1529.
13. **Hemmi, H., T. Kaisho, K. Takeda, and S. Akira.** 2003. The roles of Toll-like receptor 9, MyD88, and DNA-dependent protein kinase catalytic subunit in the effects of two distinct CpG DNAs on dendritic cell subsets. J. Immunol. **170:**3059–3064.
14. **Hornung, V., J. Schlender, M. Guenthner-Biller, S. Rothenfusser, S. Endres, K. K. Conzelmann, and G. Hartmann.** 2004. Replication dependent potent IFN-α induction in human plasmacytoid dendritic cells by a single-stranded RNA virus. J. Immunol. **173:**5935–5943.
15. **Ito, T., R. Amakawa, M. Inaba, T. Hori, M. Ota, K. Nakamura, M. Takebayashi, M. Miyaji, T. Yoshimura, K. Inaba, and S. Fukuhara.** 2004. Plasmacytoid dendritic cells regulate Th cell responses through OX40 ligand and type I IFNs. J. Immunol. **172:**4253–4259.
16. **Izaguirre, A., B. J. Barnes, S. Amrute, W. S. Yeow, N. Megjugorac, J. Dai, D. Feng, E. Chung, P. M. Pitha, and P. Fitzgerald-Bocarsly.** 2003. Comparative analysis of IRF and IFN-alpha expression in human plasmacytoid and monocyte-derived dendritic cells. J. Leukoc. Biol. **74:**1125–1138.
17. **Kawai, T., S. Sato, K. J. Ishii, C. Coban, H. Hemmi, M. Yamamoto, K. Terai, M. Matsuda, J. Inoue, S. Uematsu, O. Takeuchi, and S. Akira.** 2004. Interferon-alpha induction through Toll-like receptors involves a direct interaction of IRF7 with MyD88 and TRAF6. Nat. Immunol. **5:**1061–1068.
18. **Kerkmann, M., S. Rothenfusser, V. Hornung, A. Towarowski, M. Wagner, A. Sarris, T. Giese, S. Endres, and G. Hartmann.** 2003. Activation with CpG-A and CpG-B oligonucleotides reveals two distinct regulatory pathways of type I IFN synthesis in human plasmacytoid dendritic cells. J. Immunol. **170:**4465–4474.
19. **Krug, A., G. D. Luker, W. Barchet, D. A. Leib, S. Akira, and M. Colonna.** 2004. Herpes simplex virus type 1 activates murine natural interferon-producing cells through toll-like receptor 9. Blood **103:**1433–1437.
20. **Krug, A., A. Towarowski, S. Britsch, S. Rothenfusser, V. Hornung, R. Bals, T. Giese, H. Engelmann, S. Endres, A. M. Krieg, and G. Hartmann.** 2001. Toll-like receptor expression reveals CpG DNA as a unique microbial stimulus for plasmacytoid dendritic cells which synergizes with CD40 ligand to induce high amounts of IL-12. Eur. J. Immunol. **31:**3026–3037.
21. **Le Bon, A., and D. F. Tough.** 2002. Links between innate and adaptive immunity via type I interferon. Curr. Opin. Immunol. **14:**432–436.
22. **Lin, R., Y. Mamane, and J. Hiscott.** 2000. Multiple regulatory domains control IRF-7 activity in response to virus infection. J. Biol. Chem. **275:**34320–34327.
23. **Lund, J., A. Sato, S. Akira, R. Medzhitov, and A. Iwasaki.** 2003. Toll-like receptor 9-mediated recognition of Herpes simplex virus-2 by plasmacytoid dendritic cells. J. Exp. Med. **198:**513–520.
24. **Lund, J. M., L. Alexopoulou, A. Sato, M. Karow, N. C. Adams, N. W. Gale, A. Iwasaki, and R. A. Flavell.** 2004. Recognition of single-stranded RNA viruses by Toll-like receptor 7. Proc. Natl. Acad. Sci. USA. **101:**5598–5603.
25. **Marie, I., E. Smith, A. Prakash, and D. E. Levy.** 2000. Phosphorylation-induced dimerization of interferon regulatory factor 7 unmasks DNA binding and a bipartite transactivation domain. Mol. Cell. Biol. **20:**8803–8814.
26. **McWhirter, S. M., K. A. Fitzgerald, J. Rosains, D. C. Rowe, D. T. Golenbock, and T. Maniatis.** 2004. IFN-regulatory factor 3-dependent gene expression is defective in Tbk1-deficient mouse embryonic fibroblasts. Proc. Natl. Acad. Sci. USA **101:**233–238.
27. **Moss, W. J., M. O. Ota, and D. E. Griffin.** 2004. Measles: immune suppression and immune responses. Int. J. Biochem. Cell Biol. **36:**1380–1385.
28. **Mukaida, N., S. Okamoto, Y. Ishikawa, and K. Matsushima.** 1994. Molecular mechanism of interleukin-8 gene expression. J. Leukoc. Biol. **56:**554–558.
29. **Naniche, D., A. Yeh, D. Eto, M. Manchester, R. M. Friedman, and M. B. Oldstone.** 2000. Evasion of host defenses by measles virus: wild-type measles virus infection interferes with induction of Alpha/Beta interferon production. J. Virol. **74:**7478–7484.
30. **Palosaari, H., J. P. Parisien, J. J. Rodriguez, C. M. Ulane, and C. M.**

Horvath. 2003. STAT protein interference and suppression of cytokine signal transduction by measles virus V protein. J. Virol. **77:**7635–7644.
31. **Schlender, J., B. Bossert, U. Buchholz, and K. K. Conzelmann.** 2000. Bovine respiratory syncytial virus nonstructural proteins NS1 and NS2 cooperatively antagonize alpha/beta interferon-induced antiviral response. J. Virol. **74:** 8234–8242.
32. **Schlender, J., J. J. Schnorr, P. Spielhoffer, T. Cathomen, R. Cattaneo, M. A. Billeter, V. Ter Meulen, and S. Schneider-Schaulies.** 1996. Interaction of measles virus glycoproteins with the surface of uninfected peripheral blood lymphocytes induces immunosuppression in vitro. Proc. Natl. Acad. Sci. USA **93:**13194–13199.
33. **Schlender, J., G. Walliser, J. Fricke, and K. K. Conzelmann.** 2002. Respiratory syncytial virus fusion protein mediates inhibition of mitogen-induced T-cell proliferation by contact. J. Virol. **76:**1163–1170.
34. **Schlender, J., G. Zimmer, G. Herrler, and K. K. Conzelmann.** 2003. Respiratory syncytial virus (RSV) fusion protein subunit F2, not attachment protein G, determines the specificity of RSV infection. J. Virol. **77:**4609–4616.
35. **Schneider-Schaulies, S., I. M. Klagge, and V. Ter Meulen.** 2003. Dendritic cells and measles virus infection. Curr. Top. Microbiol. Immunol. **276:**77–101.
36. **Servant, M. J., N. Grandvaux, and J. Hiscott.** 2002. Multiple signaling pathways leading to the activation of interferon regulatory factor 3. Biochem. Pharmacol. **64:**985–992.
37. **Shaffer, J. A., W. J. Bellini, and P. A. Rota.** 2003. The C protein of measles virus inhibits the type I interferon response. Virology **315:**389–397.
38. **Sharma, S., B. R. tenOever, N. Grandvaux, G. P. Zhou, R. Lin, and J. Hiscott.** 2003. Triggering the interferon antiviral response through an IKK-related pathway. Science **300:**1148–1151.
39. **Spann, K. M., K. C. Tran, B. Chi, R. L. Rabin, and P. L. Collins.** 2004. Suppression of the induction of alpha, beta, and lambda interferons by the NS1 and NS2 proteins of human respiratory syncytial virus in human epithelial cells and macrophages. J. Virol. **78:**4363–4369.
40. **Takeda, K., and S. Akira.** 2004. TLR signaling pathways. Semin. Immunol. **16:**3–9.
41. **tenOever, B. R., M. J. Servant, N. Grandvaux, R. Lin, and J. Hiscott.** 2002. Recognition of the measles virus nucleocapsid as a mechanism of IRF-3 activation. J. Virol. **76:**3659–3669.
42. **Ulevitch, R. J.** 2004. Therapeutics targeting the innate immune system. Nat. Rev. Immunol. **4:**512–520.
43. **Valarcher, J. F., J. Furze, S. Wyld, R. Cook, K. K. Conzelmann, and G. Taylor.** 2003. Role of alpha/beta interferons in the attenuation and immunogenicity of recombinant bovine respiratory syncytial viruses lacking NS proteins. J. Virol. **77:**8426–8439.
44. **Yoneyama, M., M. Kikuchi, T. Natsukawa, N. Shinobu, T. Imaizumi, M. Miyagishi, K. Taira, S. Akira, and T. Fujita.** 2004. The RNA helicase RIG-I has an essential function in double-stranded RNA-induced innate antiviral responses. Nat. Immunol. **5:**730–737.
45. **Yoneyama, M., W. Suhara, Y. Fukuhara, M. Fukuda, E. Nishida, and T. Fujita.** 1998. Direct triggering of the type I interferon system by virus infection: activation of a transcription factor complex containing IRF-3 and CBP/p300. EMBO J. **17:**1087–1095.
46. **Yonezawa, A., R. Morita, A. Takaori-Kondo, N. Kadowaki, T. Kitawaki, T. Hori, and T. Uchiyama.** 2003. Natural alpha interferon-producing cells respond to human immunodeficiency virus type 1 with alpha interferon production and maturation into dendritic cells. J. Virol. **77:**3777–3784.

JOURNAL OF VIROLOGY, Nov. 2004, p. 12333–12343 Vol. 78, No. 22
0022-538X/04/$08.00+0 DOI: 10.1128/JVI.78.22.12333–12343.2004

Tracking Fluorescence-Labeled Rabies Virus: Enhanced Green Fluorescent Protein-Tagged Phosphoprotein P Supports Virus Gene Expression and Formation of Infectious Particles

Stefan Finke, Krzysztof Brzózka, and Karl-Klaus Conzelmann*

Max-von-Pettenkofer Institute & Gene Center, Ludwig-Maximilians-University Munich, Munich, Germany

Received 2 April 2004/Accepted 7 July 2004

Rhabdoviruses such as rabies virus (RV) encode only five multifunctional proteins accomplishing viral gene expression and virus formation. The viral phosphoprotein, P, is a structural component of the viral ribonucleoprotein (RNP) complex and an essential cofactor for the viral RNA-dependent RNA polymerase. We show here that RV P fused to enhanced green fluorescent protein (eGFP) can substitute for P throughout the viral life cycle, allowing fluorescence labeling and tracking of RV RNPs under live cell conditions. To first assess the functions of P fusion constructs, a recombinant RV lacking the P gene, SAD ΔP, was complemented in cell lines constitutively expressing eGFP-P or P-eGFP fusion proteins. P-eGFP supported the rapid accumulation of viral mRNAs but led to low infectious-virus titers, suggesting impairment of virus formation. In contrast, complementation with eGFP-P resulted in slower accumulation of mRNAs but similar infectious titers, suggesting interference with polymerase activity rather than with virus formation. Fluorescence microscopy allowed the detection of eGFP-P-labeled extracellular virus particles and tracking of cell binding and temperature-dependent internalization into intracellular vesicles. Recombinant RVs expressing eGFP-P or an eGFP-P mutant lacking the binding site for dynein light chain 1 (DLC1) instead of P were used to track interaction with cellular proteins. In cells expressing a DsRed-labeled DLC1, colocalization of DLC1 with eGFP-P but not with the mutant P was observed. Fluorescent labeling of RV RNPs will allow further dissection of virus entry, replication, and egress under live-cell conditions as well as cell interactions.

Rabies virus (RV) of the *Lyssavirus* genus and related members of the *Rhabdoviridae*, such as vesicular stomatitis virus (VSV, *Vesiculovirus* genus), are composed of only five multifunctional viral proteins, namely, nucleoprotein (N), phosphoprotein (P), matrix protein (M), glycoprotein (G), and a large (L) RNA-dependent RNA polymerase. The viral RNA is enwrapped with N and associated with P and L to form a typical helical ribonucleoprotein (RNP) complex, which is active in RNA synthesis. During RV assembly, highly condensed RNPs of the typical rhabdovirus or bullet shape are enwrapped into an envelope containing the M and G proteins (31, 32). Entry of rhabdoviruses into cells involves receptor-mediated endocytosis, pH-dependent fusion of the viral and endosomal membranes (21), release into the cytoplasm, and uncoating of RNPs from M (35) such that gene expression can resume. Although these basic principles of the rhabdovirus infection pathway have been known for some time, details of many particular steps during entry, uncoating, gene expression, and virus egress await illumination. The possibility of real-time visualization of the entire infection pathway of rhabdoviruses and of tracking virus components such as RNPs in living cells is one highly desirable tool for the study of the rhabdovirus life cycle. A widely used approach in imaging of proteins or viruses in live cells is to fuse autofluorescent proteins such as green fluorescent protein (GFP) to either the amino or the carboxy terminus of the protein of interest and to examine fluorescence within the cells over time. However, in view of the multiple functions of all rhabdovirus RNPs, their multiple interactions with viral and cellular proteins, and possible structural constraints, there may be uncertainty as to the success of this approach.

We here assessed the feasibility of labeling RV RNPs and rabies virus virions by N- and C-terminal fusion of enhanced GFP (eGFP) to the phosphoprotein P. P is not just a structural component of the RNP but is crucially involved in numerous events during the virus life cycle, including proper formation of viral RNPs and virus particles and viral RNA synthesis. In rhabdovirus-infected cells, P is present in the form of oligomers (20). Binding of P to N is thought to chaperone N such that it specifically encapsidates viral RNA (9, 23, 26), making it a suitable template for RNA synthesis by the viral polymerase complex. In addition, P is an essential cofactor of the polymerase complex itself and directly binds the catalytic L protein (6). During RNA synthesis, RV RNPs or the polymerase complex interact with the M protein, which is involved in regulating the balance of mRNA transcription and RNP replication (17, 18). Moreover, RV P protein may also be involved in interactions with cellular factors important for in vivo infection. P was shown to bind to dynein light chain 1 (DLC1), suggesting a function in the transport of RNPs by motor proteins (27, 33, 34). In addition, an N-terminally truncated form of P has been found to enter the nucleus and to colocalize with promyelotic leukemia bodies (1).

* Corresponding author. Mailing address: Max-von-Pettenkofer Institute & Gene Center, Feodor-Lynen-Str. 25, D-81377 München, Germany. Phone: 49 89 2180 76851. Fax: 49 89 2180 76899. E-mail: conzelma@lmb.uni-muenchen.de.

Since it was not clear whether the fusion of eGFP to the N or C terminus of RV P affected its essential functions, recombinant P fusion proteins were first used for complementation of a recombinant RV lacking the P gene. Successful complementation was possible with N- and C-terminally fused P proteins, but differential activity in RNA synthesis and virus formation were noticed. The eGFP-P fusion protein allowed effective production of fluorescent extracellular virions that could be detected by conventional epifluorescence microscopy or laser-scanning microscopy and could be tracked during attachment to cells and internalization. The recovery of a viable recombinant RV expressing eGFP-P instead of P and its interaction with the cellular DLC1 protein further suggested that such recombinant viruses represent promising and reliable tools to study diverse aspects of rhabdovirus biology in living cells.

MATERIALS AND METHODS

Cells and viruses. Viruses were grown on BHK-21 clone BSR cell monolayers maintained in Glasgow minimal essential medium supplemented with 10% newborn calf serum. BSR T7/5 cells constitutively expressing bacteriophage T7 RNA polymerase (2) was used for recovery of RV from transfected cDNA. BSR cells that constitutively express the authentic RV P protein were generated by cotransfection of 2.0 μg of p4P plasmid containing the P gene after the simian virus 40 promoter and of 0.2 μg of pMamNeo containing the neomycin resistance gene and subsequent cultivation in the presence of G418 (1 mg/ml). Cells expressing P fused to the N or C terminus of eGFP (BSR T7-eGFP-P and BSR T7-P-eGFP) were selected after cotransfection of BSR T7/5 cells with 5.0 μg of pEGFP-P or pP-EGFP and 0.5 μg of pTRE-Hyg (Clontech) and subsequent cultivation in the presence of hygromycin (1 mg/ml). The expression plasmids pEGFP-P and pP-EGFP are derivates of pEGFP-C3 and pEGFP-N3 (Clontech), with different linkers of 14 and 16 amino acids, respectively. BSR T7/5 cells that constitutively express DLC1 fused to the N terminus of a modified red fluorescent protein from *Discosoma* sp. (DsRed) were selected after cotransfection of the expression vector pDLC1-DsRed and pTRE-Hyg and selection as described above for eGFP-P cells. pDLC1-DsRed was constructed by an insertion of the coding sequence of DLC1 from human 293 cells into the pDsRed-Express-N1 vector (Clontech).

Recombinant RV lacking P expression, SAD ΔP, was generated from pSAD ΔP, which is a cDNA derivative of pSAD L16 (36). A deletion of 934 bp in the P-gene sequence (SAD B19 [7] nucleotides 1500 to 2434) resulted in the complete deletion of the P-protein-encoding sequence. In SAD eGFP-P, the authentic P coding sequence was replaced with the eGFP-P fusion encoding sequence from pEGFP-P. For generation of SAD eGFP-PI, the P protein coding sequence in pTIT-P (16) was mutated with the mutagenesis primer (5′-CCAGGAAAGT CTTCAGCAGCGGCAGCGGCAGCGGCAGCGGGCCGAGAGCTCAAGA AG-3′) using the Chameleon mutagenesis kit (Stratagene) as specified by the supplier. In pTIT-PI, 8 amino acids (142-EDKSTQTT-149) were thus replaced by alanine residues, deleting the DLC1 binding motif. The corresponding recombinant SAD eGFP-PI was generated by insertion of the mutated P gene sequence into the pSAD eGFP-P cDNA clone. A detailed description of all cloning steps and the final sequences are available from the authors on request by e-mail.

cDNA rescue experiments. cDNA plasmids were transfected into cells after calcium phosphate precipitation (mammalian transfection kit; Stratagene) as specified by the suppliers. Vaccinia virus-free rescue of recombinant RV was performed as described previously (16) by transfection of 10 μg of full-length cDNA and plasmids pTIT-N (5 μg), pTIT-P (2.5 μg), and pTIT-L (2.5 μg) in 10^6 BSR T7/5 cells grown in 8-cm^2 culture dishes. For recovery and subsequent amplification of the P-deficient RV SAD ΔP, culture supernatants from transfected cells were transferred onto BSR P cells at 3 days postinfection and incubated until almost 100% of the cells were infected.

Density gradient centrifugation. Supernatants from 3×10^6 virus-infected cells were harvested on day 2 after infection at a multiplicity of infection (MOI) of 1, and the virions were pelleted through 20% sucrose in TEN buffer (50 mM Tris-HCl, 1 mM EDTA, 150 mM NaCl [pH 7.4]) on a 60% sucrose cushion. The interphase fraction was diluted in TEN buffer and was loaded on a 12-ml 20 to 40% iodixanol (Optiprep; Axis-Shield) density gradient. After 18 h of centrifugation (Beckman SW28 instrument; 27,000 rpm at 4°C), 12 fractions of 1 ml each were collected and the quality of the density gradients was controlled by determination of the refraction index of each fraction. After polyacrylamide PAA gel electrophoresis and Western blotting, fractions were analyzed with RV N, P, and M protein-specific sera or with a polyclonal serum recognizing eGFP.

Cell binding and virus uptake. To observe binding of virus to the surface of cells, BSR T7/5 cells were trypsinized and the suspension was incubated with virus for 2 h at 4°C. The cells were then pelleted, resuspended in ice-cold phosphate-buffered saline and transferred onto the slides. After fixation and counterstaining with propidium iodide, the cells were mounted (Vectashield) and analyzed by confocal laser-scanning microscopy. To monitor virus uptake, the cells were incubated at 37°C for 30 min after incubation of cells for 2 h at 4°C.

Fluorescence microscopy. Epifluorescence microscopy was performed on an inverse Zeiss Axiovert 200M microscope with 20× and 63× (NA 1.4) objectives, using Zeiss Filtersets (FS) 10 for GFP (excitation, BP450 to 490 nm; emission, BP515 to 565 nm) and FS 00 (excitation, BP530 to 585 nm; emission, LP615 nm) for DsRed. Images were taken with a Zeiss Axiocam HRm microscope using the Axiovision 3.1 software. Confocal laser-scanning microscopy was performed with the Leica TCS NT laser system, using a Leica DM IRB microscope or with a Zeiss LSM510 Meta laser system using a Zeiss Axivert200 microscope.

RNA analysis. RNA from cells was isolated with the RNeasy mini kit (Qiagen). Northern blot analyses and hybridizations with [α-^{32}P]dCTP-labeled cDNAs recognizing the RV N or P gene sequences were performed as described previously (8). Hybridization signals were quantified by PhosphorImager analysis (Molecular Dynamics Storm).

RESULTS

Recovery of a P-deficient RV and complementation with eGFP fusion proteins. To establish a versatile system for assaying activities of different RV P constructs, we constructed an RV cDNA in which the complete P open reading frame was deleted (Fig. 1A). Rescue of the cDNA into recombinant RV SAD ΔP was achieved after transfection of BSR T7/5 cells with plasmids encoding RV N, P, L, and SAD ΔP antigenome RNA as described previously (16, 36). For further propagation of the newly generated viruses, supernatants from transfected cells were then transferred to a cell line constitutively expressing RV P (BSR-P) that was generated as described in Materials and Methods. The low levels of P expressed in BSR-P cells (not shown) supported the amplification of SAD ΔP; however, infectious-virus titers did not exceed 10^5 infectious units (IU) per ml of cell culture supernatant (not shown).

To test whether P proteins to which fluorescent eGFP was fused at the N or C terminus (eGFP-P or P-eGFP, respectively) would support the growth of SAD ΔP and provide a possibility to label virus RNPs and virus particles, two cell lines constitutively expressing the fluorescent proteins were generated. Expression of both fusion proteins led to a diffuse green cytoplasmic fluorescence with no significant signal in the nucleus of cells (Fig. 1B, bottom). However, when BSR eGFP-P and BSR P-eGFP cells were infected with the P-deficient SAD ΔP or the standard RV SAD L16 at an MOI of 0.1, fluorescence was concentrated in granular structures similar to the typical inclusion bodies that are usually observed in RV-infected cells (Fig. 1B, top and middle). Since coexpression of the RV N and P proteins is sufficient for formation of the inclusion bodies (5), the appearance of these fluorescent dots in SAD ΔP-infected cells demonstrated successful viral N gene expression by the activity of the two fluorescent P fusion proteins. In addition, it indicated typical interaction of eGFP-P and P-eGFP with N. Indeed, immunostaining with antibodies recognizing RV N protein revealed colocalization with the fusion proteins. In wild-type (wt) RV infection, this interaction

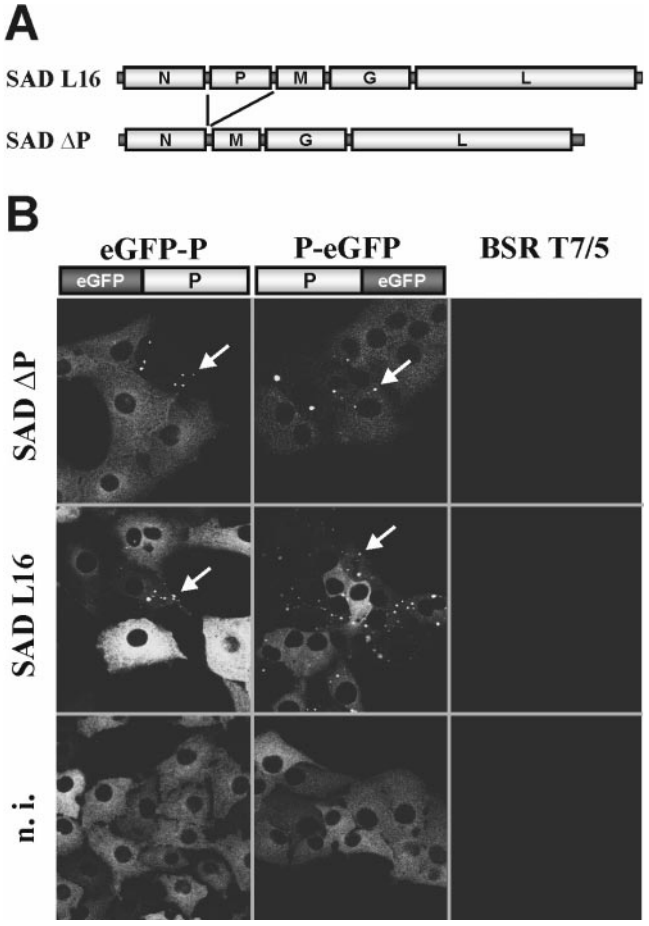

FIG. 1. Complementation of a P-deficient RV in cells expressing eGFP-tagged P proteins. (A) Genome organization of SAD ΔP, lacking the entire P open reading frame, and the parental SAD L16. (B) Recruitment of cellular eGFP-tagged P proteins into RV inclusion bodies. Cells expressing the indicated P fusion proteins were infected with SAD ΔP or SAD L16. The appearance of fluorescent inclusion bodies at 1 day postinfection demonstrated nucleoprotein gene expression from SAD ΔP. Both eGFP-P and P-eGFP proteins also colocalized to inclusion bodies of wt SAD L16. In noninfected cells (n.i.), diffuse fluorescence was exclusively observed.

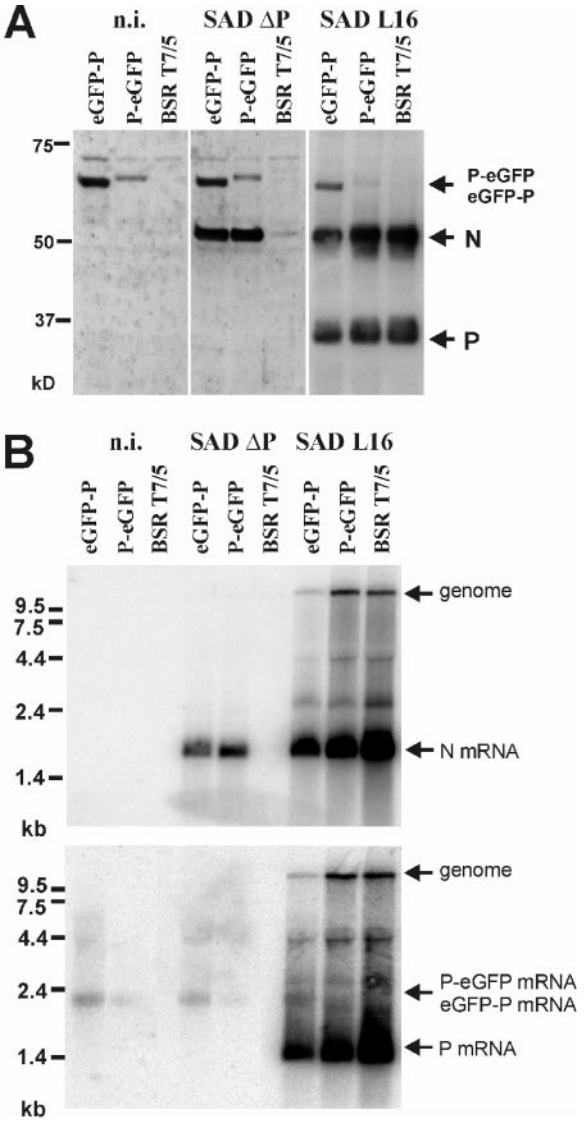

FIG. 2. Gene expression of SAD ΔP and SAD L16 in eGFP-P and P-eGFP protein-expressing cells. Cells were infected with the indicated viruses at an MOI of 0.5 for 2 days and processed for analysis of viral proteins and RNA. (A) Western blot with a serum recognizing RV N and P proteins. For SAD L16-infected cells, three times less extract was loaded. (B) Northern blot hybridization with N- and P-specific cDNA probes. n.i., not infected.

took place in the presence of excess authentic P expressed from the virus. Moreover, similar to SAD L16, further spread of SAD ΔP in the cell cultures could be directly observed by the appearance the autofluorescent inclusion bodies in previously homogenously fluorescing cells (data not shown). This suggested that infectious-virus particle formation may also be supported by the eGFP-P fusions.

The effects of the P fusion proteins on virus gene expression and protein synthesis were further investigated by Western and Northern blot analyses (Fig. 2). In both cell lines the cell-derived GFP fusions with an expected size of approximately 62 kDa were detectable with a serum recognizing RV P protein (Fig. 2A). Infection with SAD ΔP led to the synthesis of considerable amounts of N protein only in the cell lines expressing the tagged P proteins. A faint signal for N was also detectable in noncomplementing BSR T7/5 cells, which could represent viral input N and newly expressed N protein through primary transcription of input virus. Notably, although eGFP-P was apparently present at higher levels than P-eGFP, similar levels of N protein accumulated in the two cell lines, suggesting a somewhat higher specific activity of P-eGFP in viral gene expression (Fig. 2A). This was supported by the finding of lower levels of cellular P-eGFP mRNA than of eGFP-P mRNA (Fig. 2B, bottom), combined with slightly more abundant N mRNAs in SAD ΔP-infected P-eGFP cells (Fig. 2B, top). Thus, it appears that P-eGFP is less impaired than eGFP-P in its function in viral mRNA synthesis. Moreover, expression of eGFP-P had a considerable negative effect on RNA synthesis and protein expression of wt RV, illustrated by reduced N and P mRNA and protein levels (Fig. 2, right panels), whereas viral RNA

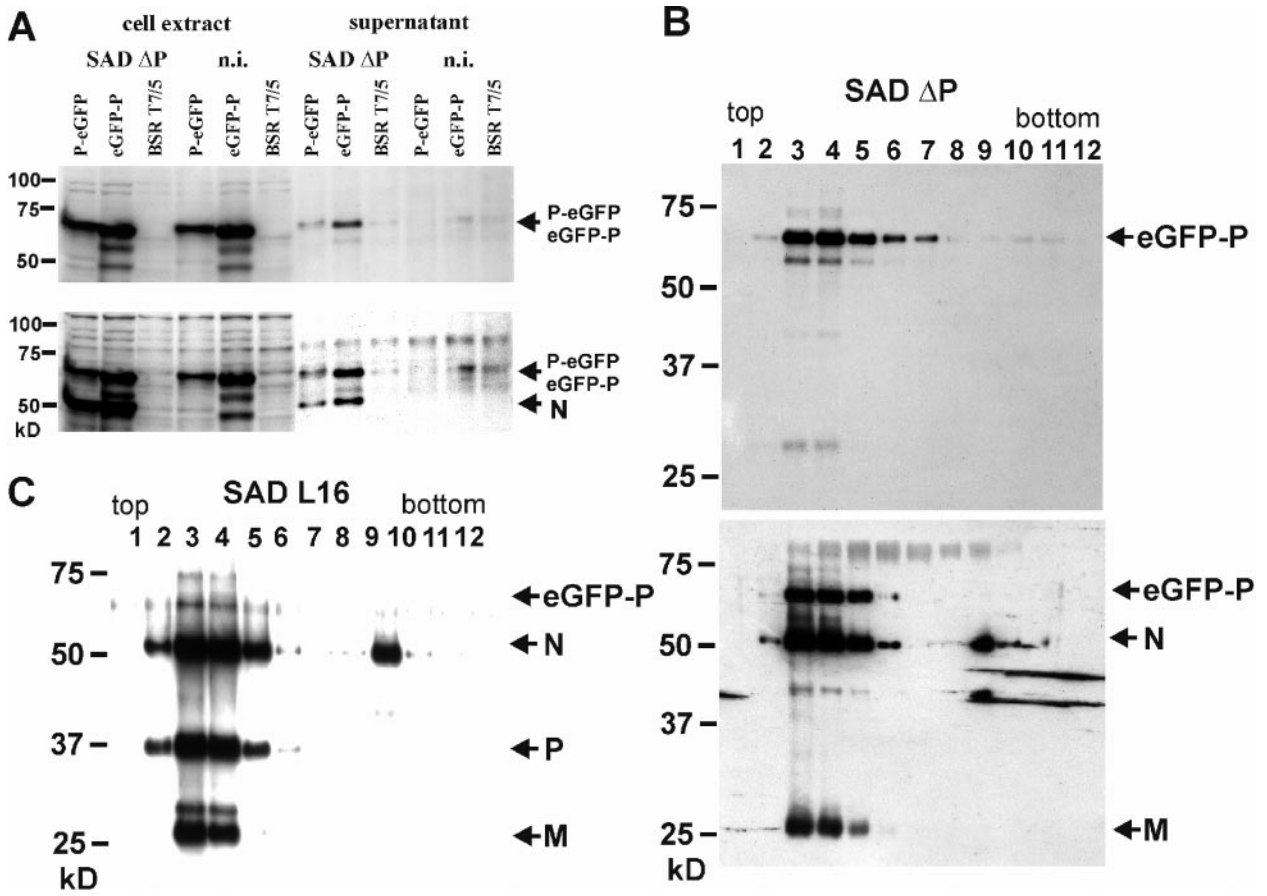

FIG. 3. Incorporation of eGFP-P into RV virions. (A) Supernatants from cells expressing the indicated P fusion proteins and infected for 4 days with SAD ΔP virus were centrifuged through 20% sucrose and analyzed by Western blotting using sera recognizing eGFP (upper blot) and RV N and P proteins (lower blot). n.i., not infected. (B) Purification of supernatant virions from SAD ΔP-infected eGFP-P cells in a 20 to 40% iodixanol density gradient. Fractions were analyzed by Western blotting with sera recognizing GFP (upper blot) or RV N, P, and M proteins (lower blot). (C) Incorporation of eGFP-P into gradient-purified SAD L16 virions from eGFP-P expressing cells. Fractions were analyzed with RV N, P, and M protein-specific sera.

synthesis in P-eGFP cells was more similar to that in the control BSR T7/5 cells.

Incorporation of eGFP-P into virions. Although SAD ΔP virus gene expression was readily detected in the complementing cell lines, the yield of infectious virus was low, reaching maximum titers of 7×10^5 IU per ml of cell culture supernatant, i.e., 1,000-fold lower than standard virus SAD L16 titers in BSR cells. Most interestingly, infectious titers on P-eGFP cells were the same as or lower than those on eGFP-P cells, in spite of the obviously more rapid accumulation of viral RNAs in P-eGFP cells. To study virus formation and incorporation of the P-fusion proteins, supernatant virions from SAD ΔP-infected cells were enriched 4 days after infection at an MOI of 0.1 by centrifugation through 20% sucrose on a 60% sucrose cushion. Western blot analysis with sera recognizing GFP or RV N and P revealed the presence of both P fusion proteins along with N and suggested the formation of virus particles containing the P fusion proteins (Fig. 3A). Consistently, supernatants from eGFP-P cells were found to contain more viral protein, suggesting that its poor transcription activity is compensated by better permitting particle formation. Further purification by iodixanol density gradient centrifugation confirmed the formation of typical virus particles containing eGFP-P. A common protein peak of RV N, M, and the cell-derived 62-kDa eGFP-P protein, which also represented the peak of infectious virus (not shown), was demonstrated by Western blot analyses using sera against viral proteins and GFP (Fig. 3B, fractions 3 to 5). The complemented SAD ΔP(eGFP-P) virions completely lacked the authentic 37-kDa RV P protein abundantly present in particles from SAD L16-infected cells (Fig. 3C). As indicated by the appearance of a faint band representing eGFP-P in virions from e-GFP-expressing cells infected with SAD L16, incorporation of eGFP-P into virions was possible, although at low efficiency, in the presence of excess amounts of authentic viral P protein (Fig. 3C).

Detection of labeled virus particles by fluorescence microscopy. To check whether the amount of virus-incorporated eGFP-P is sufficient for detection of virions by fluorescence microscopy, density gradient-purified SAD ΔP(eGFP-P) virions were transferred to glass coverslips and, without further treatment, were analyzed by confocal laser-scanning microscopy. Bright punctiform green fluorescence was observed, with individual dots of rather uniform size (Fig. 4A). Such typical

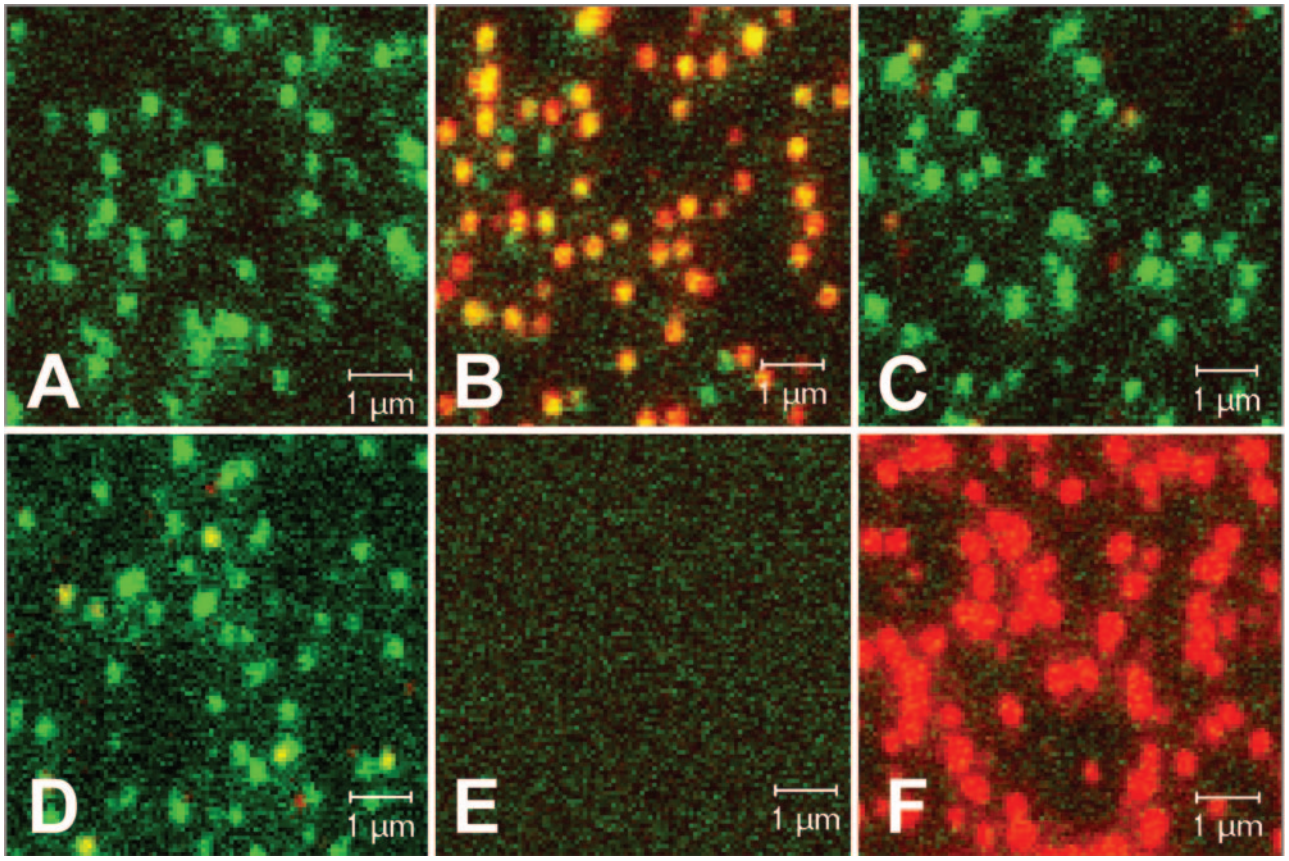

FIG. 4. Autofluorescence of eGFP-P-containing SAD ΔP virions and coimmunostaining for viral proteins. (A to D) Density gradient-purified SAD ΔP virions complemented with eGFP-P were adhered to glass coverslips and directly analyzed by confocal laser-scanning microscopy (A) or were immunostained (red fluorescence) with sera recognizing RV G (B), M (C), or N (D). (E) Negative control: no virus, anti-RV G immunostain. (F) SAD L16 virions stained with anti-G antibodies. Overlays of the eGFP-P fluorescence (green) and of the immunostainings (red) are shown.

patterns were not observed with purified supernatants from noninfected eGFP-P-expressing cells (Fig. 4E) or with wt virions (Fig. 4F), indicating that the fluorescent dots represent single extracellular, labeled virions. To further characterize the fluorescent structures observed, immunostaining of the unfixed and unpermeabilized virions was performed with antibodies specific for different virus proteins and Cy3-labeled secondary antibodies. Incubation with an antibody recognizing the viral surface glycoprotein G resulted in costaining (yellow) of most of the dots (Fig. 4B). Antibodies to the internal matrix protein M, which is located underneath the viral lipid bilayer, costained only a few dots (Fig. 4C), most probably as a result of disruption of the viral membrane during the course of virus purification. A similar staining was observed for the nucleoprotein N, a component of the inner RNP (Fig. 4D). These data strongly suggest that the punctuate structures observed by confocal microscopy represented intact fluorescent RV particles.

Cell binding and uptake of fluorescent virions. To further investigate the biological behavior of green fluorescent virions, cell infection experiments were performed. To monitor binding to target cells, BSR cells grown in suspension were incubated with gradient-purified SAD ΔP(eGFP-P) for 2 h at 4°C, thereby preventing receptor-mediated endocytosis. Typical green dots associated with the surface of propidium iodide-counterstained cells could be visualized by confocal microscopy (Fig. 5A, top). The dots were of homogenous size, less than 1 μm, and were present exclusively at the surface of cells. These dots were not present in preparations of mock-incubated cells (Fig. 5A, bottom), suggesting that they represent virus particles. Notably, when virus-neutralizing antibodies were added prior to incubation with the cells, fluorescent signals were also associated with the surface of cells. However, the fluorescent structures were much larger (>1 μm), suggesting that they represent cross-linked virus aggregates (Fig. 5A, middle).

To further monitor the fate of fluorescent virions during cell entry, binding assays were performed as above, followed by a temperature shift to 37°C, which should allow receptor-mediated endocytosis. After 30 min at 37°C, the nonneutralized green dots were found internalized into intracellular vesicles (Fig. 5B, top). In contrast, the vast majority of the larger cross-linked complexes remained bound at the cell surface, although some of the complexes were also internalized (Fig. 5B, middle). Such temperature-dependent internalization and accumulation of dots in large vesicular structures indicate that eGFP-labeled virus particles were internalized by receptor-mediated endocytosis as described for natural RV.

Recombinant RV expressing eGFP-P fusion protein: live interaction of eGFP-P with DLC1. Successful complementa-

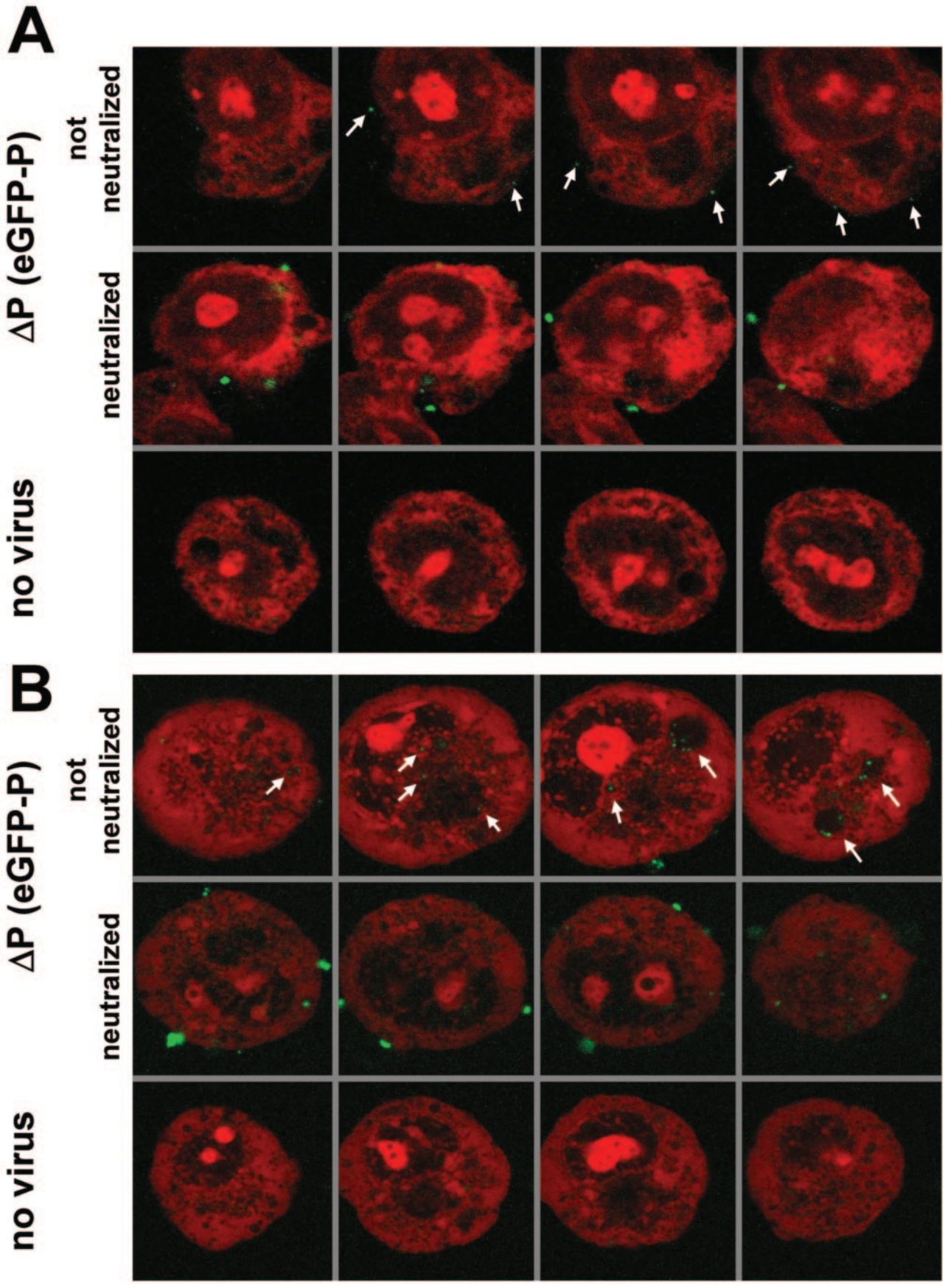
A
ΔP (eGFP-P)
not neutralized
neutralized
no virus
B
ΔP (eGFP-P)
not neutralized
neutralized
no virus

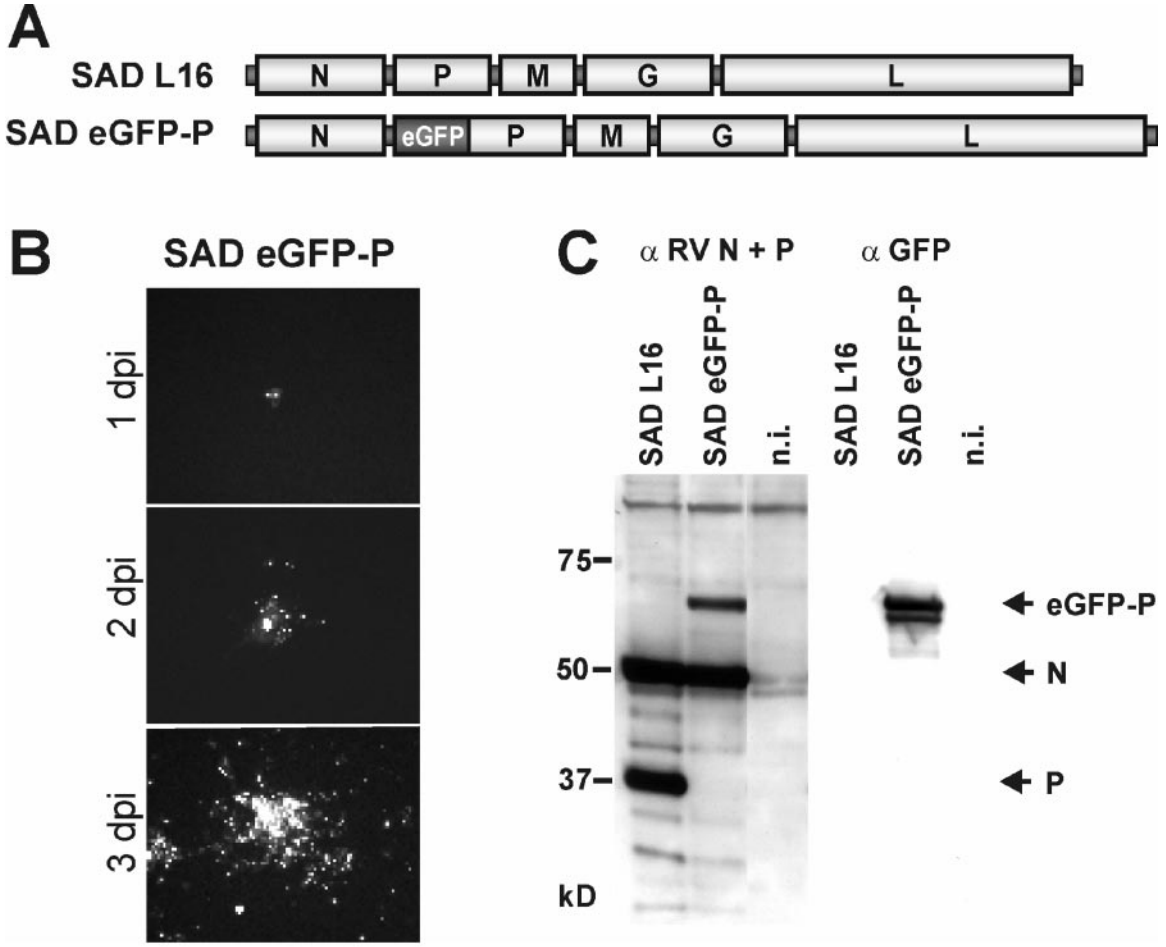

FIG. 6. Recovery of autonomously replicating RV expressing the eGFP-P fusion. (A) Genome organization of SAD L16 and SAD eGFP-P in which eGFP is fused to the N terminus of P. (B) Spread of SAD eGFP-P in noncomplementing BSR T7/5 infected at a MOI of 0.001 observed in live cells by fluorescence microscopy at the indicated time points. (C) Expression of eGFP-P in cells infected with SAD ΔP at a MOI of 1 after 2 days by Western blots with the indicated sera. n.i., not infected.

tion of SAD ΔP in the eGFP-P expressing cell line to yield fluorescent intact virions led us to construct a full-length RV cDNA encoding the eGFP-P fusion protein instead of P (Fig. 6A). Successful rescue of viable virus from cDNA in standard transfection experiments was indicated by the appearance of the typical fluorescent inclusion bodies in foci of transfected BSR T7/5 cells at 5 days posttransfection and their further spread throughout the culture. In standard virus stock preparations, SAD eGFP-P virus yielded infectious titers of 2×10^6 focus-forming units (FFU)/ml, which is about 100-fold lower than those of the parental SAD L16 virus. Infection of cells and spread in cell culture could be monitored by fluorescence microscopy (Fig. 6B). Control immunostaining of the RV N protein revealed that all infected cells expressed eGFP-P protein (not shown), confirming the absence of virus in which the GFP sequence had been deleted during virus amplification. In live cells, green fluorescence was confined to the cytoplasm and was not observed in the nucleus, as is the case with a virus expressing GFP from an extra gene (not shown).

Interactions of the virus-derived fluorescent eGFP-P fusion with other virus proteins were analyzed in more detail by immune staining of the RV N, P, or L protein and examination by confocal laser-scanning microscopy. Both N and L most exclusively colocalized with eGFP-P in the typical inclusion bodies

FIG. 5. Cell binding and internalization of fluorescent virus. (A) Binding at 4°C of density gradient-purified SAD ΔP(eGFP-P) to the cell surface. BSR cells were incubated for 2 h at 4°C with virus, fixed, and counterstained with propidium iodide. Small green dots (<1 μm) were detectable at the cell surface (top row). Neutralization with anti-G antibodies prior to incubation with cells resulted in larger aggregates (>1 μm [middle row]) that were still able to attach. Analysis of multiple sections of cells revealed that fluorescent signals were detectable exclusively at the cell surface. No comparable signals were obtained in the absence of virus (bottom row). (B) Internalization of bound SAD ΔP virus particles into large vesicular structures was observed after subsequent temperature shift to 37°C (top row). Most neutralized virus (anti-G antibodies) remained at the cell surface; however, some virus aggregates were also internalized (middle row). No green fluorescence was observed in cells not infected with SAD ΔP(eGFP-P) virus (bottom row). All laser scans shown in the figure were made at identical parameter settings.

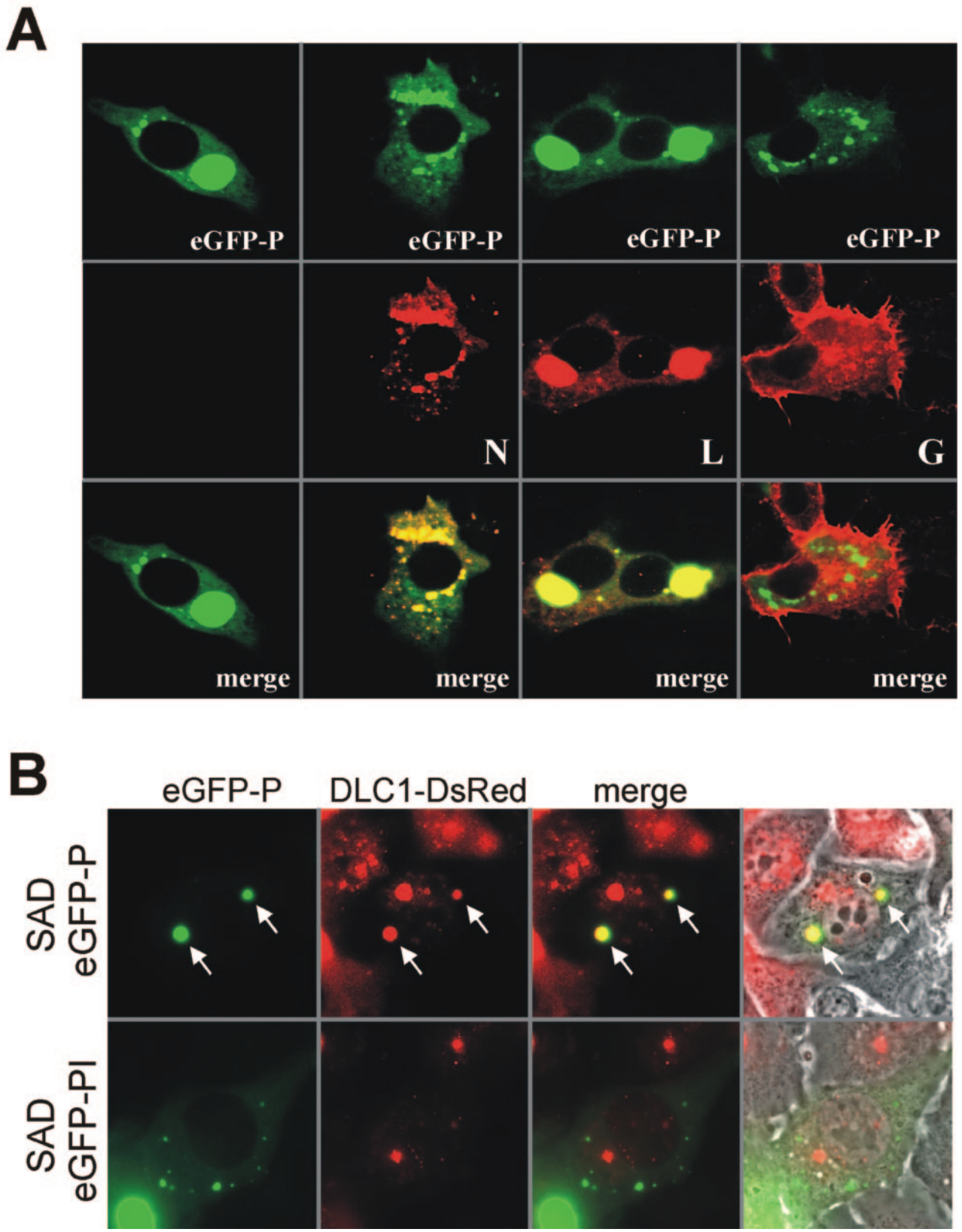

FIG. 7. Interaction of eGFP-P with viral proteins (A) and cellular DLC1 (B). (A) SAD eGFP-P-infected BSR T7/5 cells were fixed at 2 days postinfection, immunostained with sera recognizing the RV N, G, or L proteins (red fluorescence), and analyzed by confocal laser-scanning microscopy. As a negative control, the infected cells were only incubated with fluorophor-conjugated secondary antibody (first column). (B) A cell line constitutively expressing DsRed-tagged DLC1 was infected with SAD eGFP-P and a mutant virus lacking the DLC1 binding site, SAD eGFP-PI. Autofluorescence of eGFP-P (green) and DsRed-DLC1 (red) was observed in live cells 1 day postinfection by conventional epifluorescence microscopy. Whereas DsRed perfectly colocalized with the SAD eGFP-P inclusion bodies (upper lane, arrows), no colocalization was observed in cells infected with the inclusion bodies of SAD eGFP-PI. Right-hand column, fluorescence and phase contrast.

(Fig. 7A). As expected, G protein was located predominantly in Golgi-endoplasmic reticulum compartments and at the cytoplasm membrane and did not co-localize with eGFP-P.

RV P protein interacts with cellular DLC1. To check whether eGFP-P has retained this feature, a cell line expressing DLC1 fused to red fluorescent protein DsRed was generated as described in Materials and Methods and was infected with SAD eGFP-P virus. At 1 day postinfection, the distribution of DLC1-DsRed in living cells was analyzed (Fig. 7B, top). Most eGFP-P inclusion bodies showed red fluorescence, demonstrating interaction of the DLC1 and P subunits of the fusion proteins. To confirm the specificity of the interaction, an SAD eGFP-P mutant virus was generated in which the binding motif for DLC1 was replaced by a stretch of 8 alanine residues, SAD eGFP-PI. On infection of DLC1-dsRED cells with the mutant, costaining of inclusion bodies was no longer observed (Fig. 7B, bottom), demonstrating that eGFP-PI has lost the specific ability of eGFP-P to bind to DLC1-DsRed.

DISCUSSION

The availability of proteins tagged with GFP or other autofluorescent proteins, combined with progress in optical imaging, has recently allowed us to address the dynamics of many biological processes in living cells (15). This technology is particularly attractive to monitor virus infection in vitro and in vivo. Compared to chemical labeling, which allows input virus to be tracked (11, 22, 28, 37, 38), genetic labeling of virus proteins allows us to study all aspects of the virus life cycle in real time. For instance, successful labeling by GFP has been reported for human immunodeficiency virus, herpes simplex virus, and rotavirus particles (3, 12, 29). Structural and functional constraints of highly organized viruses, such as rhabdoviruses, however, may preclude the inclusion of entire fluorescent proteins or protein domains. We report here the successful construction of a viable, fluorescent RV which behaves like natural virus in many aspects and which allows live tracking of virus and virus components throughout the viral live cycle. Of note, even single virus particles were detectable by conventional live fluorescence microscopy, which is highly preferable over integrated imaging for kinetic studies.

Several reasons argued for the strategy to select the P protein for fusion with eGFP. Since P is a component of the viral RNP, fluorescent P therefore allows tracing not only of extracellular virions but also of RNPs following entry into cells and uncoating. Of the RNPs, P is of intermediate abundance. With approximately 450 copies of P present in VSV RNPs (40), it greatly exceeds the 120 molecules of eGFP required to visualize single rotavirus particles (3). Previously, an elegant study described successful labeling of the L protein of measles virus (*Paramyxoviridae*) by inserting GFP into an internal flexible loop of the protein and without disrupting its basic functions in RNA synthesis (14). However, single virus particles have not been observed, probably due to the lower content of L in RNPs. Approximately 50 copies of L were reported to be present in VSV RNPs (40). Approaches to labeling rhabdovirus proteins have so far been confined to the G protein of VSV. However, GFP fused to the cytoplasmic tail of VSV G allowed the generation of recombinant virus only when the authentic G protein was coexpressed (10).

Since RV P is instrumental in several essential virus functions, we first wanted to assess the functions of P proteins with N- and C-terminal eGFP extensions in virus complementation assays. We therefore constructed a recombinant P-deficient RV (SAD ΔP) and a P-cell line in which this virus could be amplified. The subsequent establishment of cell lines that express either P-eGFP or eGFP-P fusion proteins allowed versatile testing of protein functions related to virus gene expression and formation of virions.

RV gene expression could be visualized simply by infection and subsequent fluorescence microscopy. The redistribution of the diffuse cytoplasmic green fluorescence into the typical inclusion bodies demonstrated successful expression of N from the SAD ΔP genome (Fig. 1). Moreover, the appearance of inclusion bodies, first in single cells and later in neighboring cells, illustrated virus formation and spread (not shown) and provided strong evidence that both eGFP-P and P-eGFP were able to support the entire virus life cycle. This was confirmed by the detection of infectious virions in the cell culture and their repeated passage in the complementing cells.

Although both P fusion proteins were able to rescue the P deficiency of SAD ΔP, both were obviously disrupted in P functions. Moreover, fusion of eGFP to either the N terminus or C terminus resulted in different phenotypes, as may have been expected from the complex organization of the RV P protein and, in particular, the importance of the terminal regions of the P protein. The first 19 residues of P represent a binding site for L (6), whereas the C terminus of P is involved in binding to N (5, 6).

It was therefore interesting that SAD ΔP mRNA transcription was more effective in P-eGFP-expressing cells than in eGFP-P expressing cells, in spite of higher levels of the latter protein (Fig. 2). The decreased efficiency of eGFP-P in gene expression may therefore be due to steric hindrance, by the N-terminal GFP, of proper formation of the viral RNA polymerase complex, which, in VSV, is thought to contain three P molecules (19). The interesting observation of impaired gene expression of SAD L16 in eGFP-P-expressing cells may also be explained by a dominant negative effect of the eGFP-P fusion on the polymerase complex. Either incorporation of an eGFP-P molecule in the multimeric polymerase complex, leading to reduced activity, or a reduced binding of the viral polymerase to N/eGFP-P complexes might be responsible. In addition, the N-terminal extension of eGFP-P should abolish the expression of a series of N-terminally truncated P proteins (P2, P3, and P4) which are expressed in wt RV-infected cells from the P gene by translation initiation at downstream in-frame initiation codons (4). However, the recovery of viable SAD eGFP-P virus illustrated that these truncated forms of P do not represent essential virus proteins. Moreover, the dominant negative effect of eGFP-P on RNA synthesis of SAD L16, which does express the truncated P forms (not shown), strongly suggests that the intrinsic functions of the eGFP-P full-length protein rather than the lack of truncated P proteins is responsible for the poor RNA synthesis of SAD eGFP-P.

Compared to eGFP-P, the C-terminally extended P-eGFP showed less impairment in RNA synthesis; however, it was less effective in supporting infectious-virus formation. Comparison of supernatant virions from complementing cell lines indicated a less efficient release of virus particles from SAD ΔP-infected

P-eGFP-expressing cells (Fig. 3A). The C-terminal moiety of RV P is involved in N binding. In particular, the C-terminal residues aa 268 to 297 were reported to strongly bind N (5). Thus, the defect of P-eGFP in virus particle formation might be due to an impairment of N binding. If so, however, it is notable that this defect in N binding did not greatly affect RNA replication, which is thought to depend on proper P/N interaction and interaction of the P/L polymerase with the RNP template. The poor formation of virus particles in P-eGFP-expressing cells is most probably due to its poor activity in assembly (see above; Fig. 2). In addition, the expression levels may be limiting, thus contributing to the low-efficiency virus production.

In the approach of generating fluorescent RV virions similar to wt RV, the phenotype of eGFP-P with reduced RNA synthesis and reasonable virus formation was preferable to that of P-eGFP, where viral RNA and protein accumulation was expected due to more severe defects in virus assembly. Therefore, eGFP-complemented SAD ΔP virus and recombinant SAD eGFP-P virus were used for further analysis of fluorescent RV. Comigration of eGFP-P with the virion marker proteins N and M in density gradients demonstrated the formation of typical RV virions and efficient incorporation of the eGFP-tagged P protein. As already suggested by the occurrence of strong Western blot signals (Fig. 3B), the level of incorporated eGFP-P was high enough to enable detection of extracellular virus particles by confocal laser-scanning microscopy (Fig. 4) and conventional epifluorescence microscopy (not shown). Moreover, a series of different experiments demonstrated that even single virus particles could be identified. Untreated purified virions appeared as green individual dots of homogenous size. Staining with antibodies against external (G) and internal (M and N) virus proteins supported the identity of the dots as individual virus particles rather than protein aggregates. Virtually all dots stained for the surface G protein; some, in which the membrane was probably disrupted, stained for M; and virtually none stained for the RNP protein P. This is in agreement with the proposed structure of RV, with a tight M protein layer located underneath the lipid envelope, completely protecting the RNP from access by antibodies (32).

Results of binding and internalization assays also suggest that we have observed single and intact virus particles which behave like natural virus. RV enters the cells by receptor-mediated endocytosis (39). Binding of fluorescent dots of uniform size to the surface of cells was demonstrated at low temperature. In the presence of neutralizing antibodies, fluorescent aggregates of larger and different size were present, some of which were also bound to the cell surface. Increasing the temperature to 37°C then allowed internalization of the individual dots into vesicles, within 30 min, reflecting virus uptake by receptor-mediated endocytosis (Fig. 5B). Also, some of the large aggregates formed by neutralizing antibodies were internalized. These observations are in full agreement with previous studies showing that binding of antibody-cross-linked RV to cells is still possible and internalization is not completely prevented (13). This indicates typical attachment and entry of SAD eGFP-P into target cells, suggesting that this virus is a promising tool to further dissect molecular and kinetic details of RV binding, uptake, membrane fusion, and uncoating.

Further experiments with SAD eGFP-P were aimed at validating whether some prominent function of authentic P in the interaction with host cell proteins is maintained by eGFP-P. RV P has been described to efficiently bind DLC1 (27, 34). Although deletion of the DLC1 binding site of P does not affect virus transcription and growth in standard cell culture (30, 33; unpublished data), a role of wt P in the intracellular retrograde transport of RNPs along microtubules was suggested, with a potentially important impact on the spread and pathogenesis of RV. To examine the interaction of P with DLC1 in live cells, a cell line was generated that constitutively expressed DsRed-labeled DLC1 as well as a SAD eGFP-P mutant virus in which the DCL1 binding motif was replaced with a stretch of alanine residues (SAD eGFP-PI; see Materials and Methods). This modification in P did not change the growth characteristics of the virus in BSR cultures (not shown). On infection with SAD eGFP-P, DsRed DCL1 colocalized with viral inclusion bodies. eGFP-P was exclusively responsible for recruitment of DsRed-DLC1 into the inclusion bodies, since in SAD eGFP-PI-infected cells, colocalization was never observed (Fig. 7). The availability of recombinant RV expressing fluorescent P now also provides the possibility of directly monitoring the movement of virus or viral RNPs in more specialized cell cultures such as neurons, or in vivo, and addressing the disputed question whether dynein motor transport of intracellular RNPs or transport of vesicles containing entire virus makes the greater contribution to the famous retrograde axonal transport of RV to the central nervous system.

In summary, tagging of the RV P with eGFP-P appears to allow many aspects of the entire RV life cycle. For instance, monitoring of RV binding to cells and neurons in vitro and in vivo may facilitate investigations of the distribution and nature of RV receptors, virus endocytosis, and membrane fusion. As viral RNPs are labeled, release of the RNP into the cytoplasm, uncoating of the RNP from the M layer (35), and onset of RNA synthesis may be tracked as well. As for studies on the mechanisms involved in entry, approaches to inhibit virus entry are more easily done with fluorescent virions and may be automated in the future. Further work will reveal whether the assembly and egress of rhabdovirus, which seems to usurp cellular vesicle transport mechanisms and budding (24, 25), can also be visualized in live cells.

ACKNOWLEDGMENTS

We thank N. Hagendorf for perfect technical assistance.

This work was supported by the Deutsche Forschungsgemeinschaft, SFB 455 A3.

REFERENCES

1. **Blondel, D., T. Regad, N. Poisson, B. Pavie, F. Harper, P. P. Pandolfi, H. de The, and M. K. Chelbi-Alix.** 2002. Rabies virus P and small P products interact directly with PML and reorganize PML nuclear bodies. Oncogene **21:**7957–7970.
2. **Buchholz, U. J., S. Finke, and K. K. Conzelmann.** 1999. Generation of bovine respiratory syncytial virus (BRSV) from cDNA: BRSV NS2 is not essential for virus replication in tissue culture, and the human RSV leader region acts as a functional BRSV genome promoter. J. Virol. **73:**251–259.
3. **Charpilienne, A., M. Nejmeddine, M. Berois, N. Parez, E. Neumann, E. Hewat, G. Trugnan, and J. Cohen.** 2001. Individual rotavirus-like particles containing 120 molecules of fluorescent protein are visible in living cells. J. Biol. Chem. **276:**29361–29367.
4. **Chenik, M., K. Chebli, and D. Blondel.** 1995. Translation initiation at alternate in- frame AUG codons in the rabies virus phosphoprotein mRNA is mediated by a ribosomal leaky scanning mechanism. J. Virol. **69:**707–712.
5. **Chenik, M., K. Chebli, Y. Gaudin, and D. Blondel.** 1994. In vivo interaction

of rabies virus phosphoprotein (P) and nucleoprotein (N): existence of two N-binding sites on P protein. J. Gen. Virol. **75:**2889–2896.
6. **Chenik, M., M. Schnell, K. K. Conzelmann, and D. Blondel.** 1998. Mapping the interacting domains between the rabies virus polymerase and phosphoprotein. J. Virol. **72:**1925–1930.
7. **Conzelmann, K. K., J. H. Cox, L. G. Schneider, and H. J. Thiel.** 1990. Molecular cloning and complete nucleotide sequence of the attenuated rabies virus SAD B19. Virology **175:**485–499.
8. **Conzelmann, K. K., J. H. Cox, and H. J. Thiel.** 1991. An L (polymerase)-deficient rabies virus defective interfering particle RNA is replicated and transcribed by heterologous helper virus L proteins. Virology **184:**655–663.
9. **Curran, J., J. B. Marq, and D. Kolakofsky.** 1995. An N-terminal domain of the Sendai paramyxovirus P protein acts as a chaperone for the NP protein during the nascent chain assembly step of genome replication. J. Virol. **69:**849–855.
10. **Dalton, K. P., and J. K. Rose.** 2001. Vesicular stomatitis virus glycoprotein containing the entire green fluorescent protein on its cytoplasmic domain is incorporated efficiently into virus particles. Virology **279:**414–421.
11. **Da Poian, A. T., A. M. Gomes, R. J. Oliveira, and J. L. Silva.** 1996. Migration of vesicular stomatitis virus glycoprotein to the nucleus of infected cells. Proc. Natl. Acad. Sci. USA **93:**8268–8273.
12. **Desai, P., and S. Person.** 1998. Incorporation of the green fluorescent protein into the herpes simplex virus type 1 capsid. J. Virol. **72:**7563–7568.
13. **Dietzschold, B., M. Tollis, M. Lafon, W. H. Wunner, and H. Koprowski.** 1987. Mechanisms of rabies virus neutralization by glycoprotein-specific monoclonal antibodies. Virology **161:**29–36.
14. **Duprex, W. P., F. M. Collins, and B. K. Rima.** 2002. Modulating the function of the measles virus RNA-dependent RNA polymerase by insertion of green fluorescent protein into the open reading frame. J. Virol. **76:**7322–7328.
15. **Ehrhardt, D.** 2003. GFP technology for live cell imaging. Curr. Opin. Plant Biol. **6:**622–628.
16. **Finke, S., and K. K. Conzelmann.** 1999. Virus promoters determine interference by defective RNAs: selective amplification of mini-RNA vectors and rescue from cDNA by a 3′ copy-back ambisense rabies virus. J. Virol. **73:**3818–3825.
17. **Finke, S., and K. K. Conzelmann.** 2003. Dissociation of rabies virus matrix protein functions in regulation of viral RNA synthesis and virus assembly. J. Virol. **77:**12074–12082.
18. **Finke, S., R. Mueller-Waldeck, and K. K. Conzelmann.** 2003. Rabies virus matrix protein regulates the balance of virus transcription and replication. J. Gen. Virol. **84:**1613–1621.
19. **Gao, Y., N. J. Greenfield, D. Z. Cleverley, and J. Lenard.** 1996. The transcriptional form of the phosphoprotein of vesicular stomatitis virus is a trimer: structure and stability. Biochemistry **35:**14569–14573.
20. **Gao, Y., and J. Lenard.** 1995. Cooperative binding of multimeric phosphoprotein (P) of vesicular stomatitis virus to polymerase (L) and template: pathways of assembly. J. Virol. **69:**7718–7723.
21. **Gaudin, Y.** 2000. Rabies virus-induced membrane fusion pathway. J. Cell Biol. **150:**601–612.
22. **Georgi, A., C. Mottola-Hartshorn, A. Warner, B. Fields, and L. B. Chen.** 1990. Detection of individual fluorescently labeled reovirions in living cells. Proc. Natl. Acad. Sci. USA **87:**6579–6583.
23. **Green, T. J., S. Macpherson, S. Qiu, J. Lebowitz, G. W. Wertz, and M. Luo.** 2000. Study of the assembly of vesicular stomatitis virus N protein: role of the P. protein. J. Virol. **74:**9515–9524.
24. **Harty, R. N., M. E. Brown, J. P. McGettigan, G. Wang, H. R. Jayakar, J. M. Huibregtse, M. A. Whitt, and M. J. Schnell.** 2001. Rhabdoviruses and the cellular ubiquitin-proteasome system: a budding interaction. J. Virol. **75:**10623–10629.
25. **Harty, R. N., J. Paragas, M. Sudol, and P. Palese.** 1999. A proline-rich motif within the matrix protein of vesicular stomatitis virus and rabies virus interacts with WW domains of cellular proteins: implications for viral budding. J. Virol. **73:**2921–2929.
26. **Horikami, S. M., J. Curran, D. Kolakofsky, and S. A. Moyer.** 1992. Complexes of Sendai virus NP-P and P-L proteins are required for defective interfering particle genome replication in vitro. J. Virol. **66:**4901–4908.
27. **Jacob, Y., H. Badrane, P. E. Ceccaldi, and N. Tordo.** 2000. Cytoplasmic dynein LC8 interacts with lyssavirus phosphoprotein. J. Virol. **74:**10217–10222.
28. **Lakadamyali, M., M. J. Rust, H. P. Babcock, and X. Zhuang.** 2003. Visualizing infection of individual influenza viruses. Proc. Natl. Acad. Sci. USA **100:**9280–9285.
29. **McDonald, D., M. A. Vodicka, G. Lucero, T. M. Svitkina, G. G. Borisy, M. Emerman, and T. J. Hope.** 2002. Visualization of the intracellular behavior of HIV in living cells. J. Cell Biol. **159:**441–452.
30. **Mebatsion, T.** 2001. Extensive attenuation of rabies virus by simultaneously modifying the dynein light chain binding site in the P protein and replacing Arg333 in the G protein. J. Virol. **75:**11496–11502.
31. **Mebatsion, T., M. Konig, and K. K. Conzelmann.** 1996. Budding of rabies virus particles in the absence of the spike glycoprotein. Cell **84:**941–951.
32. **Mebatsion, T., F. Weiland, and K. K. Conzelmann.** 1999. Matrix protein of rabies virus is responsible for the assembly and budding of bullet-shaped particles and interacts with the transmembrane spike glycoprotein G. J. Virol. **73:**242–250.
33. **Poisson, N., E. Real, Y. Gaudin, M. C. Vaney, S. King, Y. Jacob, N. Tordo, and D. Blondel.** 2001. Molecular basis for the interaction between rabies virus phosphoprotein P and the dynein light chain LC8: dissociation of dynein-binding properties and transcriptional functionality of P. J. Gen. Virol. **82:**2691–2696.
34. **Raux, H., A. Flamand, and D. Blondel.** 2000. Interaction of the rabies virus P protein with the LC8 dynein light chain. J. Virol. **74:**10212–10216.
35. **Rigaut, K. D., D. E. Birk, and J. Lenard.** 1991. Intracellular distribution of input vesicular stomatitis virus proteins after uncoating. J. Virol. **65:**2622–2628.
36. **Schnell, M. J., T. Mebatsion, and K. K. Conzelmann.** 1994. Infectious rabies viruses from cloned cDNA. EMBO J. **13:**4195–4203.
37. **Seisenberger, G., M. U. Ried, T. Endress, H. Buning, M. Hallek, and C. Brauchle.** 2001. Real-time single-molecule imaging of the infection pathway of an adeno- associated virus. Science **294:**1929–1932.
38. **Suomalainen, M., M. Y. Nakano, S. Keller, K. Boucke, R. P. Stidwill, and U. F. Greber.** 1999. Microtubule-dependent plus- and minus end-directed motilities are competing processes for nuclear targeting of adenovirus. J. Cell Biol. **144:**657–672.
39. **Superti, F., M. Derer, and H. Tsiang.** 1984. Mechanism of rabies virus entry into CER cells. J. Gen. Virol. **65:**781–789.
40. **Thomas, D., W. W. Newcomb, J. C. Brown, J. S. Wall, J. F. Hainfeld, B. L. Trus, and A. C. Steven.** 1985. Mass and molecular composition of vesicular stomatitis virus: a scanning transmission electron microscopy analysis. J. Virol. **54:**598–607.